



Virginia Commonwealth University  
VCU Scholars Compass

---

Theses and Dissertations

Graduate School

---

2011

## Synthesis of cyclen based receptors and their use in separations biotechnology.

Vivek Kaushik  
*Virginia Commonwealth University*

Follow this and additional works at: <https://scholarscompass.vcu.edu/etd>

 Part of the [Chemistry Commons](#)

© The Author

---

Downloaded from

<https://scholarscompass.vcu.edu/etd/2611>

This Dissertation is brought to you for free and open access by the Graduate School at VCU Scholars Compass. It has been accepted for inclusion in Theses and Dissertations by an authorized administrator of VCU Scholars Compass. For more information, please contact [libcompass@vcu.edu](mailto:libcompass@vcu.edu).

© Vivek Kaushik, 2011

All Rights Reserved

SYNTHESIS OF CYCLEN BASED RECEPTORS FOR PYRENE  
DYES AND THEIR USE IN SEPARATIONS BIOTECHNOLOGY

A Dissertation submitted in partial fulfillment of the requirements for the degree of Doctor of  
Philosophy at Virginia Commonwealth University.

by

VIVEK KAUSHIK

Master of Chemistry, Maharshi Dayanand University, 2004

Director: VLADIMIR A SIDOROV, Ph.D.

ASSOCIATE PROFESSOR, DEPARTMENT OF CHEMISTRY

Virginia Commonwealth University

Richmond, Virginia

Aug 2011

## Acknowledgement

My sincerest gratitude goes to my advisor Dr. Vladimir Sidorov, who has inspired, motivated and guided me through my years as a graduate student. I would also like to thank the department for accepting me into the program and supporting me throughout.

I'm also indebted to my fellow students/lab mates Christine Winschel, Rick Uhl and Andrew Voegel, who have been a pleasure to work with and constant source of inspiration.

Finally, I'd like to thank my friends and family, especially my parents who encouraged a young aspiring student from Bhiwani to pursue his passion in research. It was their constant love and support that pushed me through all the highs and lows of these past few years.

Thank you all.

## Table of Contents

	Page
Acknowledgements.....	ii
List of Figures.....	vi
List of Schemes.....	viii
List of Tables.....	x
List of Abbreviations.....	xi
Abstract.....	xiii
 Chapter	
1 Separations technology-Affinity chromatography and chemoselective precipitation.....	1
1.1 Introduction.....	1
1.2 Affinity chromatography.....	2
1.2.1 Immunoaffinity chromatography.....	3
1.2.2 Immobilized metal-ion affinity chromatography.....	9
1.2.3 Dye-ligand affinity chromatography.....	15
1.3 Chemoselective precipitation.....	19
1.3.1 Precipitons.....	19
1.4 Cyclen based receptors for pyrene dyes and their use in separations technology.....	26

2	Synthesis of cyclen based receptors for pyrene dyes.....	29
	2.1 Introduction.....	29
	2.2 Structure- activity studies.....	33
	2.3 Synthesis of new receptors.....	35
	2.4 Fluorometric titrations and results.....	36
	2.5 Conclusions.....	39
3	Chemoselective precipitation of Lactose from a Lactose/Sucrose mixture: Proof of concept for a new separation methodology.....	40
	3.1 Introduction.....	40
	3.2 Irreversible labeling of lactose with APTS and its chemoselective separation from lactose/sucrose mixture.....	42
	3.3 Reversible labeling of lactose with APTS and recovery of all the components used for the chemoselective precipitation.....	46
	3.4 Conclusions.....	48
4	Immobilization of cyclen based receptors for pyrene dyes on solid supports: beginning of a new affinity chromatography technique.....	50
	4.1 Introduction.....	50
	4.2 Synthesis of <i>p</i> -NO <sub>2</sub> -Bn-Cyclen (core cyclen <b>9a</b> ).....	50
	4.3 Synthesis of functionalized receptor.....	52
	4.4 Immobilization of functionalized receptor on solid support.....	56

4.5	Synthesis of functionalized receptor with a spacer arm.....	60
4.6	Immobilization of the receptor <b>13</b> .....	61
4.7	Fluorometric titrations of receptor <b>11</b> immobilized on the solid support.....	62
4.8	Conclusions.....	63
5	Future work.....	64
5.1	Introduction.....	64
5.2	Separation of a mixture of dyes.....	64
5.3	Separation of low molecular weight heparin (LMWH).....	64
5.4	Mapping of cells expressing ligand-gated ion channels.....	66
	Experimental Section.....	69
	References.....	82
	Appendix.....	97
	<sup>1</sup> H NMR and <sup>13</sup> C NMR.....	97
	VITA.....	127

## List of Figures

	Page
Figure 1.1 Structure of antibody and mechanism of antigen recognition.....	5
Figure 1.2 Immobilization of antibody by random coupling methods.....	6
Figure 1.3 Structure of some reactive dyes.....	16
Figure 1.4 Structure of cyclen <b>1</b> and various pyrene dyes.....	27
Figure 2.1 Structure of DPX.....	30
Figure 2.2 Microcalorimetric characterization of interactions of cyclen <b>1</b> with pyranine and calcein in methanol.....	32
Figure 2.3 Structure of various fluorescein dyes.....	33
Figure 2.4 Structure of compounds used in structure and activity studies.....	34
Figure 2.5 Structure of various synthesized cyclen based receptors.....	35
Figure 2.6. Fluorometric titrations of 50 nM PBS solution of HPTS with receptor <b>7</b> .....	38
Figure 3.1 Quenching of lactose-sucrose conjugate fluorescence on addition of cyclen <b>1</b> ....	44
Figure 3.2 <sup>1</sup> H NMR spectra of various stages of chemoselective precipitation protocol 1....	45
Figure 3.3 <sup>1</sup> H NMR spectra of various stages of chemoselective precipitation protocol 2.....	46
Figure 3.4 <sup>1</sup> H NMR spectra of various stages of chemoselective precipitation protocol 3.....	47
Figure 4.1 Raw fluorescence data for 50 nM solution of HPTS in the presence of the resins and (or) receptor <b>11</b> .....	60
Figure 4.2 Raw fluorescence data for 50 nM solution of HPTS in the presence	



of the resin and (or) free or immobilized receptor <b>11</b> .....	63
Figure 5.1 Major repeating disaccharide of heparin.....	64
Figure 5.2 Structure of receptor <b>12</b> .....	67

## List of Schemes

	Page
Scheme 1.1 A schematic representation of various affinity chromatography steps.....	2
Scheme 1.2 Selected activation and coupling pathways.....	7
Scheme 1.3 Synthesis of precipiton 3Z.....	20
Scheme 1.4 A general scheme for the synthesis of isoxazolines.....	21
Scheme 1.5 Synthesis of precipiton bound alkene substrate.....	21
Scheme 1.6 A general scheme for the synthesis of precipiton bound isoxazoline product....	22
Scheme 1.7 Illustration of the “precipiton” process for isoxazoline isolation.....	22
Scheme 1.8 Methanolytic cleavage to furnish precipiton E-3 and product.....	23
Scheme 1.9 Synthesis of acetoacetate ester 4Z.....	23
Scheme 1.10 Synthesis and isolation of precipiton bound product.....	24
Scheme 1.11 Methanolytic removal of precipiton to give free product.....	24
Scheme 1.12 A general scheme for the synthesis of Baylis-Hillman product.....	25
Scheme 1.13 Synthesis of precipiton acrylate 5Z.....	25
Scheme 1.14 Synthesis and isolation of precipiton bound product.....	26
Scheme 1.15 Hydrolysis of precipiton bound product to afford precipiton and product.....	26
Scheme 1.16 Complexation mechanism of HPTS dye with cyclen1.....	27
Scheme 2.1 A) pH-Stat experiment; B) Membrane leakage assay.....	29

Scheme 2.2 Synthetic scheme for the cyclen based receptors.....	36
Scheme 3.1 Structures of lactose, sucrose, APTS dye and receptor cyclen <b>1</b> .....	42
Scheme 3.2 General representation of protocols for chemoselective precipitation.....	43
Scheme 4.1 Synthesis of <i>p</i> -NO <sub>2</sub> -Bn-Cyclen (core cyclen <b>9a</b> ).....	51
Scheme 4.2 Synthesis of functionalized cyclen receptor.....	53
Scheme 4.3 Alternative scheme for the synthesis of functionalized cyclen receptor.....	55
Scheme 4.4 Synthesis of functionalized receptor with spacer arm.....	61
Scheme 4.5 Immobilization of receptor <b>11</b> on NHS activated agarose.....	62
Scheme 5.1 Acid catalyzed and enzymatic depolymerization of heparin.....	65
Scheme 5.2 A general scheme for the detection of ligand-gated ion channels.....	68

## List of Tables

	Pages
Table 2.1 Thermodynamic parameters assessed for the complexation of pyranine with cyclen <b>1</b> in methanol.....	32
Table 2.2 Binding constants and maximum fluorescence loss assessed for the complexes of HPTS with pyrene based receptors from fluorometric titrations .....	37

## List of Abbreviations

Ab	Antibody
Ag	Antigen
APTS	8 - Aminopyrene - 1,3,6 - trisulfonic acid, trisodium salt
CNBr	Cyanogen bromide
DABCO	1,4-diazabicyclo[2.2.2]octane
DIEA	Ethyl-diisopropylamine
DMF	Dimethylformamide
DMAP	4-Dimethylaminopyridine
DMSO	Dimethyl sulfoxide
DOPE	1,2-dioleoyl-sn-glycero-3-phosphoethanolamine
DPX	p-xylene-bis-pyridinium bromide
EDC	1-Ethyl-3-(3-dimethylaminopropyl)carbodiimide
EDTA	Ethlenediaminetetraacetic acid
HEPES	(4-(2-hydroxyethyl)-1-piperazineethanesulfonic acid )
HPIAC	High pressure immunoaffinity chromatography
HPTS	8 - Hydroxypyrene - 1,3,6 - trisulfonic acid, trisodium salt
IAC	Immunoaffinity chromatography
IMAC	Immobilized Metal-ion affinity chromatography

IgG	Immunoglobulin G
ITC	Isothermal thermal calorimetry
KCl	Potassium chloride
KHMDS	Potassium bis(trimethylsilyl)amide
KSCN	Potassium thiocyanate
LMWH	Low molecular weight heparin
LUV	Unilamellar vesicles
MAb	Monoclonal antibody
MES	2-( <i>N</i> -morpholino)ethanesulfonic acid
MOPS	3-( <i>N</i> -morpholino)propanesulfonic acid
TFA	Trifluoroacetic acid
THF	Tetrahydrofuran

## Abstract

# SYNTHESIS OF CYCLEN BASED RECEPTORS FOR PYRENE DYES AND THEIR USE IN SEPARATIONS BIOTECHNOLOGY

By Vivek Kaushik, Ph.D.

A Dissertation submitted in partial fulfillment of the requirements for the degree of Doctor of  
Philosophy at Virginia Commonwealth University.

Virginia Commonwealth University, 2011

Major Director: Vladimir A Sidorov, Ph.D.

Associate Professor Department of Chemistry

A number of purification techniques such as adsorption, centrifugation, chromatography, extraction, distillation, filtration, precipitation etc. to name a few, are commonly used for the purification. However, due to a constant need of purification of even more complex crude mixtures, be it reaction mixtures, various proteins and DNA from cell extracts or medicinal compounds and fragrances from plant extracts, scientists needed to consistently develop new and improved techniques of purification. One such great advancement in the field of chromatography was the development of affinity chromatography. It revolutionized the field of bioseparations technology, and the dream of single stage purification of complex biological substrates such as proteins, enzymes, co-enzymes, DNA, RNA etc. was realized.

Development of various precipitation techniques involving phase tags, acid-base induced precipitation, host-guest interactions, chemoselective precipitation etc. further simplified

purification procedures for few substrates. However, only a few examples of chemoselective precipitation are known in literature.<sup>1, 2</sup>

In 2005, our group synthesized a cyclen-based receptor.<sup>9</sup> This receptor showed very strong and very specific affinity for the pyrene based dyes (HPTS, APTS, PTA) under physiological conditions, similar to that of the natural receptors for their ligands. Upon interaction with the dye, this artificial receptor formed a low solubility complex which had micromolar stability.

Various structure and activity studies established the essentiality of the macrocyclic structure of the receptor for the dye recognition. We further decided to study the effect of various substituents on the aromatic ring on the binding and quenching affinity of the receptor. A series of receptors bearing electron-withdrawing and electron-donating substituents were synthesized (receptor **4-6**). We also synthesized a receptor having aliphatic groups instead of aromatic groups attached to the thiourea group (receptor **7**) as well as a receptor lacking thiourea linkage (receptor **8**). The results of fluorometric titrations of these receptors were consistent with the previous structure and activity studies, as the receptors having electron withdrawing nitro- and bromo substituents (receptor **4** and **6** respectively) on the aromatic groups (have increased  $\pi$ -stacking) were better receptor than cyclen **1**. Interestingly, the receptor **5**, bearing an electron-donating methoxy groups on the aromatic ring, has also shown an increase in the affinity towards HPTS. We speculated that this increased affinity could be due to the higher affinity of receptor **5** towards  $\text{Na}^+$  which was essential for the proper arrangement of the receptor binding arms. The receptor with the aliphatic chain (receptor **7**) showed a complicated complexation process and showed variable fluorescence quenching at various receptor concentrations. This behaviour was probably due to the formation of complexes of a various stoichiometries. Expectedly, the receptor lacking thiourea group (receptor **8**) did not show any interaction.



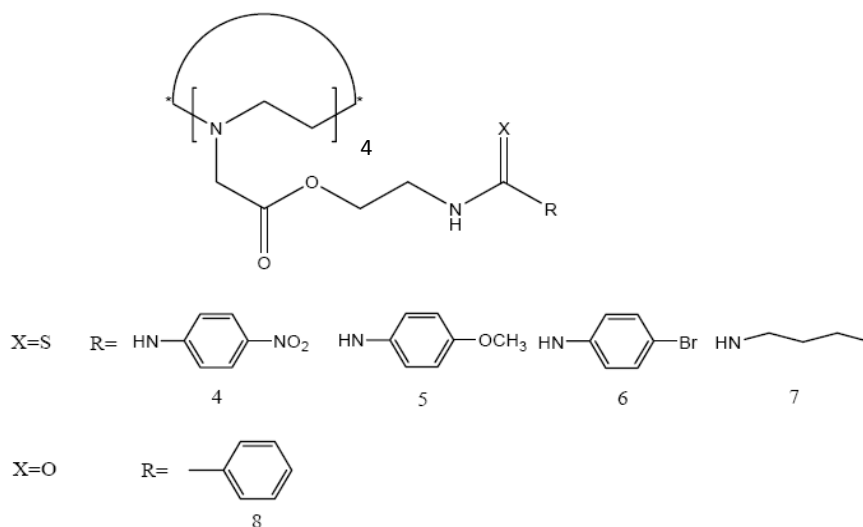
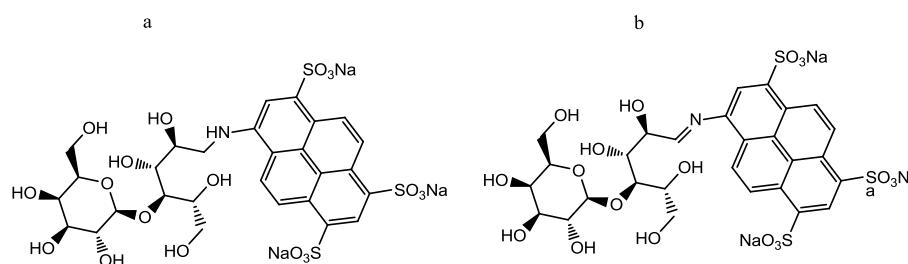


Figure 1. Structure of various receptors synthesized having different X and R groups. For stability upon interaction, we hypothesized that this receptor-dye pair can be used in the selective separation of substrates by chemoselective precipitation. We reasoned that if the substrate of interest can be attached to the dye, this dye-substrate conjugate then can be selectively precipitated from the reaction mixture upon addition of the receptor. We tried our concept for the separation of lactose from lactose/sucrose mixture. Being a reducing sugar, lactose was labeled with APTS dye, whereas sucrose that lacks the reducing end, remained unmodified. Application of the cyclen receptor to this mixture resulted in precipitation of APTS-lactose conjugate, leaving sucrose as the only component in the solution.<sup>10</sup> By coupling APTS dye with lactose via an imine bond, we were able to successfully isolate unmodified lactose from the conjugate by subsequent hydrolysis of the conjugate.<sup>10</sup>



Scheme 1. Structure of a) fully reduced lactose-APTS conjugate b) partially reduced lactose-APTS conjugate.

Next, we decided to use this dye-receptor pair in affinity chromatography. We hypothesized that if the receptor can be immobilized on some solid support then it can be specifically used as an affinity support for the substrates which are attached to the pyrene-based dyes. A new receptor with a functional group on the cyclen core was needed to immobilize the receptor on the solid support. The receptor **11** (fig. 2.A) having an aromatic primary amine group was synthesized. This receptor was successfully immobilized on the NHS activated agarose resin. A series of fluorometric experiments were performed to determine the specificity and binding ability of the affinity support towards the pyrene dyes. Initial results of these experiments indicated that the affinity support was very effective as indicated by almost 95% fluorescence quench of a solution of 50 nM HPTS and affinity resin (fig. 2.B).

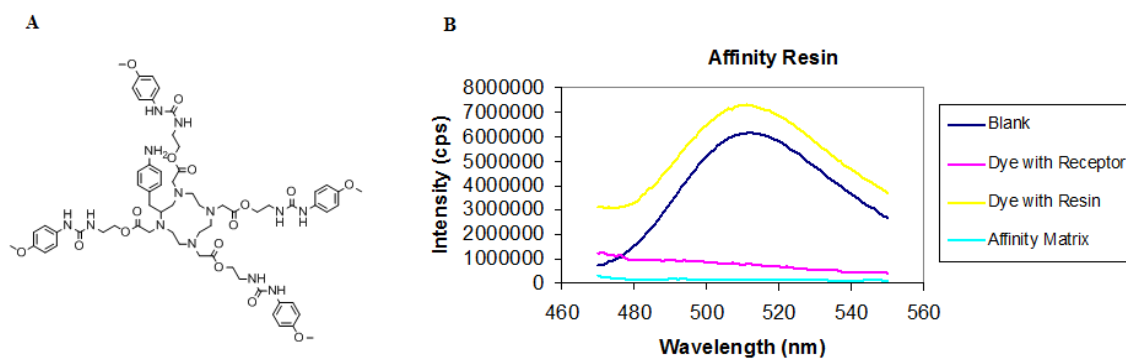


Figure 2. A) Structure of receptor **11**; B) Emission spectra of 50 nM HPTS dye in the presence of the resin and (or) free or immobilized receptor **11**.

This work has opened several new venues of research, and the applicability of this dye-receptor pair in the fields of biochemistry, pharmacology, cell biology etc. will be explored.

## Chapter 1

# Separations Technology-Affinity chromatography and chemoselective precipitation

### 1.1 Introduction

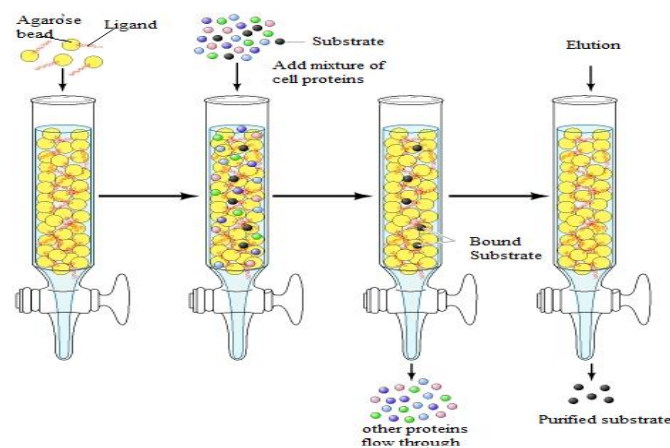
Since ancient times, people have used methods of separating and purifying chemical substances for improving the quality of life. The extraction of metals from ores and of medicines from plants is older than recorded history. Gold was mined as early 2<sup>nd</sup> and 3<sup>rd</sup> century AD in India as proved by the gold objects found in Harappa and Mohenjo-daro. Fragrances were first extracted from various plants and flowers by ancient Egyptians. One very common and modern example which revolutionized human history is purification of crude oil. It is a mixture of various hydrocarbons and each has a significant use. Crude oil is purified by fractional distillation into individual hydrocarbons such as gasoline, diesel, jet fuel, lubricating oil, asphalt etc.

Nowadays, discovery of most of the new compounds results from synthesis in the laboratory. Laboratory preparation of a compound often yields a crude mixture containing some quantities of the unreacted starting materials as also impurities that are by-products from side reactions. A substance that occurs in a natural source is also rarely present as a single entity in that source. The first demand on the chemist or the biochemist is the isolation of the pure compound from the crude mixture that has resulted from either the laboratory synthesis of the compound or its extraction from one of its natural sources. The chemist or the biochemist proceeds to study the properties or details of the structure of a compound only after it has become available in the pure state.

A number of purification techniques such as adsorption, centrifugation, chromatography, extraction, distillation, filtration, precipitation etc. to name a few, are commonly used for the purification. However, due to this constant need of purification of complex crude mixtures like reaction mixtures, various proteins or DNA from cell extracts, scientists needed to develop new and improved techniques of purification. One such great advancement in the field of chromatography was the development of affinity chromatography. It revolutionized the field of bioseparations technology and as a consequence, the goal of single stage purification of complex biological substrates such as proteins, enzymes, co-enzymes, DNA, RNA etc. was realized. Development of various precipitation techniques involving phase tags, acid-base induced precipitation, host-guest interactions etc. further simplified purification procedures for few substrates.

## 1.2 Affinity Chromatography:

Affinity chromatography is a purification technique based on highly specific and reversible interactions between two molecules. Interactions between antibody and antigen, protein and metal-ion, enzyme and substrate, dye and protein etc. are few very common examples of such interactions which formed the bases of affinity chromatographic separation of these substrates from the complex mixtures.



Scheme 1.1. A schematic representation of various affinity chromatography steps.<sup>85</sup>

### 1.2.1 Immunoaffinity Chromatography (IAC)

The concept of immunoaffinity chromatography goes back as early as 1924 when Engelgardt suggested "the method of fixed partner" and used immobilized antibodies to catch free antigen in fluids.<sup>11</sup> In early 1950s Campbell et al. successfully isolated antibodies with antigens immobilized on azide-activated cellulose.<sup>12</sup> Even though, the idea of immunoaffinity chromatography originated in early twentieth century, it took several decades to expand the use of the method for the separation of different types of antigen and antibody fragments.<sup>13-15</sup> Discovery of monoclonal antibodies in 1970s greatly accelerated development of IAC.<sup>16</sup>

IAC is a separation method based on specific and reversible interaction between an antigen (Ag) and a matrix bound antibody (Ab), and is capable of effecting high yield single stage purification of many biomolecules.<sup>11</sup> IAC can be used in the separation of various biomolecules such as proteins of pharmaceutical interest,<sup>17-20</sup> vaccines, small biomolecules<sup>21</sup> and virtually anything for which monoclonal antibody (MAb) can be made. Separation by IAC involves a number of steps. First is to find an ideal support, followed by activation and immobilization of affinity ligand on the support. This support is then loaded with the crude extract having desired product and finally eluted to separate the desired product from other impurities.

#### **Matrix:**

The matrix is the solid support on which antibodies are immobilized for IAC. An ideal immunoabsorbent should be macroporous, stable, highly functionalized, easy to activate, hydrophilic and inert.<sup>22-24</sup>

The most popular support matrix for affinity chromatography is beaded agarose. The favorable characteristics of agarose include its high porosity, hydrophilicity, chemical

stability, and its relative inertness towards nonspecific adsorption.<sup>25</sup> However, agarose is not very stable.<sup>26</sup> This problem was overcome by cross linking agarose with epichlorohydrin.<sup>26</sup> A major disadvantage of beaded agarose is its inability to withstand high pressure gradients, even when cross linked.

Another popular support is polyacrylamide porous beads. These are prepared by the copolymerization of acrylamide and N-N' methylene-bis-acrylamide. Polyacrylamide gels are hydrophilic, free of fixed charge, stable in aqueous environment between pH 2-10, and tolerate dilute organic acids.<sup>26</sup> A major disadvantage is microporosity which hinders the efficient immobilization of Ab.<sup>16</sup>

Poly(HEMA), a copolymer of hydroxyl methacrylate and ethylene glycol dimethacrylate; azalactone functional copolymer beads, made by copolymerization of azlactone functional vinyl monomers with acrylamides or acrylates; and cellulose are other supports used in affinity chromatography.

Silica is the inorganic support used in IAC. However, pure silica, due to irreversible adsorption and denaturation of many biomolecules, has limited use in immunoaffinity chromatography.<sup>16</sup> Synthesis of modified silica, covered with a hydrophilic surface layer, made it more compatible for IAC. High stability and its ability to withstand high pressure have made silica an ideal support for high performance immunoaffinity chromatography (HPIAC).<sup>27</sup>

### **Activation and Coupling:**

All the matrices discussed above are highly functionalized; however, not all of them are reactive enough for the immobilization of the Ab on the matrix. Hence, these functional groups need to be activated in order to attach Ab to the solid support. Several activation

strategies have been successfully used to activate the solid support. These methods fall under two basic categories: 1) those that produce randomly oriented immobilized Abs 2) those that produce more uniformly oriented Abs. Proper orientation of Ab is necessary for effective binding to the Ag. Antibodies have Y shaped structure with antigen binding region (Fab region) located in the tip of arms. The base of the Y is called Fc region (fig. 1.1).<sup>28</sup>

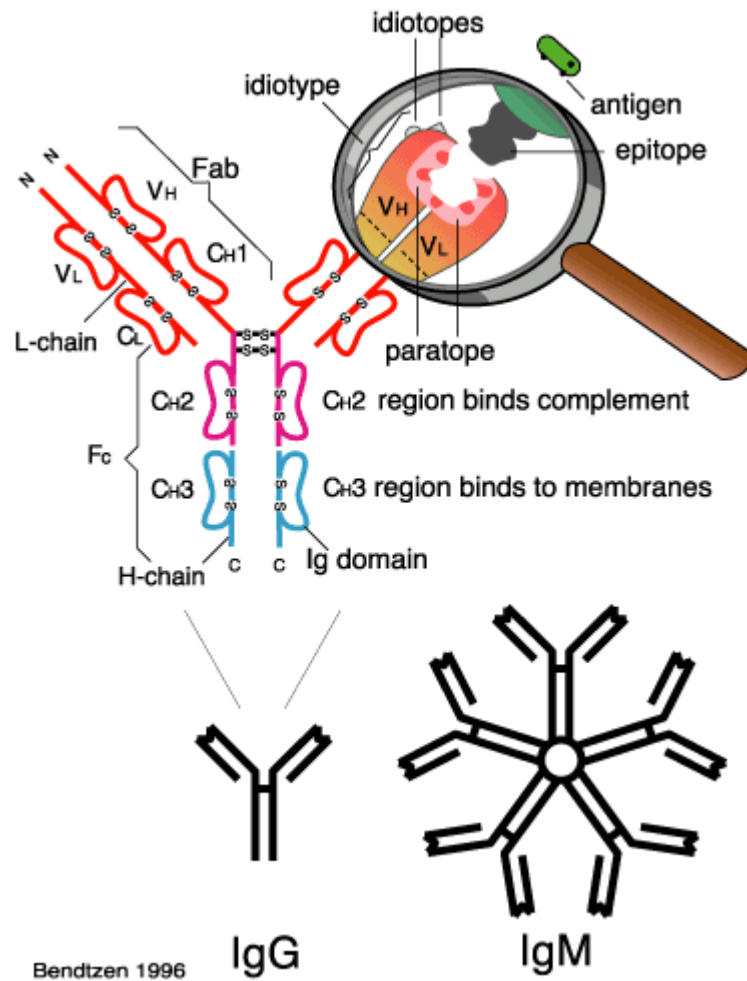


Figure 1.1. Structure of antibody showing Fab and Fc regions and mechanism of recognition of antigen by antibody.<sup>190</sup>

Abs immobilized using Fc region retain full activity and bind with the Ag. However, Abs immobilized on the solid support using Fab region, loses partial or complete ability to bind the Ag depending on whether one or both the Fab regions of the Ab are used for immobilization (fig. 1.2).<sup>29</sup>

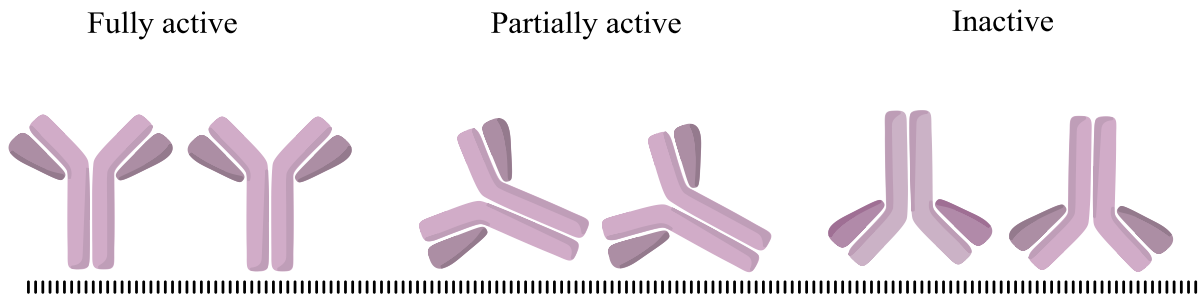


Figure 1.2. Idealized representation of Ab immobilized by random coupling procedure.

Cyanogen bromide (CNBr): It is the most popular and very effective method for the activation of solid supports.<sup>30, 31</sup> One big advantage of using CNBr is its ability to activate most matrix surfaces under aqueous conditions. However, CNBr is volatile and toxic, hence, newer procedures employing cyanylating agents<sup>32</sup> such as p-nitrophenylcyanate (pNPC) or 1-cyano-4-(dimethyl-amino)-pyridinium tetrafluoroborate (CDAP) have been introduced. One disadvantage of CNBr-activated supports with respect to Ab immobilization is the slow leakage of the protein over time.<sup>33</sup> This can be attributed to the inherent instability of the isourea bond through which Ab is coupled to the support.<sup>32</sup>

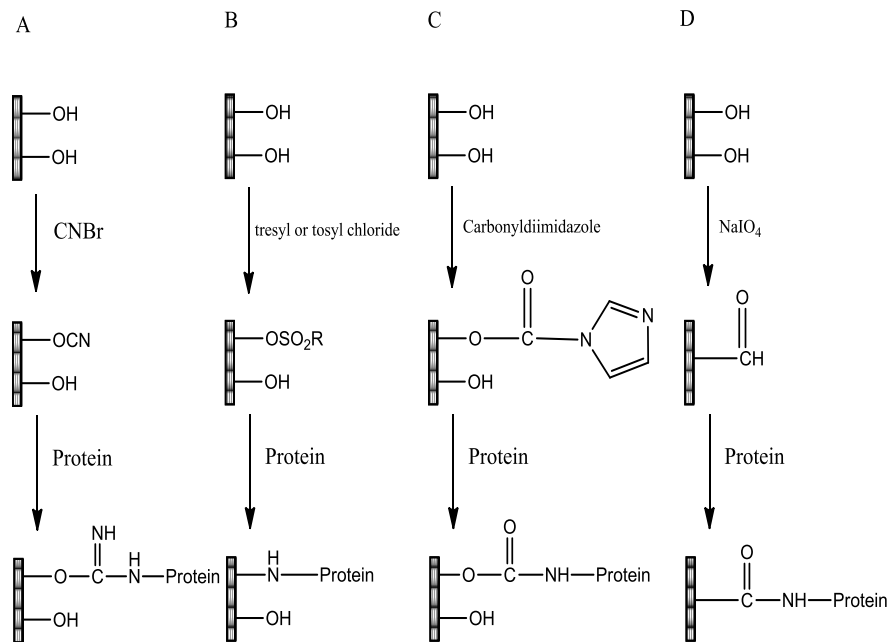
Sulfonyl chlorides: Tresyl chloride and tosyl chloride are the two most commonly used sulfonyl chlorides for the activation of solid supports.<sup>34</sup> Tresyl chloride is preferred as it forms sulfonates more readily and is easily displaced at neutral pH and 4<sup>0</sup>C.<sup>34</sup>

Carbonyldiimidazole: Another activation procedure for hydroxyl groups uses 1, 1'-carbonyldiimidazole to introduce activated carbamates as the reactive species.<sup>35, 36</sup>

Periodate oxidation: Supports containing vicinal diol groups can be activated by sodium metaperiodate, oxidizing the diols to aldehyde group. Amino group on the protein reacts with the aldehyde group under mild conditions (aqueous buffer at pH 7-8) and forms an imine bond which is subsequently reduced with sodium borohydride or sodium cyanoborohydride to produce a stable secondary amine bond.



Activation by hydrazine, azalactone and N-hydroxy succinimide are some other methods used to activate solid supports having functional groups other than –OH group.



Scheme 1.2. Selected activation and coupling pathways: A) Cyanogen bromide; B) Sulfonyl chloride; C) Carbonyldiimidazole; D) Periodate oxidation

### Methods for oriented Ab immobilization:

All of the above mentioned methods results in random orientation of coupled Ab, which tend to reduce its ability to bind Ag. Several schemes for achieving oriented coupling have been reported. One such scheme involves immobilization of Protein A on the solid support, which has strong affinity for the Fc region of many IgG subclasses.<sup>37, 38</sup> This protein is then cross linked to Ab with dimethyl pimelidate. Using Protein A agarose, Sisson and Castor reported complete Ab attachment and full Ab activity.<sup>38</sup>

Another approach involves oxidation of carbohydrate moiety of IgG with periodates to produce reactive aldehyde groups, located mostly within the hinge region of Ab molecule. The modified IgG is either coupled to a surface containing amines or more reactive hydrazide

groups.<sup>39, 40</sup> Prisyazhuoy et al., utilized the SH groups of the Fab' fragment to create an oriented Ab fragment.<sup>41</sup>

### **Loading:**

The objective of loading is to retain only the desired product on the support. Usually pre-column clarification of the crude extract is done prior to loading in order to prevent fouling or clogging of the column. This solution is then introduced in the column. The flow rate of the crude solution is limited either by the mechanical rigidity of the support matrix or the time required for the diffusion of the product into the pores of column matrix. In stirred tanks, the matrix and crude mixture are mixed together for a fixed time, after which solid phase is collected.<sup>16</sup> One variation of stirred tank methods uses magnetic affinity beads which can be separated from other insoluble compounds by collecting them in a magnetic field.<sup>29, 42</sup>

### **Washing:**

Following the loading, column is washed with physiological buffers (e.g. phosphate buffered saline, pH 7.2). The column is washed to remove unbound impurities present in the fluid volume of the column as well as those bound nonspecifically to the affinity support. However, one must be careful with washing as excessive washing can result in product loss. Thus, it may be necessary to compromise between yield and purity.

### **Elution:**

In this step, product is recovered from the column by using a solvent that reduces affinity of Ag to Ab. A number of procedures have been described. These includes use of either high<sup>43</sup> or low pH,<sup>16, 44</sup> chaotropic agents such as KSCN,<sup>45</sup> organic solvents such as ethylene glycol,<sup>46</sup> DMSO,<sup>47</sup> or acetonitrile,<sup>48</sup> high<sup>49</sup> or low ionic strength,<sup>50, 51</sup> increased temperature,<sup>52</sup> denaturing agents<sup>11</sup> such as 8M urea or 6M guanidine and others. Alternatively, gentler

elution methods that have been described include electrophoretic elution,<sup>53</sup> pressure induced elution<sup>54</sup> and metal ion elution<sup>18</sup> in which Ag-Ab binding depends on the presence or absence of a metal ion.

### **Regeneration and cycling:**

Since Ab and MAb are expensive, it is absolutely necessary to regenerate the immunoaffinity columns for further use to make it economically viable process. In this step column is washed with the solutions to remove elution buffers, as well as component of the crude extracts that have bound nonspecifically to the column and have not been released by either washing or elution. One protocol suggests a routine wash with 2M KCl/6M urea after each use.<sup>11</sup>

### **Applications of IAC:**

The most important application of IAC is protein purification. IAC has been used both for laboratory scale and preparative scale purification of proteins.<sup>29</sup> At laboratory scale cost is not a primary concern as the scale is small, and main focus is placed on the development of new purification methods for the substances that have not been previously purified. In contrast, the cost is the most significant factor at preparative scale purification. This requires careful selection of support, the coupling chemistry, the ligand and the elution and washing conditions such that the column capacity is retained over repeated cycles.<sup>29</sup> Other uses involve use in assays and subtractive chromatography.

#### **1.2.2 Immobilized Metal-Ion affinity chromatography (IMAC)**

The basis of the method was first introduced by Helfferich<sup>55</sup> in 1961 when he showed that metal ions immobilized on the resins can be used for the separation of the compounds which form complexes with them. Everson and Parker<sup>56</sup> were the first, who adopted immobilization of the chelating compounds for the separation of metalloproteins. The method became

popular through the research work of Porath,<sup>57, 58</sup> and Sulkowski,<sup>59-62</sup> who laid the foundation of this technique, mainly on its use for the separation and isolation of proteins.

In IMAC, metal ions are loaded on a sorbent or matrix using multidentate chelating groups which are covalently attached to the matrix. Chelating groups and metal ions form complexes, as a result of which metal ions are secured for subsequent interaction with the compound to be resolved. To this end, the metal ions must have free coordination sites in order to allow the interaction with proteins. These interactions between metal-ions and proteins are extremely complex in nature and can involve electrostatic, hydrophobic and donor-acceptor interactions. It has been found that histidine, tryptophan and cysteine residues in proteins are critical for protein separation in IMAC,<sup>63</sup> due to the strong interactions of these residues with the metal ions. Since there are a limited number of cysteine residues on the surfaces of proteins, histidine plays the role of a major target for metal ion complexation.<sup>64, 65</sup>

### **Metal Ions:**

Metal ions can be divided into three categories: Hard, borderline or intermediate and soft ions, based on the principle of hard and soft acids and bases (HSAB) described by Pearson.<sup>66</sup> Fe (III), Al (III), Ca (II), Mg (II), and K (I) belongs to the hard metal ions group, which show preference for oxygen, aliphatic nitrogen and phosphorus. Soft metal-ions such as Cu (I), Hg (II), Ag (I), etc., prefer sulfur containing ligands and borderline metal-ions Cu (II), Ni (II), Zn (II), and Co (II) coordinate aromatic nitrogen, oxygen and sulfur.<sup>64</sup> The most commonly used metal-ions are transition ones, Cu (II), Ni (II), Zn (II), Co (II), and Fe (III), especially Ni (II) as it provides a coordination number of six, electrochemical stability under chromatographic conditions, borderline polarizability and redox stability.<sup>22</sup>

### **Chelating Ligands:**

In IMAC metal-ions are immobilized on the matrix using chelating ligands. These are compounds that form complexes with metal ions and retain them on the solid support. Various types of multidentate ligands are commonly used for the immobilization of metal-ions.<sup>55</sup> The stability of metal ion complex with a chelating ligand depends upon multiplicity of the chelate, hence order of stability is penta> tetra> tridentate<sup>58, 64, 65</sup> which implies a lower metal-ion leakage in higher dentate chelate. However, the stronger metal-chelate complex comes at the expense of weaker protein binding. Therefore, the order of biomolecule adsorption strength is tridentate> tetradentate> pentadentate.<sup>58, 65</sup> As a result, most of the investigations have focused on the use of tri and tetradentate ligands which hold on the metal ions sufficient strength without sacrificing too much binding affinity of the metal ion to the proteins.

Triazine dyes such as Cibacron blue, Cibacron red, Procion brown etc. are also used as chelating agents in IMAC.<sup>67-69</sup> However, their use is very limited as they form weaker complex compared to multidentate chelates. Also, the dye ligands are used as affinity ligands themselves, which implies that part of biomolecule adsorption on this kind of immobilized metal affinity matrix may be through the dye affinity adsorption and not completely due to the metal ion interaction.<sup>68-70</sup>

### **Matrix:**

For an adequate use in IMAC, the matrix must be stable, have functional groups on the surface that are easy to derivatize, hydrophilic, have high porosity with fairly large pore size, allow the use of high flow rate and provide a stable bed. Classical stationary phases are based on soft gel matrices, such as agarose, beaded cellulose or cross linked dextran.<sup>71, 72</sup> However,

these matrices are compressible and restricted to low flow rate, hence their use on the large scale in industry is limited.<sup>65</sup>

Silica is an ideal rigid support, as it can be manufactured with large pores and narrow pore size distribution to efficiently increase the macromolecular transfer inside the matrix.<sup>73</sup> However, nonspecific adsorption of proteins to silica by complex hydrophobic interactions and instability under basic conditions ( $\text{pH} > 8.0$ ) limits the use of silica in IMAC. In order to overcome these problems silica-based matrices are normally coated with hydrophilic polymers such as agarose,<sup>65, 74, 75</sup> dextran<sup>74-77</sup> and chitosan<sup>73, 78, 79</sup>. Not only such coatings reduce the nonspecific adsorption through the increased hydrophilicity, but they also increase chemical stability and loading capacity of the coated silica.

#### **Activation and ligand immobilization conditions:**

While immobilizing ligand on the matrix, care should be taken that only the least critical regions of the ligand are used for immobilization. Reaction conditions should be chosen in such a way that the loss of ligand activity is minimal. Steric hindrance between the ligand and the protein is another major concern, as active sites of the biological molecules are often located deep within the three-dimensional structure of the molecule which can severely hinder protein binding capability of the ligand. This problem can be overcome by use of spacer arms between matrix and the ligand molecule. An ideal spacer arm must be bifunctional so that it can react with both matrix and the ligand. It should not have any active center to cause extra non-specific adsorption.<sup>23</sup>

Two alternative procedures may be followed. The matrix is first activated with an activation agent, and then spacer arm is attached covalently to the matrix through the active points.<sup>80</sup>

The ligand is then reacted with the other end of the spacer molecules. Alternatively, the

ligand-spacer arm conjugate is first synthesized and then attached to the matrix in one single step.

Cyanogen bromide, activation of –OH groups to oxiran groups with bisoxiranes, epichlorohydrin, or epoxy bromopropane and oxidation of two vicinal cis-hydroxyl groups to aldehyde using sodium peroxide are few commonly used activation methods.<sup>30, 80, 81</sup>

### **Loading:**

The interactions between protein and the immobilized metal ion are very complex in nature and vary from electrostatic interactions between charged biomolecule and (a) positively charged metal-ions, (b) negatively charged sites remaining on the matrix, hydrophobic interactions between biomolecule and the matrix surface and/or donor-acceptor interactions of the exposed amino acid residues with the metal-ions.<sup>23, 81-83</sup> Various factors such as the nature of chelating ligand, metal ion, surface amino acid composition, nature of buffer salts, pH, and ionic strength of the loading buffer determine the dominant interaction over the others during loading. It has been found that at higher ionic strengths protein adsorption become more selective.<sup>84-86</sup> The protein adsorption is controlled by the pH of the medium as protons affect the net charge on the immobilized metal-ions as well as the surface properties of the proteins resulting in an altered retention behavior.<sup>58, 84, 85, 87, 88</sup>

### **Elution:**

In this step, buffer solutions of a pH value lower than the pKa of surface exposed electron donating amino acids or high ionic strengths are used to elute proteins from the column. If harsher conditions are needed, a high displacement agent e.g., imidazole or stronger metal chelating agent e.g., EDTA could be used.<sup>58</sup> Some elution protocols involving the

simultaneous use of both imidazole addition and pH decreasing gradient in order to achieve a better chromatographic resolution have been described.<sup>64</sup>

### **Application:**

#### **Protein purification:**

Histidine residues are found on most of the natural proteins, but due to their mild hydrophobicity, only few of them are located on the protein surface.<sup>65</sup> Also, there are steric concerns as well, as proper accessibility is required to form stable complex between the histidine residue and the metal ion chelate conjugate.

Hochuli et al.<sup>89</sup> showed that affinity tags attached to the C- or N-terminus of the recombinant proteins can be used for the purification of proteins by IMAC. Usually histidine tags of various lengths have been used as affinity tags. His<sub>6</sub> having six consecutive histidine residues is the most commonly used affinity tag.<sup>89-96</sup> Histidine tagging and IMAC have become a routine for easy first-time isolation of newly expressed proteins.

#### **IMAC and protein refolding:**

Inclusion bodies produced in *E. coli* are composed of densely packed denatured protein molecules. These proteins are biologically inactive and need elaborate solubilization, refolding and purification to yield the functionally active product. But these processes are highly cumbersome, result in poor recovery and account for the major cost in the production of recombinant proteins from *E. coli*.<sup>97</sup>

Recently, a new IMAC based matrix assisted method has been developed for the production of soluble and functional proteins from inclusion bodies. It involves production of tagged proteins in inclusion bodies which are then solubilized, denatured and immobilized on a charged resin. These immobilized proteins are then renatured or refolded (using various



denaturing and renaturing procedures)<sup>98-106</sup> on the matrix followed by elution of protein from the matrix in its native and soluble form.

Other uses of IMAC involve separation and enrichment of phosphoproteins and phosphopeptides using Fe (III) and Ga (III) embedded matrices.<sup>107</sup>

### **1.2.3 Dye-ligand affinity chromatography**

Most of the affinity chromatography techniques involve immobilization of antibodies, amino acids, proteins, nucleic acids, oligonucleotides, enzymes, coenzymes and cofactors on the solid matrix.<sup>108, 109</sup> These ligands are expensive due to the high cost of production and/or extensive purification steps. Moreover, as use of harsh conditions can cause degradation of the ligands, it is difficult to immobilize certain ligands, as standard conditions are not sufficient to immobilize these ligands on the support. Also, precaution is required during the sorption and elution steps, as the use of harsh conditions can damage the affinity ligand.

The dye-based ligands provide exciting alternative to the natural counterparts for the specific affinity chromatography. These dyes are synthetic, inexpensive, commercially available compounds that can be easily immobilized on the matrices bearing hydroxyl groups. Dye-based ligands are able to bind most types of proteins, especially enzymes, in some cases in a remarkably specific manner.

#### **Chemical structures of the dye-based ligands:**

Triazinyl-based dyes are the most widely used in protein purification (fig. 1.3.a).Cyanuric chloride (1, 3, 5-trichloro-syn-triazine) forms the core structure of the dye. Due to the presence of the chlorine atoms these three carbons become highly susceptible to nucleophilic substitution reactions.<sup>24</sup> Chromophore molecules are easily attached to this molecule to form dichlorotriazinyl dyes. The procion MX (fig. 1.3.b) series is a typical example of this type of

dyes.<sup>110, 111</sup> By further reaction of these molecules with other nucleophilic substituents, monochlorotriazinyl dyes are synthesized. Cibacron<sup>112,113</sup> and Procion H<sup>110, 111, 114</sup> are examples of such dyes (fig. 1.3.c). Two dichlorotriazinyl molecules can be coupled with a bifunctional molecule to form bifunctional triazinyl dyes. Procion H-E is an example of this type of dye (fig. 1.3.d).<sup>114</sup>

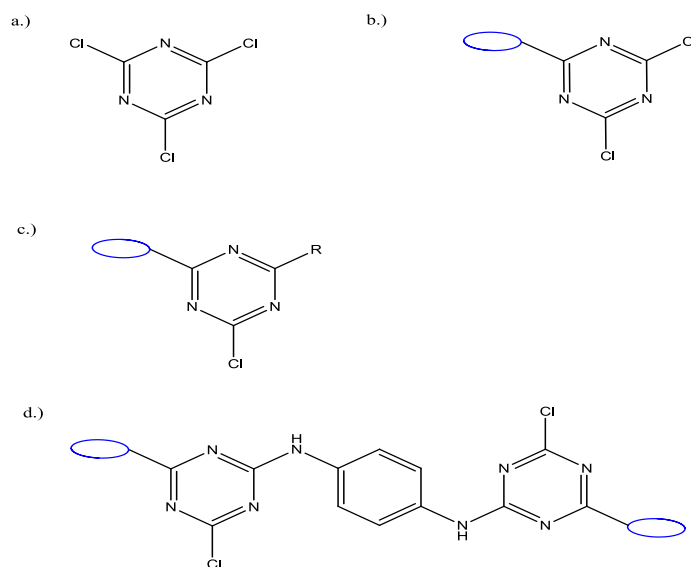


Figure 1.3. Structure of some of reactive dye molecules. a) cyanuric chloride b) Procion MX series c) Cibacron and Procion H d) Procion H-E

The latest development in the dye-ligand affinity chromatography is the use of “biomimetic dyes”.<sup>115</sup> These are synthetic dyes which mimic the structure and binding of natural biological ligands of the targeted protein. These dyes retain advantages of the parent dye but have improved specificity towards the target protein. The first biomimetic dye was prepared by linking benzamidine to the reactive chlorotriazine ring via the diaminomethylbenzene group.<sup>116</sup> It was used for the specific separation of trypsin from the chymotrypsin.<sup>117</sup> Isolation of kallikrein from a crude pancreatic extract and purification of alkaline phosphates from calf intestinal extract are few examples where biomimetic dyes were used for specific purification of the target protein.<sup>118</sup>

**Matrix:**

As discussed in previous sections, an ideal matrix should be stable, have high porosity and fairly large bead size, have functional groups, exhibit minimal nonspecific binding to the biomolecules and hydrophilic. Most commonly used matrices are cross linked agarose beads, cellulose, sephadex, acrylamide gels and controlled pore glass.<sup>71, 72</sup>

**Ligand Immobilization:**

The choice of coupling methods and the reaction conditions depends on both the matrix and the ligand. The least critical regions of the dye should be used for immobilization to ensure minimal interference with the specific interactions between immobilized ligand and the target molecule. As the active sites of the biological molecules are often located deep within the three dimensional structure of the molecule, spacer arms are frequently placed between the matrix and the ligand to ensure their accessibility to the target.

Nonreactive dyes can be coupled to the matrix by usual activation methods. Many reactive dyes are directly immobilized on the matrix by direct reaction between the reactive groups (mainly hydroxyl groups) on the matrix and the dye molecules (through chloride or fluoride atoms) on triazinyl groups.<sup>119-122</sup>

**Loading:**

Before loading, the column is washed with the equilibrating buffer solution, followed by loading of target protein on the column in a buffer solution having same pH and ionic strength as that of the equilibrating buffer solution. The pH and ionic strength of buffer is optimized for each specific case. Usually phosphate buffers are used as they reduce non specific protein-dye-ligand interactions. When the low conductivity buffers are required, MOPS, MES, HEPES or Tris buffers are often chosen. Metal ions ( $Mg^{2+}$ ,  $Ca^{2+}$ ,  $Zn^{2+}$ ,  $Fe^{3+}$ ,

Al<sup>3+</sup> etc.) may be added into the buffers to increase the affinity of the dye-ligand to the target protein, and/or to stabilize the protein molecules in the aqueous media. However, precipitation of the metal ions, which is pH dependent, may cause problems; therefore necessary precautions should be taken into consideration. Temperature is another factor that affects affinity interactions. Therefore, it should be kept constant at the optimum value both at the sorption and elution steps. The linear flow rate of the buffers should be optimized.

There are two protocols that can be followed in the adsorption step. The first one is known as the “positive binding” method. This method involves use of an adsorbent that specifically binds the target protein along with few other contaminating proteins. These contaminating proteins are then flushed out of the column using equilibrating buffer before the elution step. Alternatively, a “negative binding” protocol, in which contaminating proteins are adsorbed on the column preferentially, can be used.<sup>123, 124</sup> Higher target recovery and purity can be achieved in a two step process, in which the protein mixture is passed through a negative binding column, and effluent of this column is then directed to the second, positive binding column.

### **Elution:**

The objective of elution step is to completely elute the desired protein, at the same time minimizing the amount of the contaminating proteins which may be co-eluted. Elution of the bound proteins may be achieved by nonselective or selective processes. In the nonselective elution, pH, ionic strength, or polarity of the elution buffer is changed to elute protein of interest. If the electrostatic interactions are dominant, an increase in pH may be sufficient to elute the bound protein molecules. If the cation exchange is important, a very sharp effect of ionic strength is observed on protein elution.<sup>55</sup> If hydrophobic interactions are predominating, the polarity of eluting buffer can be reduced to promote elution. Chaotropic agents are highly

effective for protein elution.<sup>125</sup> However, chaotropes may cause significant degree of protein denaturation, and therefore they are not recommended to be used at elution step. Chaotropic solutions are effective to remove residual proteins for regeneration of dye-ligand sorbents for repeated use.

In selective elution, the affinity eluants are used, which compete with the dye ligand for the same binding site on the adsorbed target protein. Nucleotide cofactors such as NADP<sup>+</sup>, NADH, ATP and AMP have been used to elute dehydrogenases and other nucleotide dependent enzymes from immobilized Cibacron blue F3GA and other reactive dyes.<sup>126</sup>

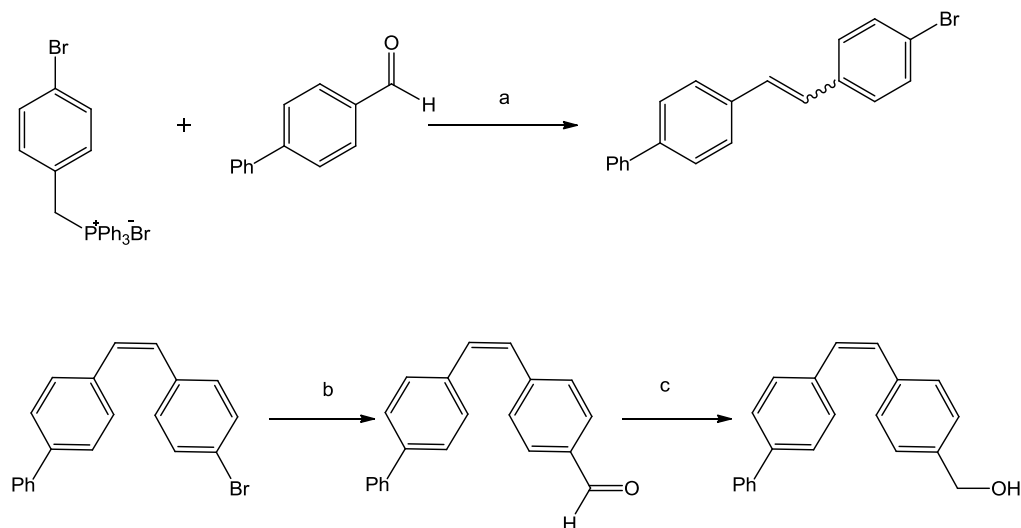
### **1.3 Chemoselective precipitation**

Only a few examples of such chemoselective precipitation are known in literature.<sup>1, 2</sup> Of most prominent examples, precipitation of C<sub>60</sub> with calixarenes and related macrocycles, developed by Atwood and coworkers, serves as a proof of efficiency of such methodology.<sup>3, 4</sup> While being efficient, Atwood's protocol lacks versatility as it is only applicable to a specific pair of substrate and macrocycle, and is not applicable to biological substrates, which must be extracted from the aqueous medium. A precipitation methodology for isolation of non-biological targets has been introduced by Wilcox et al..<sup>127, 128, 129</sup> It will be discussed in detail in the next section.

#### **1.3.1 Precipitons:**

In 2001 Craig Wilcox introduced a new concept of "precipiton" assisted separation of product from a reaction mixture. A "precipiton" is a group of atoms (molecular fragment) that is purposefully attached to a reactant molecule and can be isomerized after the reaction to facilitate precipitation or the phase transfer of the attached product.<sup>5-7</sup> Various studies showed that cis-stilbenes were more soluble than the trans-stilbenes in various organic solvents. This

varying solubility formed the basis for the development of the precipiton.<sup>8</sup> The biphenyl-derived alkenes 3Z and 3E were prepared by Wittig reaction (scheme 1.3).<sup>5</sup>

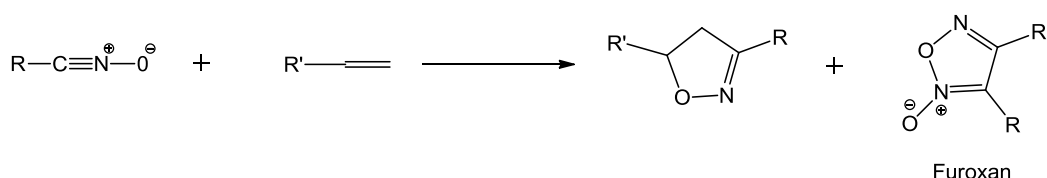


Scheme 1.3. Synthesis of precipiton 3Z. a) KHMDS, THF,  $-78^{\circ}\text{C}$ , 81%; b) 1. *t*BuLi, THF,  $-78^{\circ}\text{C}$ ; 2. DMF,  $-78-0^{\circ}\text{C}$ , 97%; c)  $\text{NaBH}_4$ , EtOH,  $0^{\circ}\text{C}$ , 98%

Alkene 3Z was freely soluble in common organic solvents such as EtoAc, THF,  $\text{Et}_2\text{O}$ ,  $\text{CH}_2\text{Cl}_2$ ,  $\text{CHCl}_3$  and  $\text{C}_6\text{H}_5\text{CH}_3$  while 3E isomer was virtually insoluble in all those solvents. Before using these auxiliary groups for isolating products, various isomerization conditions such as photochemical methods (with or without sensitization),<sup>130</sup> isomerization using diphenyl disulfide<sup>131</sup> and isomerization using iodine with benzoyl peroxide under illumination by a sun lamp were examined. However, photochemical methods were not satisfactory as the reactions were slow and side products were generated during the course of reaction. In contrast, the last two methods were very effective and afforded excellent yields of precipitated products.

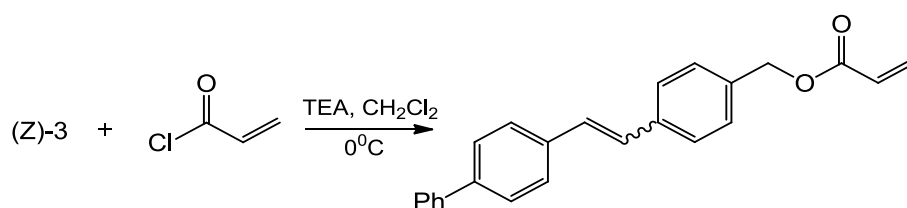
### Isolation of Isoxizolines using Precipitons:

Isoxazolines are a class of compounds synthesized by [3+2] cycloaddition reaction between alkenes and nitrile oxides (scheme 1.4).<sup>132</sup> Furoxans, formed by the dimerization of nitrile



Scheme 1.4. A general scheme for the synthesis of isoxazolines by [3+2] cycloaddition reaction between alkenes and nitrile oxides.

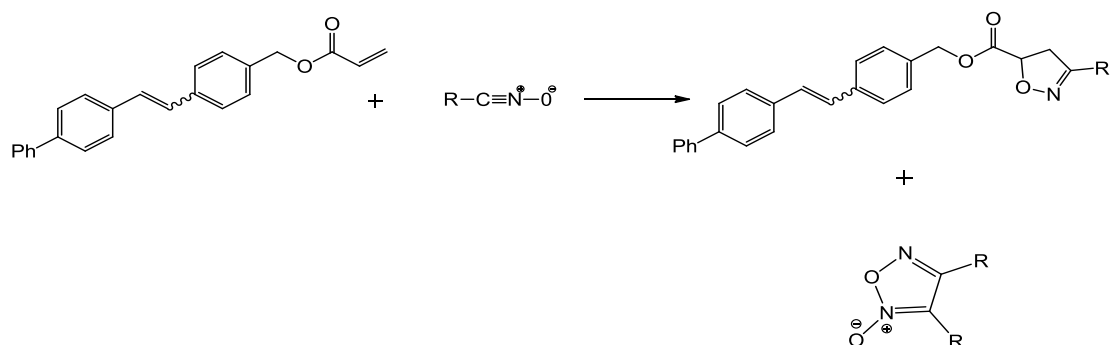
oxides, are troublesome byproducts and condition worsens when the excess of nitrile oxide is required to push the reaction to completion.<sup>133</sup> Flash column chromatography is used to purify the isoxazoline product. Wilcox et al. hypothesized and successfully used precipitons for the isolation of isoxazolines from furoxan by product. To do so, first several alkenoates were attached to precipiton 3Z by an ester linkage (scheme 1.5).



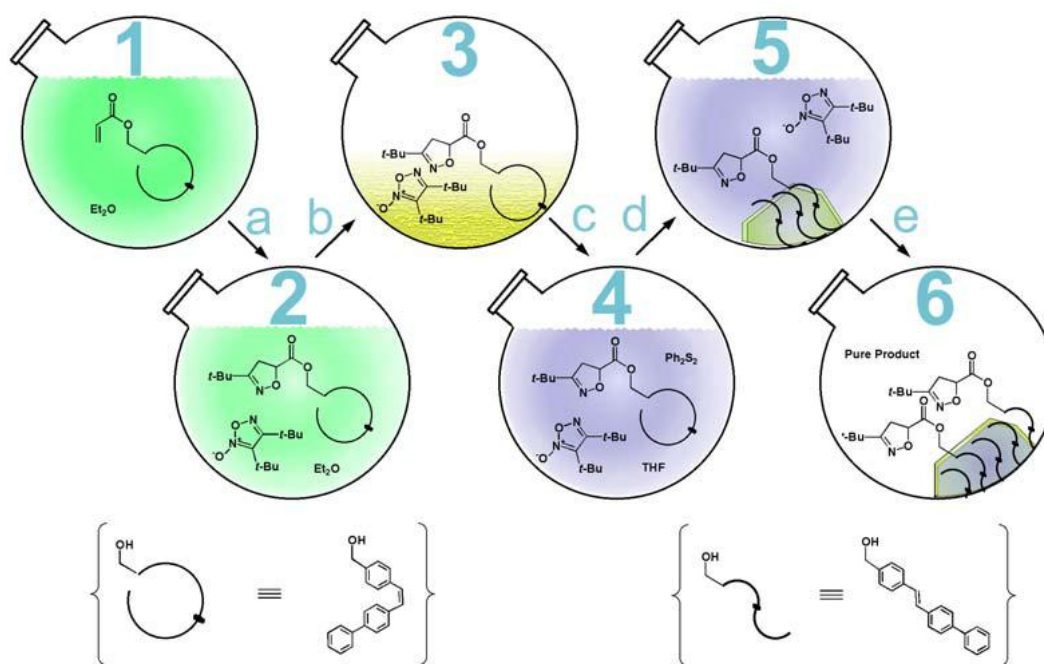
Scheme 1.5. Synthesis of precipiton bound alkene substrate for cycloaddition with nitrile oxide.

These were then subjected to cycloaddition with nitrile oxides in diethyl ether (scheme 1.6). After the reaction, the reaction mixture was washed with water and volatile components were removed. This residue was then dissolved in THF and Z/E isomerization of the precipiton auxiliary was induced by adding diphenyl disulfide and heating the solution. The solvent was removed after isomerization, the crude residue obtained was washed with Et<sub>2</sub>O, MeOH, or hexanes to remove any by product, and sparingly soluble pure products were isolated by

filtration. Precipiton-bound products were isolated in good yields and high purity (scheme 1.7).



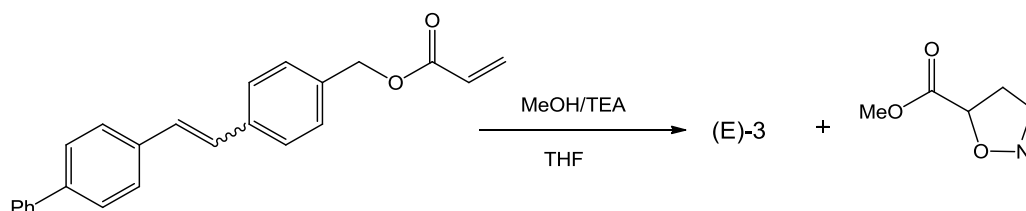
Scheme 1.6. A general scheme for the synthesis of precipiton bound isoxazoline product by [3+2] cycloaddition reaction between precipiton bound alkenes and nitrile oxides.



Scheme 1.7. Illustration of the “precipiton” process for isoxazoline isolation. a) A solution of tert-butyl nitrile is added to an ethereal solution of precipiton bound alkene. b) The  $Et_2O$  is removed to afford a crude residue. c) The crude residue is diluted with THF and one equivalent of diphenyl disulfide was added. d) The solution is heated at reflux to cause isomerization and product precipitation. e) The THF is removed and the solid is washed with hexanes,  $Et_2O$ , or methano; to afford clean solid.



Finally, precipiton was cleaved from the product by methanolytic transesterification in THF by methanol/triethylamine (scheme 1.8). The resulting methyl ester isoxazolines were obtained in high yields and purities.

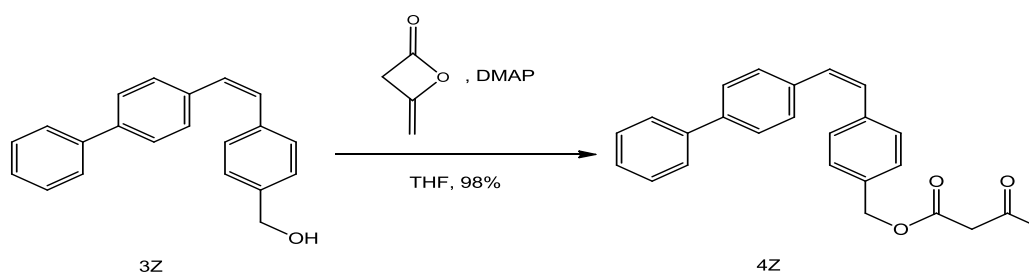


Scheme 1.8. Methanolytic cleavage of the precipiton bound product to furnish precipiton E-3 and methyl ester of desired product.

### Precipiton-assisted isolation of $\alpha$ -substituted $\beta$ -ketoesters:

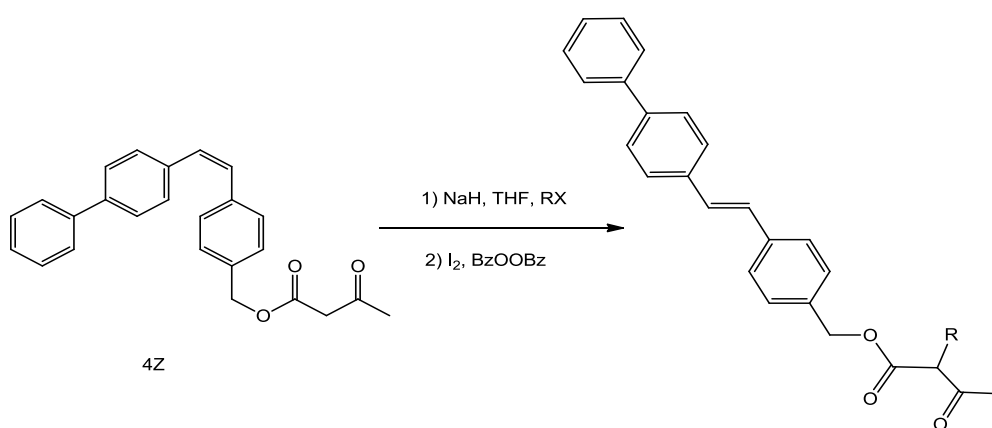
In order to demonstrate the usefulness and further extend the scope of precipiton method in separations technology, Wilcox et al. used precipitons in the separation of  $\alpha$ -substituted  $\beta$ -ketoesters.<sup>129</sup> These are the family of compounds which serve as useful intermediates in the preparation of heterocyclic compounds<sup>134</sup> and can also be chemoselectively and diastereoselectively reduced to form aldol-type products.<sup>135</sup>

Acetoacetate ester 4Z was prepared by treatment of 3Z with diketene and catalytic amount of DMAP (scheme 1.9).



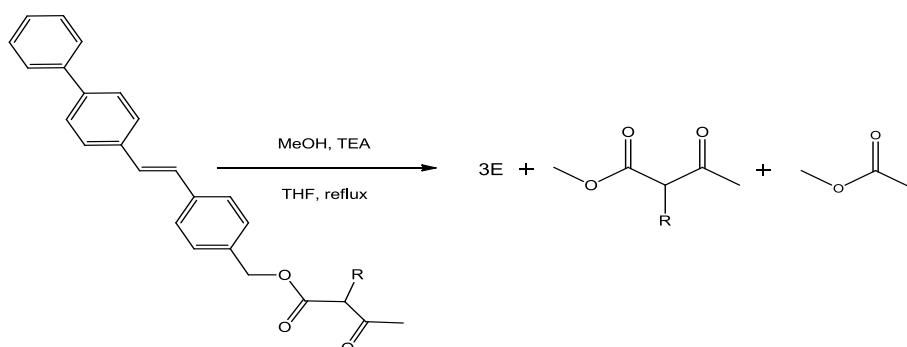
Scheme 1.9. Acetoacetate ester 4Z was synthesized by reacting precipiton 3Z with diketene in the presence of catalytic amount of DMAP.

The  $\beta$ -ketoester 4Z was deprotonated with sodium hydride to generate the enolate, which was then treated with an excess of alkylating agent. Upon completion of alkylation, the reaction mixture was partitioned between EtOAc and aqueous  $\text{NH}_4\text{Cl}$ . The organic layer was evaporated and residue was dissolved in  $\text{Et}_2\text{O}$  or  $\text{CCl}_4$  containing  $\text{I}_2$  and benzoyl peroxide to cause isomerization. Further work-ups and trituration of crude in ether, hexanes or methanol resulted in isolation of precipiton bound product in good yields and purities over 95% (scheme 1.10).



Scheme 1.10. Synthesis and isolation of precipiton bound product. 1) Alkylation of 4Z to afford precipiton bound product. 2) Isomerization of reaction crude to yield precipiton bound product.

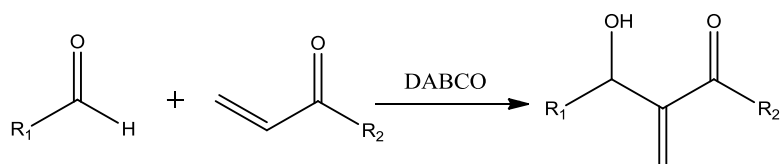
The precipiton was then cleaved by methanolysis ( $\text{MeOH}/\text{TEA}$  in  $\text{THF}$ , reflux 1-2 h) (scheme 1.11). This furnished the methyl  $\beta$ -ketoesters in good yields and high purities.



Scheme 1.11. Methanolytic removal of precipiton to give free product.

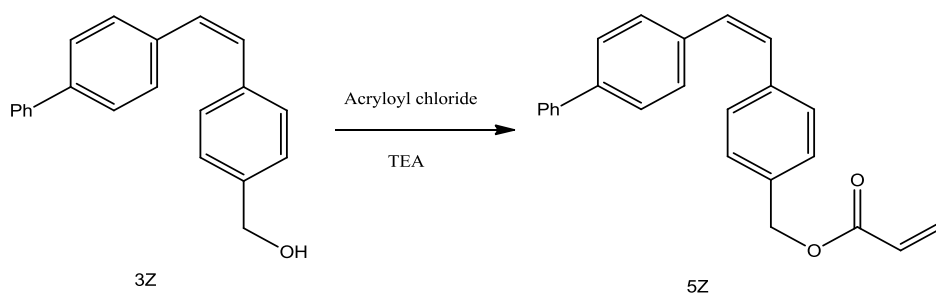
### Precipiton assisted purification of Baylis-Hillman adducts:

The Baylis-Hillman reaction is a C-C bond forming reaction between an activated alkene and an aldehyde in the presence of a tertiary amine, tertiary phosphine, or chalcogenide (scheme 1.12).<sup>136</sup> To push the reaction to completion one of the components must be used in excess,<sup>137</sup> which, in turn, will require purification of the product by column chromatography. However, the precipiton approach provides the liberty to use excess of one of the reactants without having to run a column for purification.



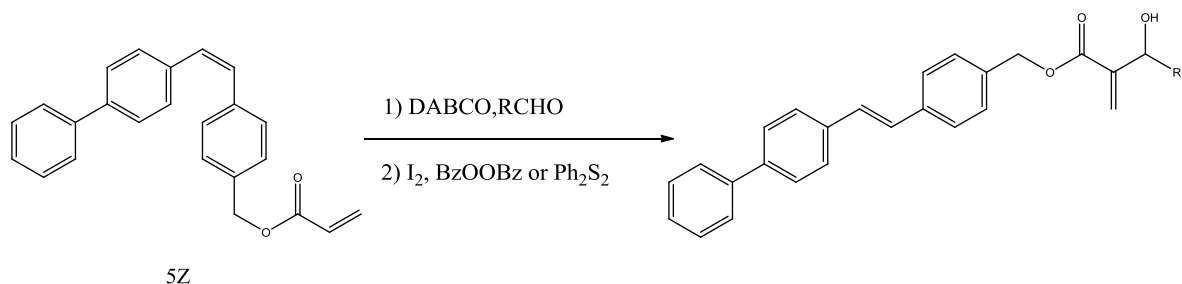
Scheme 1.12. A general scheme for the synthesis of Baylis-Hillman product by reaction of an aldehyde with an activated alkene.

Acrylate 5Z was prepared by treatment of 3Z with acryloyl chloride in the presence of triethyl amine (scheme 1.13). The acrylate 5Z was treated with catalytic amount of



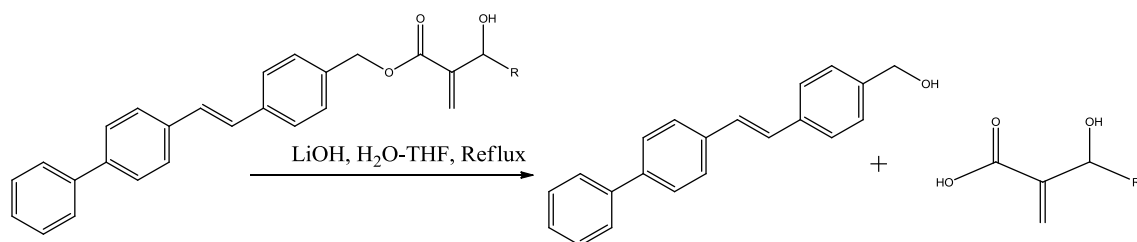
Scheme 1.13. Synthesis of precipiton acrylate 5Z by reacting precipiton 3Z and acryloyl chloride in the presence of TEA

DABCO and excess of aldehyde at room temperature.<sup>138</sup> Upon completion of the reaction of the reaction the crude mixture was diluted with a suitable solvent and treated with I<sub>2</sub> and dibenzoyl peroxide or PhSSPh. Various work-ups and trituration with hexanes, ether, or MeOH resulted in precipiton bound Baylis-Hillman product in good yields and high purity (scheme 1.14).



Scheme 1.14. Synthesis and isolation of precipiton bound product. 1) Reaction of 5Z with aldehyde in the presence of catalytic amount of DABCO to furnish precipiton bound product. 2) Isomerization of reaction crude to yield pure precipiton bound product.

hydrolysis (LiOH in THF-H<sub>2</sub>O). The acids were isolated by filtration of the insoluble precipiton, acidification of the solution, followed by extraction with EtOAc. Removal of the EtOAc furnished the desired acid in good yields and purities of  $\geq 95\%$  (scheme 1.15).



Scheme 1.15. Hydrolysis of precipiton bound product in the presence of LiOH in H<sub>2</sub>O-THF to afford precipiton and product

#### 1.4 Cyclen based receptors for pyrene dyes and their use in separation technology

In 2005 our group synthesized a cyclen based receptor.<sup>9</sup> This receptor had a macrocyclic structure and was comprised of four naphthylthiourea groups tethered to a cyclen core via an ester linkage (fig. 1.4). This receptor showed very strong and very specific affinity for the

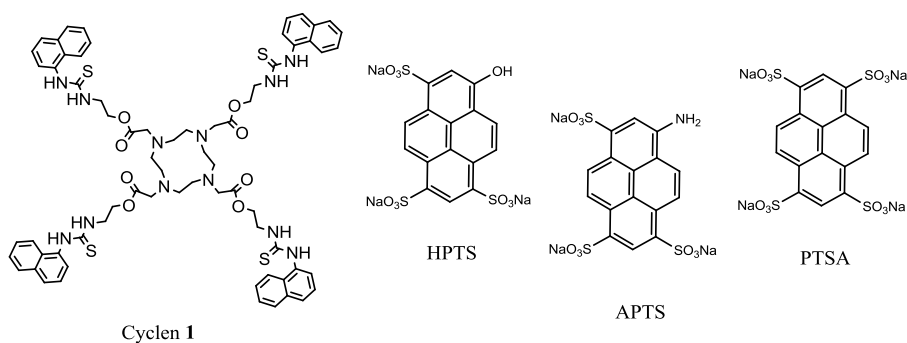
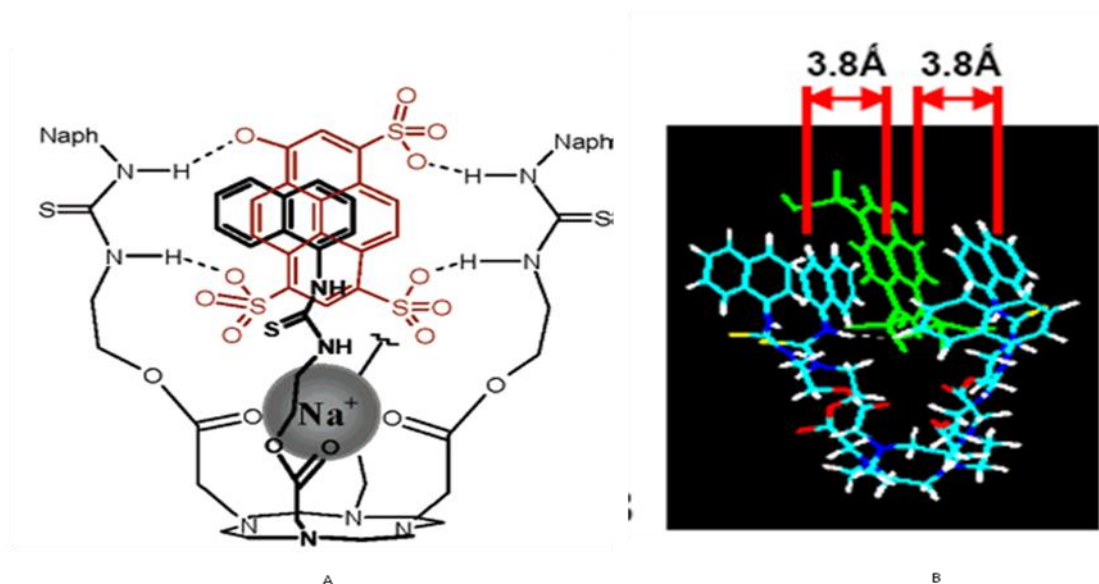


Figure 1.4. Structure of cyclen 1, HPTS, APTS and PTSA dyes.

pyrene based dyes (HPTS, APTS, PTA) (fig. 1.4) under physiological conditions. Upon interaction with the dye, the receptor formed an insoluble complex which had micromolar stability ( $K_a \cdot 10^{-6}$ ), and the complex formation resulted in quenching of the dye fluorescence. Isothermal calorimetry (ITC) and molecular mechanics simulation identified  $\pi$ -stacking between the aromatic units of the receptor and the planar core of the dye as the major driving force for the complex formation (scheme 1.16).



Scheme. 1.16. A) Envisioned binding mode for cyclen 1 and HPTS dye. The backside thiourea unit of cyclen 1 is truncated for clarity. This representation is given for pictorial purpose only. B) Structure of cyclen 1-HPTS complex optimized by molecular mechanics (AMBER) simulations in the water box. Water molecule omitted for clarity.

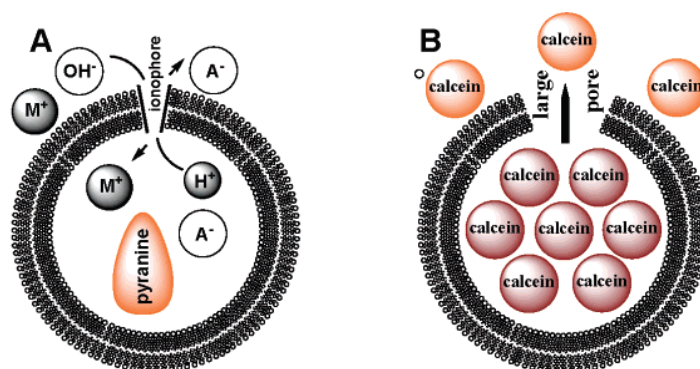
Since this receptor-dye pair formed an insoluble complex of micromolar stability upon interaction, we decided to use this receptor-dye pair in developing a new separations technology. We reasoned that if the substrate of interest can be attached to the dye, this dye-substrate conjugate then can be selectively precipitated from the reaction mixture by adding receptor in the reaction mixture. Alternatively, if this mixture is passed through a column carrying immobilized receptor on the solid support, the labeled substrate can be selectively purified. We hypothesized that this receptor-dye pair can be used in the selective separation of substrate by chemoselective precipitation as well as by affinity chromatography. This work is discussed in detail in the following chapters.

## Chapter 2

### Synthesis of cyclen-based receptors for pyrene dyes

#### 2.1. Introduction

In 2005, Winschel et al. were trying to develop a new biomembrane leakage assay,<sup>139</sup> as the current assays had some inherent shortcomings. The liposome-based pH-stat fluorometric assay is an assay routinely used for identification of physiologically relevant ionophores.<sup>140, 141</sup> In the context of this discussion, ionophores are the compounds that assist in the transport of ions across cell membranes. In this assay, a controlled amount of the base and potential ionophore is added to a suspension of liposomes containing a pH-sensitive dye, 8-hydroxypyrene-1,3,6-trisulfonate (HPTS, pyranine),<sup>142-144</sup> or sometimes fluorescein.<sup>145</sup> The resulting pH gradient across the bilayer membrane causes the efflux of hydronium ions and builds up an electrostatic potential. This potential can be compensated by the efflux of anions or influx of cations. If the compound of interest mediates such ion transport, the efflux of hydronium ions continues altering the intravesicular pH and the fluorescence of the reporter dye. The kinetic trace obtained from the dye response thus reflects the ionophoretic activity of the studied compound.



Scheme 2.1. A) pH-Stat experiment; B) Membrane leakage assay

While being rapid and reliable, the pH stat assay provides little information on the mechanism of ion transport.<sup>146</sup> A membrane leakage assay addresses some mechanistic aspects by distinguishing selective ion transport from nonslective leakage through oversized pores.<sup>147, 148</sup> This assay utilizes the ability of calcein or carboxyfluorescein (CF) dyes to self-quench their fluorescence emission at ~100 mM concentration.(ref) In a typical experiment, a set of large unilamellar vesicles (LUVs) containing the concentrated dye is challenged with the compound of interest. In the case of selective ion transport, little change in fluorescence is observed, whereas the larger pore formation results in the dye release, its subsequent dilution, and emission increase. However, this assay requires high concentration of the dye (100 mM) and at such a high concentration the membrane properties could be altered, as well as the buffer capacity, and interactions of the dye with ionophore become possible. Another assay used to detect endovesiculation requires high concentration (40mM) of quencher p-xylene-bis-pyridinium bromide (DPX) (fig. 2.1).<sup>149</sup> In such high concentrations DPX has been reported to affect the fluidity of negatively charged membranes, to alter the size of large unilamellar vesicles (LUVs), and to lower the bilayer phase transition temperatures.<sup>150</sup> As a result, both above mentioned assays cannot deliver an accurate picture of the effects produced by the ionophore on the biological membrane.

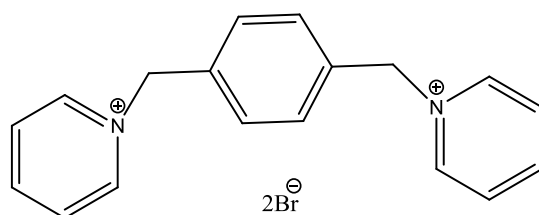


Figure 2.1. Structure of DPX.

Therefore, we hypothesized that a compound capable of selective binding to the HPTS at micromolar concentrations, impermeable to the bilayer membrane, and capable of quenching HPTS fluorescence would provide the basis for improved assays. This led to the synthesis of



cyclen **1** receptor which binds to HPTS and quenches its fluorescence at micromolar concentrations under physiological conditions. To gain more information on the thermodynamics of the complexation process, a series of isothermal titration calorimetry (ITC) experiments were performed. ITC is a quantitative technique that can directly measure the enthalpy ( $\Delta H$ ) of binding event, whereas the binding affinity ( $K_a$ ) and, subsequently, the free energy ( $\Delta G$ ) can be calculated through the fitting of the titration data into the binding isotherm. The last thermodynamic parameter, entropy ( $\Delta S$ ), can be calculated through the subtraction of the free energy of binding from the enthalpy. The stoichiometry of the complex formation can be accessed from the appearance of the binding isotherm. As a result, all important thermodynamic parameters can be obtained from a single ITC experiment.

In the case of ITC titration of the solution of HPTS with the solution of cyclen **1**, the formation of two distinct types of complexes was observed (fig. 2.2.A and 2.2.B). The assessed thermodynamic data for these complexes are summarized in Table 1. The first complex shows 1:1 stoichiometry, whereas the second complex corresponds to the overall 1:4 HPTS/cyclen **1** stoichiometry. These two complexes have different strengths and are driven by different thermodynamic forces. The originally formed 1:1 complex is 2 orders of magnitude stronger than the subsequently formed 1:4 complex. Whereas the formation of the 1:4 complex is an enthalpically driven process, the 1:1 complex formation is almost entirely an entropically driven process. The entropically driven 1:1 binding is consistent with the solvophobic effect most likely accompanying  $\pi$ - $\pi$  rather than hydrogen-bonding or electrostatic interactions.<sup>151</sup> A much weaker 1:4 complex formation is a mostly enthalpically driven process accompanied by a smaller positive entropy change. This second complexation step is probably due to the electrostatic and/or hydrogen-bonding interactions of cyclen **1** molecules with the initially formed 1:1 complex. Although the solvophobic effect plays a role in the 1:4 complex formation as well, the diminished entropy change likely stems from the

decrease in the degrees of freedom for the large aggregate formed from several molecules. Noteworthy, no additional inflection points between 1:1 and 1:4 pyranine/cyclen **1** ratios were observed in the ITC plot, suggesting that the second binding process proceeds via a concerted cooperative mechanism.

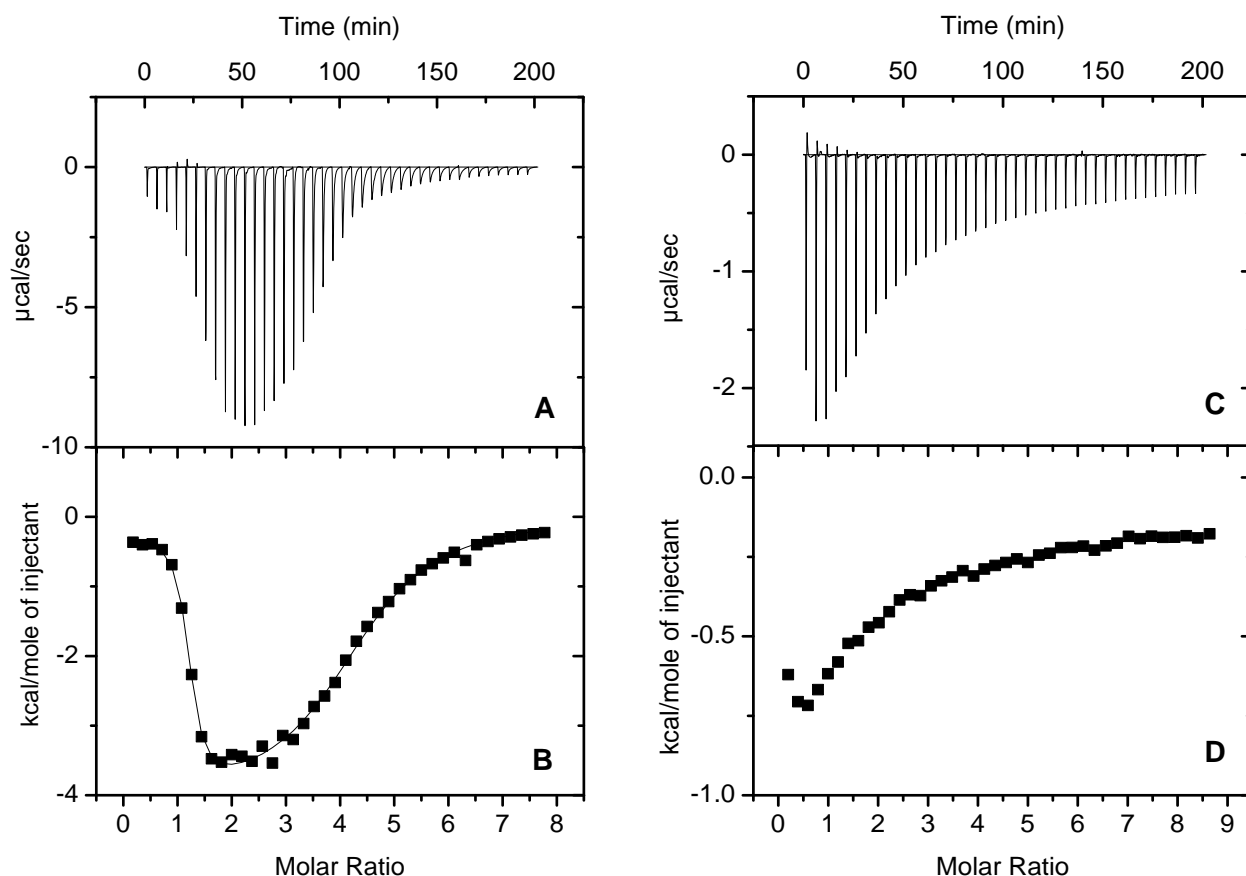


Figure 2.2. Microcalorimetric characterization of interactions of cyclen **1** with pyranine and calcein in methanol. (A) Raw data for the titration of a 0.25 mM solution of HPTS with a 10 mM solution of cyclen **1**. (B) Integrated data from (A), corrected by the heat of cyclen **1** dilution, normalized to moles of injectant and plotted as a function of cyclen **1**/pyranine ratios (solid squares). A continuous line represents the data fit in two sets of sites binding model. (C) Raw data for the titration of a 0.25 mM solution of calcein with a 10 mM solution of cyclen **1**. Note the difference in vertical scales for plots (A) and (C). (D) Integrated data from (C), corrected by the heat of cyclen **1** dilution, normalized to moles of injectant and plotted as a function of cyclen **1**/calcein ratios.

Table 2.1. Thermodynamic Parameters Assessed for the Complexation of Pyranine with Cyclen **1** in Methanol

N	$K_a(M^{-1})$	$\Delta G(kcal/mol)$	$\Delta H(kcal/mol)$	$T\Delta S(kcal/mol)$
$1.28 \pm 0.014$	$(3.16 \pm 0.75) \times 10^6$	$-8.87 \pm 0.17$	$-0.41 \pm 0.05$	8.47
$3.57 \pm 0.050$	$(1.46 \pm 0.12) \times 10^4$	$-5.68 \pm 0.05$	$-3.87 \pm 0.08$	1.81

The specificity of the cyclen **1** towards the HPTS dye was further established by the lack of interaction of cyclen **1** with fluorescein-related dyes (fig. 2.3). These dyes are negatively charged and have aromatic cores like HPTS dye, however, these dyes are not planar as the benzene ring is tilted out of plane of the second aromatic unit. The  $\pi$ -stacking of these cores with the aromatic units of the cyclen **1** was not expected to be efficient, and indeed, the ITC titrations of calcein with cyclen **1** showed no apparent binding except protonation of the basic receptor with the acidic dye (fig. 2.2.C and 2.2.D). These experiments prove that the planar aromatic core of the dye is essential for its recognition by cyclen **1**.

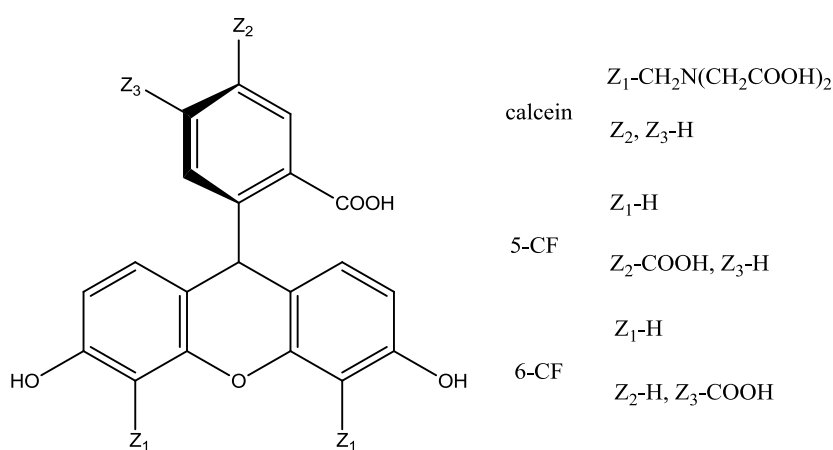


Figure 2.3. Structure of various fluorescein dyes.

## 2.2. Structure-activity relationship studies

The original receptor cyclen **1** was comprised of four naphthylthiourea groups tethered to a cyclen core via ester linkages (fig. 1.4 structure of cyclen **1**). This tetrafold macrocyclic structure of cyclen **1** with multiple functional groups placed into the specific positions was essential for HPTS recognition, as established by the results of various structure-activity studies. In the first study, the acyclic naphthyl thiourea **2** (fig. 2.4.A), which mimics the structure of a single arm of cyclen **1**, was titrated into the solution of HPTS instead of cyclen **1**. This arm replica did not bind the dye to any measurable extent, proving the necessity of the

macrocyclic arrangement of the receptor for the dye recognition. Another study indicated that ester linkers are essential for the binding as ester groups coordinate to the physiologically-abundant  $\text{Na}^+$  ion and bring the four arms closer to each other which further assists in the complexation of the dye.<sup>152, 153</sup> Indeed, when receptor **3** (fig. 2.4.B) lacking ester linkages was used for HPTS binding, a 15-fold decrease in  $K_a$  values was observed compared to the cyclen **1**. This hypothesis was further supported by a three-fold drop in cyclen **1** affinity to HPTS in  $\text{Na}^+$ -free buffer. In another study, **NH-Boc** synthetic precursor (fig. 2.4.C) showed no noticeable binding affinity to HPTS. This proved essentiality of the thio(urea) functionality as well as the terminal aromatic units for the recognition of the dye by the receptor. All these studies proved beyond any doubt that the receptor having a macrocyclic structure and specifically placed functional groups is essential for the recognition of the dye by the receptor.

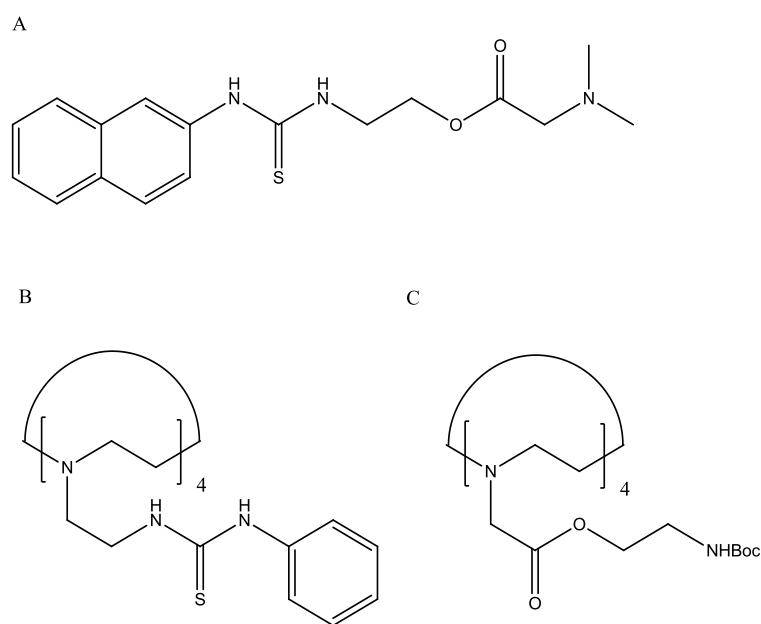


Figure 2.4. Structure of compounds used in structure and activity studies. A) acyl naphthyl thiourea **2** B) receptor **3** C) **NH-Boc** synthetic precursor

### 2.3. Synthesis of new receptors

The results of various structure and activity studies shed light on some interesting facts regarding necessity of macrocyclic structure of the receptor for the dye recognition. We further decided to explore the effects of structure of the receptor on its ability to bind the dye. The effects of various substituents on the aromatic unit of the receptor were not studied previously. Hence, a series of receptors having different X and R groups as shown in fig. 2.5 were synthesized and their fluorometric titrations were carried out to determine their affinity towards pyranine dye.

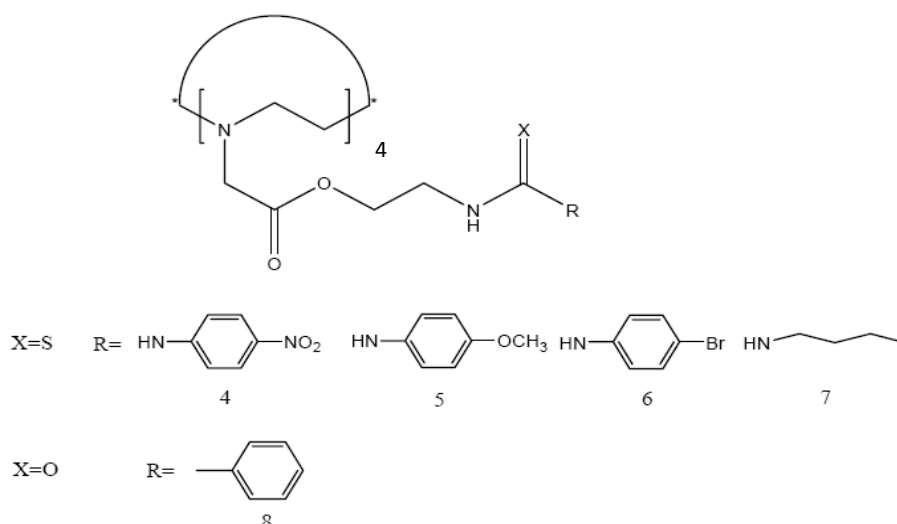
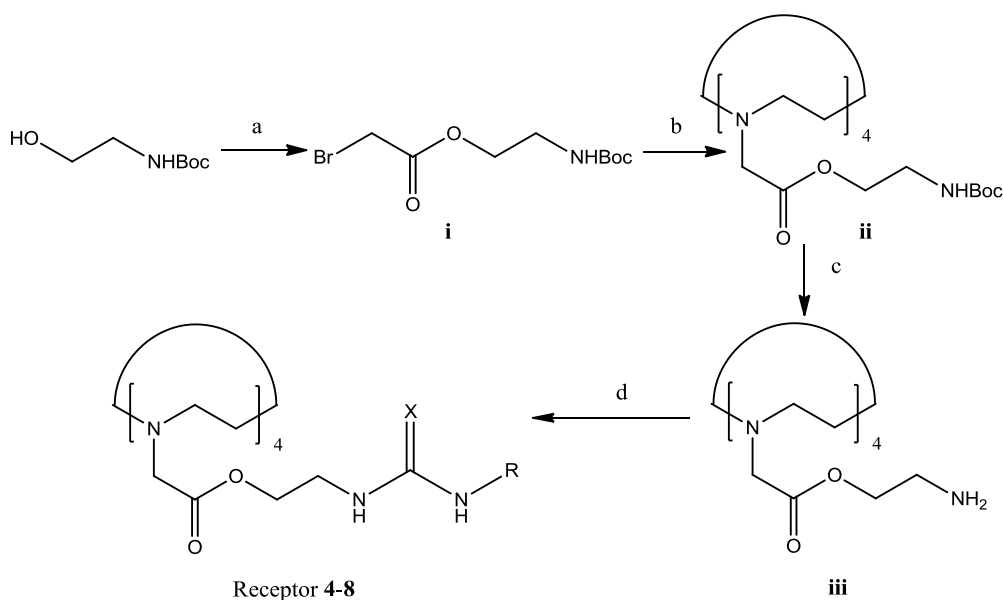


Figure 2.5: Structure of various receptors synthesized having different X and R groups

Receptors **4-8** were synthesized according to scheme 2.2. The synthesis began with N-Boc-ethanolamine, which underwent a substitution reaction with bromoacetyl bromide to give compound **i** (step a) in 90% yield. The compound **i** was then subjected to substitution reaction with the cyclen to afford compound **ii** (step b) in 56% yield. We call compound **ii** as the precursor, as it was used to synthesize all the receptors **4-8**, by reacting it with various isothiocyanate compounds. Subsequent deprotection of the precursor with trifluoroacetic acid (TFA) furnished compound **iii** (step c) in 100% yield. The compound **iii** was used without

any purification in the synthesis of receptors **4-8**. The compound **iii** was subjected to addition reaction under basic conditions with various isothiocyanate to furnish receptor **4-7** and reacted with benzoyl chloride to yield receptor **8** in yields ranging from 22-76% (step d).



Scheme 2.2. a) Bromoacetyl bromide, Et<sub>3</sub>N, CH<sub>2</sub>Cl<sub>2</sub>, rt, 5 hrs, 90%; b) cyclen, CH<sub>3</sub>CN, rt, 72 hrs, 56%; c) TFA/CH<sub>2</sub>Cl<sub>2</sub>, rt, 6 hrs; d) RNCX, i-PrOH/EtOH or THF, Et<sub>3</sub>N or i-Pr<sub>2</sub>EtN, 6-48 hrs, 22-76%

## 2.4. Fluorometric titrations and results

The receptors **4-8** synthesized according to the scheme 2.1 had different **X** and **R** groups. The receptors **4-7** have thiourea tethers but they have different **R** groups on the aromatic moieties. The receptor **3-5** varied in the electronic nature of the substituent group attached to the aromatic ring e.g. receptor **4** had an electron-withdrawing nitro group on the aromatic ring, receptor **5** was bearing an electron-donating methoxy group on the aromatic ring and receptor **6** had a weakly electron-withdrawing bromine atom on the aromatic unit. The receptor **7** lacked the aromatic unit and had an n-butyl group attached to the thiourea group instead. The receptor **8** had an amide group instead of thiourea group. In order to understand the effect of these different groups on the binding ability of the receptor, fluorometric titrations were carried out. In a typical experiment, an aqueous solution (2 mL) containing 50 nM HPTS, 100

mM NaCl, 10 mM  $\text{Na}_x\text{H}_{3-x}\text{PO}_4$  ( $x = 1, 2$ ; pH 6.4) was placed in a thermostated spectrophotometric cell set at 25°C. The solution was gently stirred during the experiment. Prior to the spectrometric recording, 20 $\mu\text{L}$  of 25-5000  $\mu\text{M}$  solution of receptors **4-8** in DMSO were added to the cell giving the final concentration of the receptors in the range of 2.5-500  $\mu\text{M}$ . The emission spectra were then recorded with the excitation wavelength of 405 nm. The emission maxima at 510 nm were monitored. Binding constant and the maximum emission loss with the confidence interval values were then computed (table 2.2) using a homemade nonlinear regression curve fitting program.

Table 2.2. Binding constants and maximum fluorescence loss assessed for the complexes of HPTS with cyclen based receptors from Fluorometric titrations in PBS

Receptor	cyclen <b>1</b>	<b>4</b>	<b>5</b>	<b>6</b>	<b>7</b>	<b>8</b>
$K_a$ ( $\text{M}^{-1}$ )	$(2.6 \pm 0.3) \times 10^6$	$(7.2 \pm 0.8) \times 10^6$	$(9.0 \pm 1.2) \times 10^6$	$(4.2 \pm 0.8) \times 10^6$	Not determined	No interaction
$I_{\text{rel}}^{\text{max}}$ loss (%)	$90.9 \pm 1.6$	$98.5 \pm 2.3$	$77 \pm 1.1$	$93.3 \pm 3.1$	Variable	0

The receptors **4** and **6** featured strong and weak electron-withdrawing groups respectively, and their affinity to HPTS was higher than that of cyclen **1** as indicated by their respective  $K_a$  and  $I_{\text{rel}}^{\text{max}}$  loss values. Receptor **4** with the strong electron-withdrawing nitro group turned out to be the most efficient receptor in terms of the fluorescence quenching. HPTS dye is negatively charged due to the presence of three sulfonate groups and an OH group with low  $\text{p}K_a$ . The electron-withdrawing groups remove electrons from the aromatic ring of the receptor's arms, making them electron-depleted, which in turn resulted in a stronger  $\pi$ -stacking of the receptor with the negatively charged HPTS dye.

Interestingly, receptor **5**, bearing an electron-donating methoxy groups on the aromatic ring, has also shown an increase in the affinity towards HPTS. While we didn't have an exact explanation for this observation, we speculated that the receptor **5** has a higher affinity to  $\text{Na}^+$  cation, which was essential for the proper arrangement of the receptor binding arms. Since

the actual affinity of ester groups to  $\text{Na}^+$  is not very high,<sup>152, 153</sup> a certain portion of receptor molecules always remain uncoordinated and hence less efficient in terms of HPTS binding. In case of receptor **5**, such a portion of molecules was lower than that for the cyclen **1**, and more efficient apparent binding of the receptor **5** could be due to this more efficient  $\text{Na}^+$  coordination. Although plausible, this explanation is a mere speculation as the further investigation of the observed phenomenon was beyond the scope of this study.

Receptor **7** showed variable fluorescence quenching at various concentrations which suggested that a complex binding mechanism was in operation. One possible explanation is a formation of complexes of a various stoichiometries. We have already seen two types of complexes in case of HPTS and cyclen **1** binding (1:1 and 1:4). As the receptor has four binding arms and HPTS has six binding sites (four sulfonates and two faces of aromatic core), it is plausible that a series of complexes ranging from 6:1 (one dye and six receptor molecules) to 1:4 (one receptor and four dye molecules) can be formed. In all these complexes, the electronic environment of the dye is different which results in different extent of quenching. This is in line with the observed variation in the quenching extent as the receptor concentration was increased in titration series (fig. 2.6).

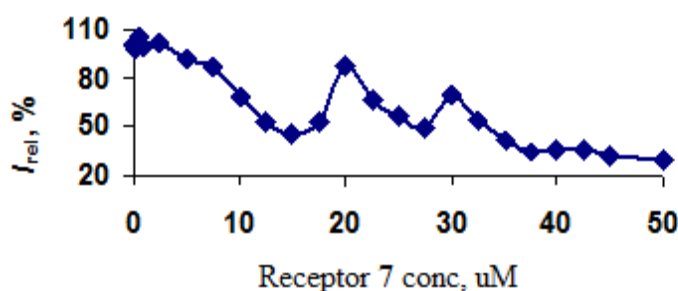


Figure 2.6. Fluorometric titrations of 50 nM PBS solution of HPTS with receptor **7**. Experimental data is normalized to the percentage of unbound dye fluorescence



Receptor **8** had amide linkages in the place of thio(urea) linkages of the receptors **1-7**, and it did not show any binding to the HPTS dye. This observation signifies the importance of thio(urea) group for the dye recognition by the receptor.

## 2.5 Conclusions

Receptor **4** and **6** with electron-withdrawing substituents were the better receptors, signifying the importance of  $\pi$ -stacking in the complexation process. The highest  $K_a$  value observed for the receptor **5** and lower quenching was somewhat intriguing and no exact explanation was possible for its complexation behavior. Receptor **7** with butyl groups showed variable quenching extent in the titration series, attributable to the formation of several complexes with different stoichiometries. Receptor **8** lacking the thio(urea) group did not bind the dye, showing the essentiality of these groups for HPTS recognition.

## Chapter 3

### Chemoselective Precipitation of Lactose from a Lactose/Sucrose Mixture:

#### Proof of Concept for a New Separation Methodology

##### 3.1 Introduction

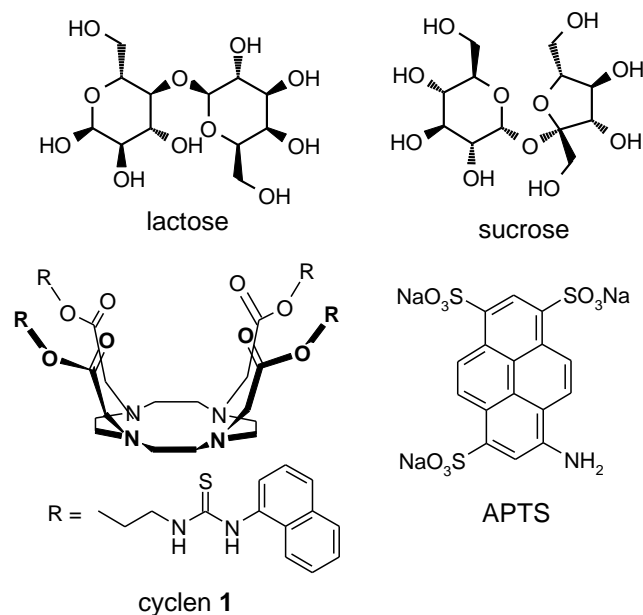
Affinity chromatography,<sup>154, 155, 156, 157</sup> immunoprecipitation<sup>158, 159, 160</sup> and electrophoresis<sup>161, 162, 163</sup> remain the most common purification techniques for biological targets. Although the efficiency of these techniques has advanced to a level where virtually any biological substrate can be isolated in pure form, large scale purification of such substrates is cost-prohibitive.<sup>164, 165</sup> Furthermore, nearly all techniques, except for immunoselective precipitation,<sup>166</sup> require a substantial excess of gel matrices or solid phase, which may pose environmental problems in association with large scale purifications. On the other hand, non-specific precipitation techniques such as protein salting out<sup>167, 168</sup> or precipitation with glycine or trichloroacetic acid<sup>169</sup> do not require excessive amounts of reagents yet they provide rapid large-scale isolation of crude mixtures of proteins. Obviously, such precipitation methods show little selectivity as they rely on non-specific desolvation of proteins that are present in the mixture. A precipitation methodology that does not require excessive amounts of components, yet is capable of targeting specific functional groups that are present or introduced into the substrate, may become a valuable addition to both highly selective microscale separations and nonselective large scale separation techniques.

To our surprise, only a few examples of such chemoselective precipitation are known in literature<sup>1, 2</sup> Of most prominent examples, precipitation of C<sub>60</sub> with calixarenes and related macrocycles, developed by Atwood and coworkers, serves as a proof of efficiency of such methodology.<sup>3, 4</sup> While being efficient, Atwood's protocol lacks versatility as it is only applicable to a specific pair of substrate and macrocycle, and is not applicable to biological

substrates, which must be extracted from the aqueous medium. A precipitation methodology for isolation of non-biological targets has been introduced by Wilcox et al.<sup>127, 128, 129</sup> In this methodology, a substrate of interest is allowed to react with a “precipiton”: an auxiliary stilbene-based molecule, solubility of which can be modulated by isomerization from highly soluble *cis*-form to insoluble *trans*-form. After the reaction, the conjugate is converted into insoluble form, the precipitate is collected, and the substrate is recovered through solvolysis. This methodology is applicable to isolation of lipophilic compounds, however, it cannot be used for separations of highly polar biological substrates due to the reaction conditions that require organic solvents of low polarity.

While our new methodology utilizes purification approach similar to that described by Wilcox, this methodology is developed for aqueous medium and therefore especially suitable for isolation of biological substrates.

Recently, we identified a family of artificial cyclen-thiourea receptors that form complexes with pyrene-based dyes under near-physiological conditions.<sup>9, 170</sup> These complexes feature micromolar stability and diminished solubility in water and methanol compared to the intrinsic solubility of the dye and receptor alone.<sup>9</sup> More interestingly, the cyclen-based artificial receptors were highly selective for the pyrene scaffold, while at the same time tolerating considerable structural variations in peripheral positions on the dye. We reasoned that the conjugates of these dyes with biological substrates should form insoluble complexes with the cyclen-thiourea receptors and afford selective separation of the desired target.

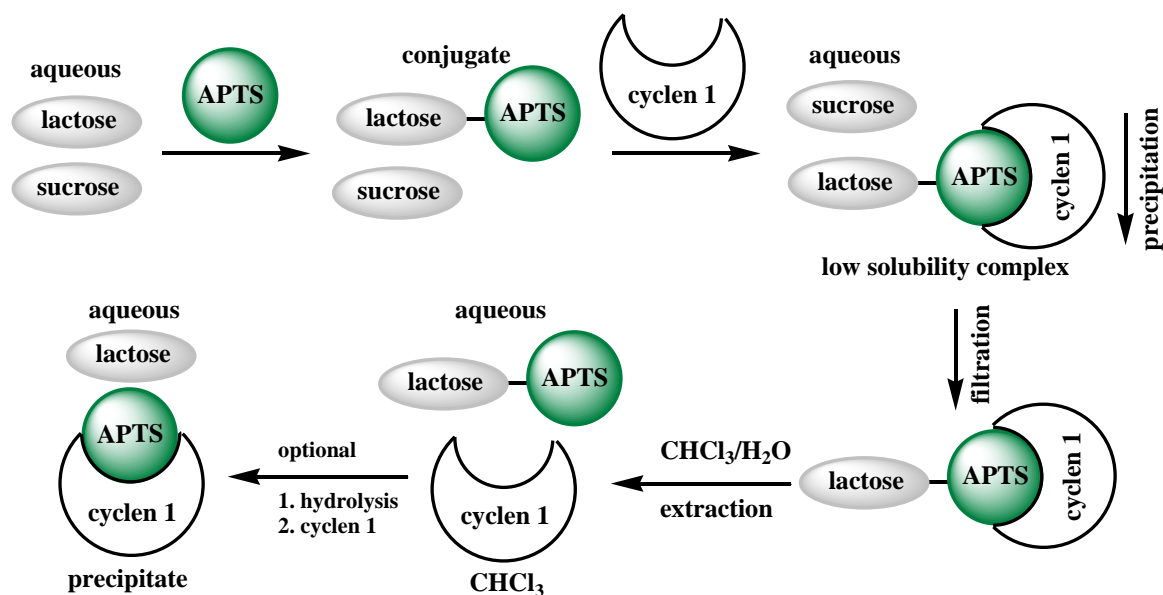


Scheme 3.1. Structures of lactose, sucrose, APTS dye and receptor cyclen **1**.

### 3.2 Irreversible labeling of lactose with APTS and its chemoselective separation from lactose/sucrose mixture

Here, we report the proof of concept for the chemoselective precipitation of biological substrates using a model system of two disaccharides: lactose and sucrose. While the physical properties of these sugars are very similar,<sup>171</sup> which makes their separation by common techniques difficult,<sup>172, 173</sup> the presence of a reducing end in lactose allows a test of our principle. 8-Aminopyrene-1,3,6-trisulfonic acid (APTS) is the dye that forms a stable complex ( $K_a = 8 \times 10^5 \text{ M}^{-1}$ ) with the naphthyl thiourea cyclen receptor (cyclen **1**, Scheme 3.1).<sup>9</sup> The presence of an amino group in this dye implies that it can be readily tethered to the reducing end of lactose via reductive amination reaction.

The combined schematic representation of chemoselective precipitation protocols is shown on scheme 3.2.



Scheme 3.2 General representation of protocols for chemoselective precipitation and isolation of lactose and sucrose from a lactose/sucrose mixture.

First, we demonstrated that the lactose-APTS conjugate can be precipitated out from the solution by interacting with cyclen **1** in the presence of sucrose. As detailed in the experimental section, the reductive amination reaction between lactose and APTS was performed according to the literature procedure<sup>174, 175</sup> and the conjugate was purified on an anion-exchange column. Then, we developed a procedure that allows precipitation of this conjugate through interaction with cyclen **1**. The most efficient results were achieved when a 1 mM solution of lactose-APTS conjugate in H<sub>2</sub>O:MeOH (1:9) was mixed with an equal volume of 2 mM cyclen **1** solution in the same solvent system. At these concentrations, both lactose-APTS conjugate and cyclen **1** were completely soluble. However, the interaction between these two components resulted in formation of a precipitate and almost complete discoloration of the originally bright greenish solution (fig. 3.1.a). The fluorometric analysis suggested that at least 89% of the lactose-APTS conjugate was precipitated from solution (fig. 3.1.b).

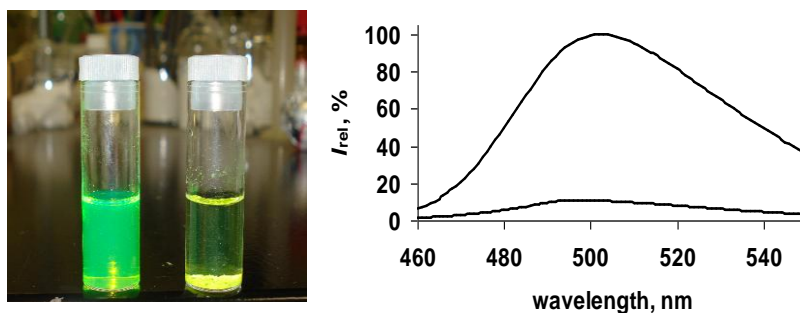


Figure 3.1. a) Image of 1 mM solution of APTS-lactose conjugate in the absence (left vial) and in the presence (right vial) of 2 mM cyclen **1**. Note a precipitate formed in the right vial upon application of cyclen **1**; b) Emission spectra of lactose-APTS conjugate (ex = 424 nm) before and after the treatment with cyclen **1**. Top spectrum was recorded for 1  $\mu$ L of 1 mM solution of lactose-APTS conjugate in H<sub>2</sub>O:MeOH (1:9) injected into 20 mL of water. Bottom spectrum was recorded for 2  $\mu$ L of the supernatant formed upon mixing of lactose-APTS conjugate and cyclen **1** solutions, diluted into 20 mL of water.

To test the selectivity of precipitation, a sample of APTS-labeled lactose was mixed with sucrose (1 eq.), dissolved in H<sub>2</sub>O:MeOH (1:9), followed by the addition of a solution of cyclen **1** (2 eq.). A precipitate immediately formed, which was removed by centrifugation, suspended in water and back-extracted with chloroform. This back-extraction led to repartitioning of cyclen **1** into the organic layer, thereby releasing APTS-labeled lactose in the aqueous layer. Comparison of the <sup>1</sup>H NMR spectra (fig. 3.2) of the mixture of sucrose and labeled lactose (spectrum 1), the supernatant following precipitation (spectrum 2) and the back extracted aqueous solution (spectrum 3) shows the chemoselective precipitation phenomenon. It is important to note that the precipitation and release is highly selective and almost quantitative as evidenced by the absence of APTS signals in spectrum 2 and cyclen **1** signals in spectrum 3. The aromatic signals observed in the supernatant correspond to a partly dissolved excess of cyclen **1**. The aromatic region shows signals of APTS label with no traces of cyclen **1**. Also note the absence of acetal signal for sucrose at 5.4 ppm in this spectrum.

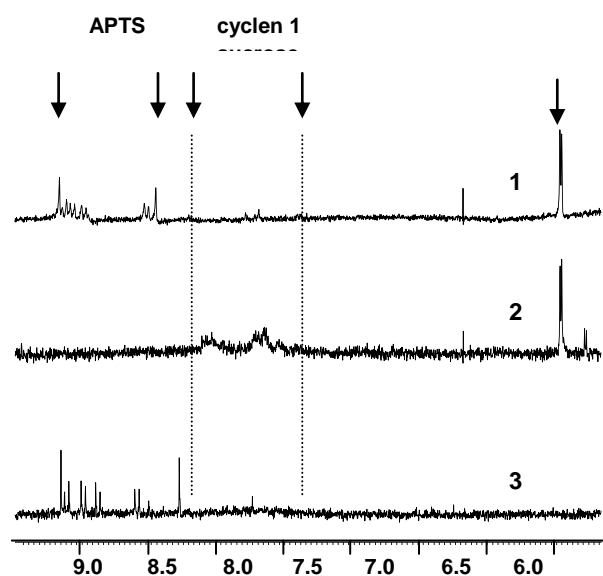


Figure 3.2.  $^1\text{H}$  NMR spectra ( $\text{D}_2\text{O}$ ) of 1) labeled lactose and sucrose mixture; 2) supernatant formed upon treatment of the mixture with cyclen **1** and 3) aqueous portion of precipitate after back-extraction with  $\text{CHCl}_3$ .

To demonstrate that lactose can be selectively removed from the sucrose-lactose mixture via the two step labeling – precipitation protocol, we then chose to carry out labeling with disaccharide mixture, rather than mix pre-labeled lactose with sucrose. Unfortunately, labeling of lactose with equimolar amounts of APTS dye was too slow, and sucrose underwent acid-catalyzed hydrolysis during this time. When a five-fold excess of APTS was used in the reductive amination, a rapid (within 2 hours) labeling of lactose took place without any detectable sucrose degradation. Even though the resulting mixture was more complex than a mixture of labeled lactose and sucrose, the additional component in this mixture was APTS dye, which was also a target substrate for cyclen **1**. Application of two-fold excess of cyclen **1** (with respect to the total amount of APTS) resulted in a complete removal of APTS and APTS-lactose conjugate, leaving sucrose as the only soluble component in this mixture (fig. 3.3). Almost 70% of sucrose was recovered.

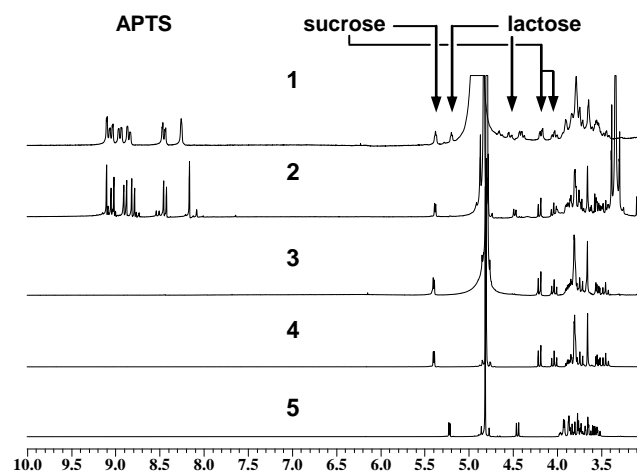


Figure 3.3. <sup>1</sup>H NMR spectra (D<sub>2</sub>O) of 1) APTS, lactose, sucrose and NaBH<sub>3</sub>CN mixture prior to the reductive amination reaction; 2) same mixture after two hours of the reduction; 3) same mixture after treatment with cyclen **1**. Please note disappearance of all peaks except those produced by sucrose; 4) sucrose; 5) lactose.

### 3.3 Reversible labeling of lactose with APTS and recovery of all the components used for the chemoselective precipitation

The protocol for chemoselective precipitation that relies on the reductive amination reaction leads to the irreversible labeling of the target molecule. Formation of an imine bond from the same carbonyl group and the amino group of the dye would introduce the label that could be hydrolyzed back to the original substrate after chemoselective precipitation. This Schiff-base chemistry has been recently used for the reversible attachment of proteins to the solid matrix.<sup>176</sup> In order to test such possibility we have developed an additional protocol to label lactose with APTS via an imine tether. Due to the reversibility of imine bond formation, the labeling of carbonyl compounds is an equilibrium process, and an excess of the amino compound is required in order to label most of the substrate. Even though such an approach results in a mixture comprising at least three components (free excess label, a conjugate and label-free substrate), our new protocol solves the problem of irreversible modification.



First, a mixture of lactose and APTS dye was dissolved in a small volume of 1 M solution of acetic acid and stirred for 12 hours, producing lactose-APTS imine conjugate and excess of free dye, as evidenced by  $^1\text{H}$  NMR. Then, an excess of cyclen **1** was applied to this solution, causing precipitation of labeled lactose and lactose-free dye. This precipitate was collected and subjected to hydrolysis with a large volume (3 mL) of 2 M aqueous acetic acid. Under such conditions, the precipitate was immediately dissolved. After 2 hours of stirring, the solvent was removed under vacuum, and 1 mL of 1 N aqueous ammonia was added to the solid residue and back extracted with chloroform. The  $^1\text{H}$  NMR analysis of organic and aqueous layers showed that only cyclen **1** was present in chloroform, and a mixture of lactose and APTS were found in the aqueous layer. Finally, lactose was separated from the APTS dye by the second application of cyclen **1**, which resulted in precipitation of cyclen **1** and APTS dye, and left lactose as the only component in aqueous layer. Resuspension of the precipitate in water and back extraction with chloroform separated cyclen **1** from APTS (fig. 3.4)

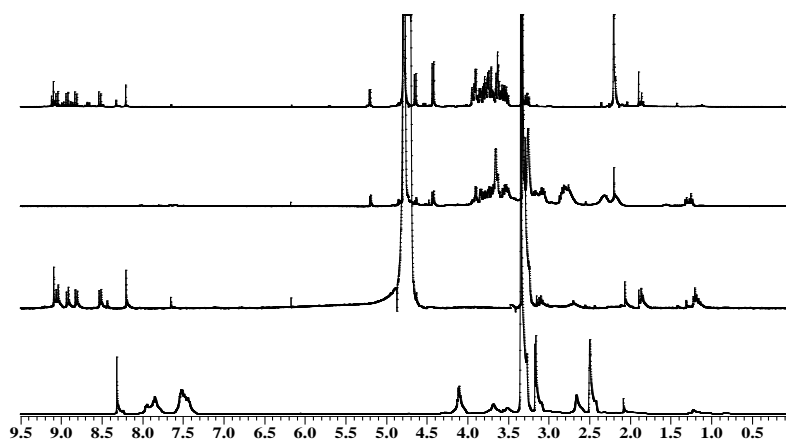


Figure 3.4.  $^1\text{H}$  NMR spectra of 1) reaction mixture comprising lactose and APTS dye in  $\text{D}_2\text{O}$ ; 2) recovered lactose in  $\text{D}_2\text{O}$ ; 3) recovered APTS dye in  $\text{D}_2\text{O}$  and 4) recovered cyclen **1** in  $\text{DMSO}-d_6$ .

With this new protocol, not only could lactose be isolated in an unaltered form, but the dye and cyclen **1** were recovered as well.

An attempt of separation of lactose from sucrose in an unmodified form reached only partial success. While the isolated precipitate gave pure lactose after hydrolysis and back extraction, the supernatant showed sucrose contaminated with some residual lactose. Apparently, precipitation of lactose was not complete because of the reversible nature of the imine bond, which set the equilibrium between labeled and label-free disaccharide. Although the methodology of separation that relies on the temporary labeling via imine bond did not allow us to separate both sugars in the pure form, it can still be used for isolation of reducing sugars. In case if non-reducing sugars are the target substrates, they can be separated from the reducing components via permanent labeling of the latter via amine bond.

Since many sugars possess reducing ends, a similar methodology can be applied to their separation. One example of practical value is the separation of low molecular weight heparin<sup>177</sup>. Heparin oligomers contain reducing ends<sup>178</sup> and therefore can be labeled with APTS dye and complexed with cyclen **1**. The overall solubility of such complexes should depend on the length of the heparin oligomers, where the complexes of the shortest oligomers will be the least soluble and the complexes of the longest oligomers will be the most soluble. Our preliminary studies indicated that labeling of a heparin digest with APTS, followed by the treatment with cyclen **1** resulted in a partial precipitation of heparin conjugates, the extent of which was dependent on the solvent composition. Chemoselective precipitation of heparin oligomers will be the focus of our future studies.

### **3.4 Conclusions**

We developed a facile method for separation of biomolecules via tethering them to the APTS dye and subsequently applying to these conjugates a synthetic receptor cyclen **1**, which binds to the APTS label. Due to the low solubility of the APTS-cyclen **1** complex, the APTS conjugate precipitates out from the solution upon interaction with cyclen **1**, thus leaving

unlabeled molecules as the only soluble components in the mixture. Whereas tethering of carbonyl-containing compounds to APTS via the reductive amination reaction makes them permanently labeled with APTS, the attachment of APTS through an imine bond allows for release of the precipitated molecule in the label-free form. Subsequent extraction of supernatant with organic solvent provides a means for the recovery of all components used for the chemoselective precipitation. This feature makes our new approach especially attractive for the large-scale separations of biological molecules. Separation of low molecular weight heparin oligomers is the focus of our future studies.

## Chapter 4

### Immobilization of cyclen based receptors for pyrene dyes on solid supports:

#### Beginning of a new affinity chromatography technique

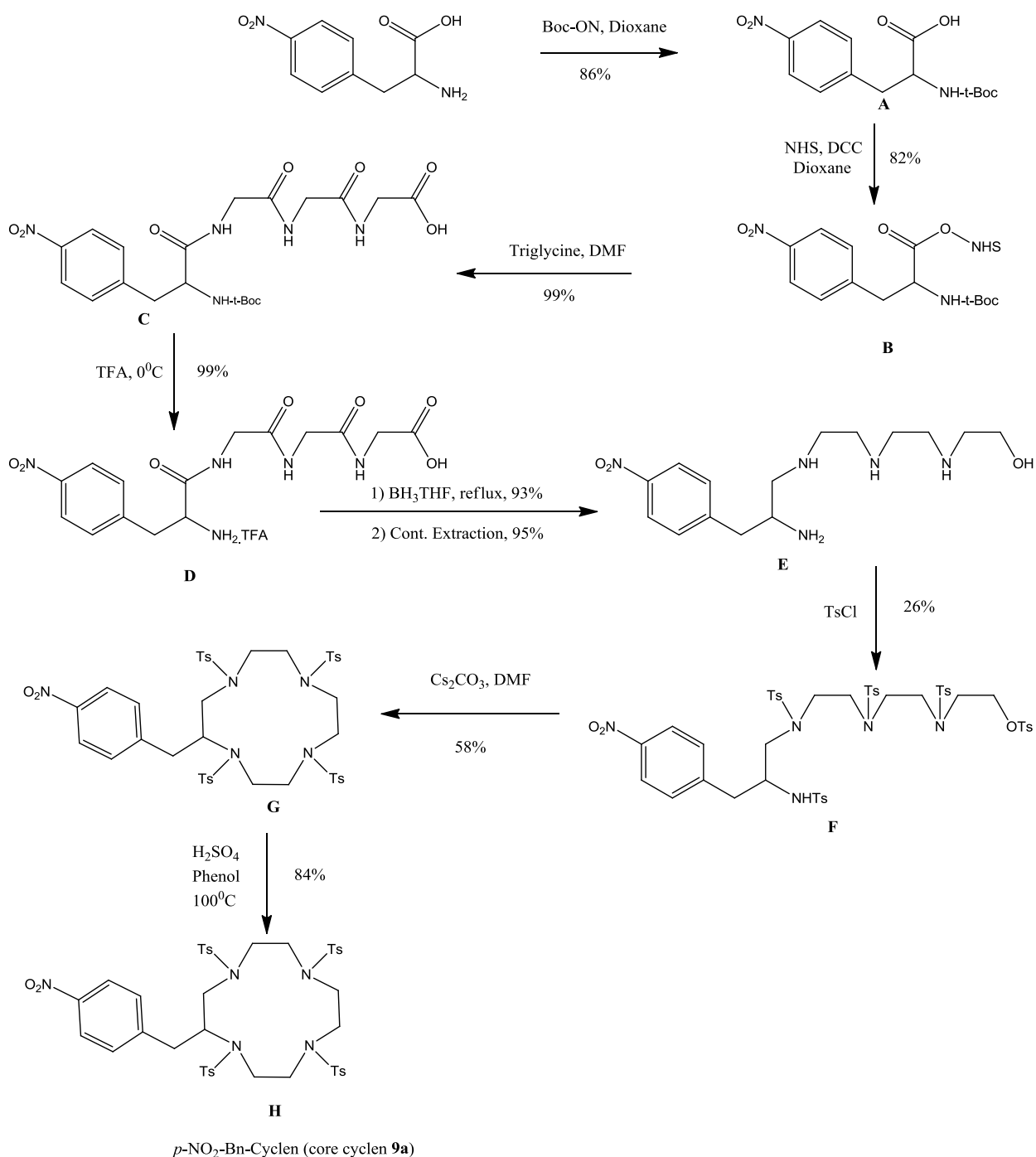
##### 4.1. Introduction

The successful use of dye-receptor pair in chemoselective precipitation of lactose from sucrose<sup>10</sup> encouraged us to further explore the use of this dye-receptor pair in separations technology. In order to broaden the scope of this dye-receptor pair in separations technology, we decided to use this pair in affinity chromatography. We hypothesized that if a receptor having a functional group on the cyclen core can be synthesized, then this receptor can be immobilized on a solid support using this functional group. The receptor for pyrene dyes, immobilized on the solid support will be used as selection auxiliary for affinity chromatography. We expected that the substrates conjugated with the pyrene dyes will exhibit elongated retention times due to the specific interactions of the label with the solid support. This approach might prove itself as valuable means for purification of biological substrates, since the pyrene labels are commonly used in biotechnology for marking the targets of interest.<sup>179, 180</sup>

##### 4.2 Synthesis of *p*-NO<sub>2</sub>-Bn-Cyclen (core cyclen 9a)

A functionalized receptor was required for the immobilization of the receptor on the affinity matrix. The *p*-NO<sub>2</sub>-Bn-Cyclen (core cyclen 9a), which has nitro benzyl group attached to the cyclen core can be used for the synthesis of functionalized receptor. Reduction of nitro group to an amine group will provide a reactive group which can be used for the immobilization of the receptor on various affinity supports. Although, this reagent was commercially available, we decided to synthesize it because of its high cost. Synthesis of *p*-NO<sub>2</sub>-Bn-Cyclen (core

cyclen **9a**) had been reported by Oliver Renn et. al.<sup>191</sup> They synthesized it according to scheme 4.1.

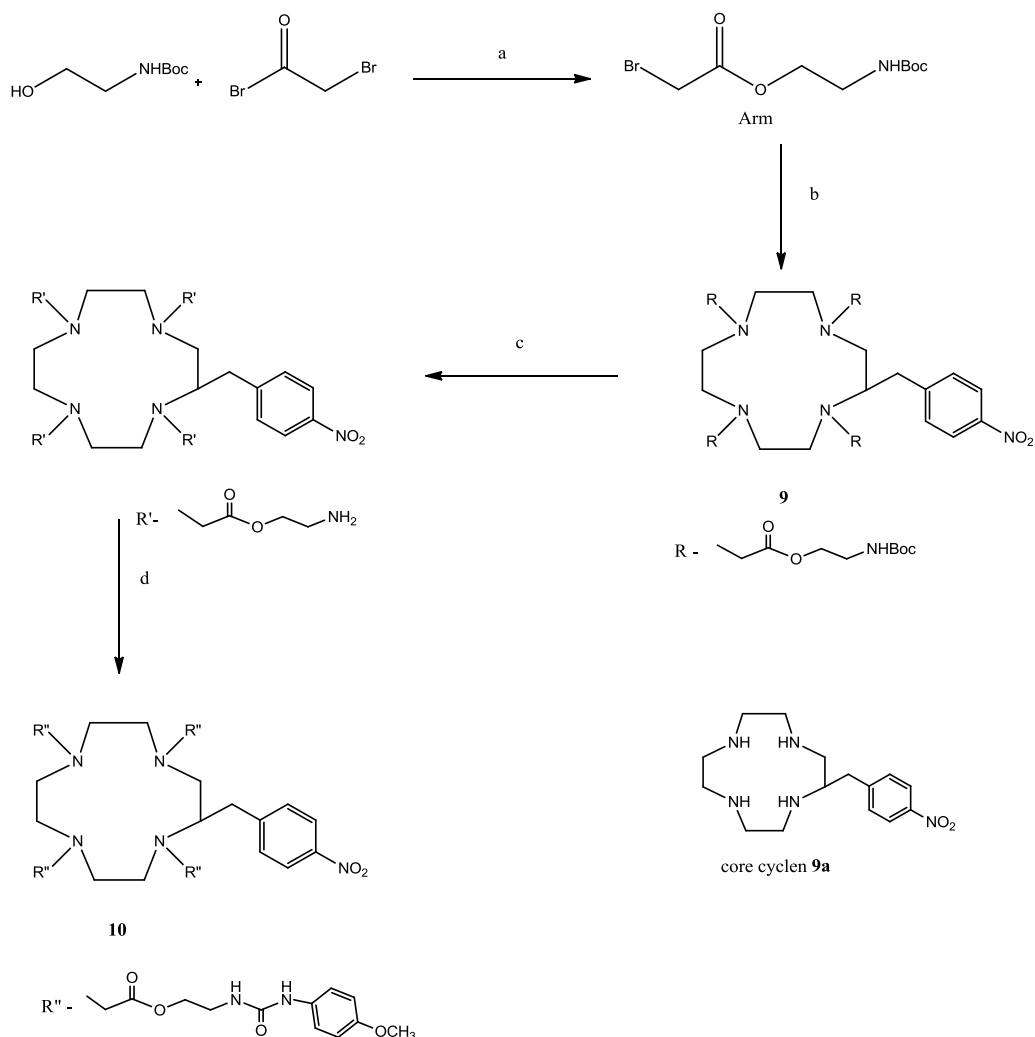


Scheme 4.1. Reaction scheme for the large scale synthesis of *p*-NO<sub>2</sub>-Bn-Cyclen (core cyclen **9a**) from nitrophenylalanine

In this scheme a number of intermediates e.g. compound **F**, **G** and **H** (*p*-NO<sub>2</sub>-Bn-Cyclen), required HPLC purification making it an expensive process. We significantly modified this scheme and successfully developed conditions where normal chromatography can be used for the purification of the compound **F** and **G**. In the last step of the synthesis where detosylation was done to synthesize compound **H** (*p*-NO<sub>2</sub>-Bn-Cyclen), barium hydroxide was used to neutralize the excess sulfuric acid. Barium hydroxide is a very corrosive compound and can cause severe burns. We replaced it with less harmful potassium carbonate. A lot of solid was generated when potassium carbonate was added to the reaction mixture. This solid was stirred with chloroform to extract the compound **H** (*p*-NO<sub>2</sub>-Bn-Cyclen) from the solid. Thus, we successfully developed an extraction procedure for the isolation of final product instead of reverse phase HPLC purification as used in the literature. These changes in the synthetic procedure significantly reduced the cost of production of *p*-NO<sub>2</sub>-Bn-Cyclen (core cyclen **9a**).

### 4.3. Synthesis of functionalized receptor

Functionalized cyclen receptor **11** was synthesized according to the scheme 4.2.<sup>9</sup> It was the same scheme used for the synthesis of the receptors **4-8** (see chapter 2), except that *p*-NO<sub>2</sub>-Bn-Cyclen (core cyclen **9a**) was used instead of cyclen. The synthesis started with the recognition arm (step a), followed by its attachment to the core cyclen **9a** (step b) to furnish the precursor **9**, which was then deprotected under acidic conditions (step c) and reacted with 4-methoxyphenyl isocyanate to yield functionalized OMe receptor **10** (step d).



Scheme 4.2: a) Bromoacetyl bromide,  $\text{Et}_3\text{N}$ ,  $\text{CH}_2\text{Cl}_2$ , rt, 5 hrs, 90%; b) functionalized cyclen, anhydrous DMF,  $\text{K}_2\text{CO}_3$ , First 6 hrs  $60^\circ\text{C}$  followed by rt overnight, 55% ; c) TFA/ $\text{CH}_2\text{Cl}_2$ , rt, 6 hrs; d) 4-methoxyphenyl isocyanate, isopropanol/ $\text{CH}_3\text{CN}$ ,  $\text{Et}_3\text{N}$ , rt, 16hrs, 40%. Overall yield: 22% in core cyclen **9a** conversion.

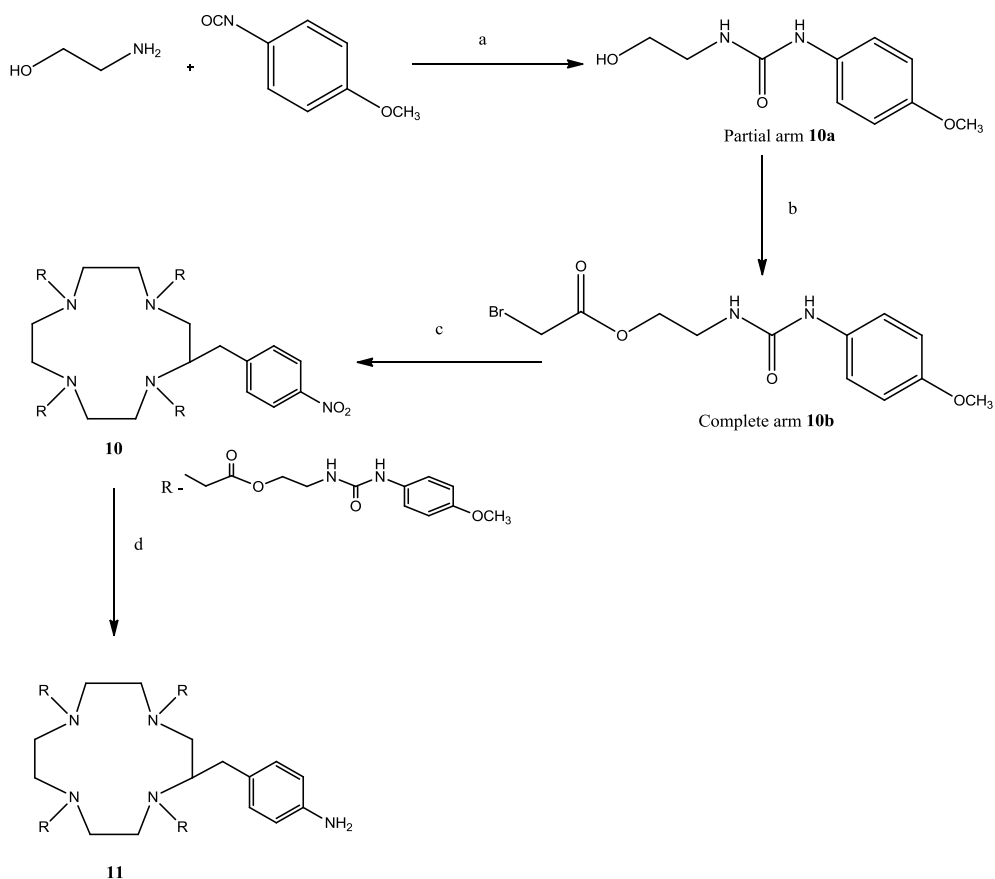
The core cyclen **9a** is an expensive compound and it was involved in the second step of the synthesis, followed by two more steps before the functionalized receptor **10** was obtained. As a result, even though the reasonable yields were acquired for the last three steps, the overall conversion of cyclen **9a** was unacceptably low.

Therefore, we decided to use an alternative scheme (scheme 4.3) which involved the use of cyclen **9a** only in the final step of the receptor synthesis. This alternative synthesis started with the addition of 4-methoxyphenyl isocyanate to ethanolamine (step a) to yield a partial

arm **10a** in almost 100% yield. It was then reacted with bromoacetyl bromide to furnish a complete arm **10b** in 90% yield. The “complete arm” **10b** was then attached to the core cyclen **9a** to afford functionalized OMe receptor **10** in a 62% with respect to the core cyclen **9a** conversion. This was almost threefold increase in the procedure efficiency, comparing to the original route outlined in the scheme 4.2. Several reaction conditions such as use of different bases (organic and inorganic), different solvents, different reaction times and different temperatures were tried to optimize the yield. The best results were obtained when the step c was carried out in dry DMF at room temperature for six hours in the presence of  $K_2CO_3$ .

Additionally, new synthetic route has not only increased the yield but it also simplified the overall procedure, as no purification was needed in the first step and the partial arm **10a** was used as such in the step b for the synthesis of complete arm **10b**.





Scheme 4.3. Synthesis of the receptor **11**. a) ethyl acetate, rt, 1hr, 97%; b) bromoacetyl bromide, Et<sub>3</sub>N, CH<sub>2</sub>Cl<sub>2</sub>, rt, 5 hrs, 90%; c) anhydrous DMF, Na<sub>2</sub>CO<sub>3</sub>, rt, 6 hrs, 62%; d) anhydrous THF, Sn/HCl<sub>(g)</sub>, rt, 4hrs, 63%.

The nitro group of functionalized OMe receptor **10** was then reduced to yield the final functionalized OMe receptor **11**. Several attempts to reduce the nitro group with reduction procedures such as Na<sub>2</sub>S<sub>2</sub>O<sub>4</sub>, Ni/H<sub>2</sub>, Co/H<sub>2</sub>, NaBH<sub>4</sub>, Ni/H<sub>2</sub> in the presence of NaBH<sub>4</sub> have either failed or gave unacceptably low yields on the target compound. Finally, the Sn/HCl<sub>(g)</sub> reagent was used for the reduction. The drawback of this reagent was in the fact that each arm of the receptor had an ester linker susceptible to the acidic hydrolysis in the presence of moisture. However, by choosing proper conditions and apparatus design, we were able to successfully reduce the nitro group in a 63% yield (scheme 4.3).

#### 4.4 Immobilization of functionalized receptor on solid support

Selection of solid support is a very important consideration in affinity systems. To be an adequate support, the matrix should be functionalized (so that the receptor can be immobilized using these functional groups), it should not show any significant nonspecific interactions neither with the target substrate nor with the receptor. The receptor is positively charged due to the cyclen core and the dye has negative charge due to the sulfonate groups. Thus, a neutral resin would be the most suitable support for immobilization, as it diminishes the nonspecific interactions between both the resin and the dye, as well as the resin and the receptor. Prior to the immobilization of the receptor, a series of fluorometric experiments of the matrix were carried out to ascertain the suitability of the given matrix for the affinity chromatography. In a typical experiment, emission spectra were recorded for a 50nM HPTS solution in the presence of the resin and (or) receptor at an excitation wavelength of 405 nm.

Benzaldehyde resin has an aldehyde group which can be used for the immobilization of the receptor **11** by the reductive amination. However, fluorometric experiments (fig. 4.1.A) showed unacceptable interactions with the HPTS dye. The fluorescence intensity of HPTS solution decreased proportionally to the amount of resin added to the fluorometric cell (fig 4.1.A, traces 1 and 2 from the bottom). This could be due to the  $\pi$ - $\pi$  stacking of the aromatic groups of the resin with the aromatic core of the HPTS. Therefore, it was not used for immobilization of the functionalized receptor.

Benzenesulfonyl chloride resin has reactive sulfonyl chloride groups which can react with the receptor **11** to form a sulfonamide bond. However, fluorometric experiments (fig. 4.1.B) showed undesirable interactions of the resin with the receptor. Whereas little change in fluorescence of HPTS was observed in the presence of the resin alone (fig 4.1.B, traces 2 and 3 from the bottom), a significant increase in fluorescence was observed in the presence of

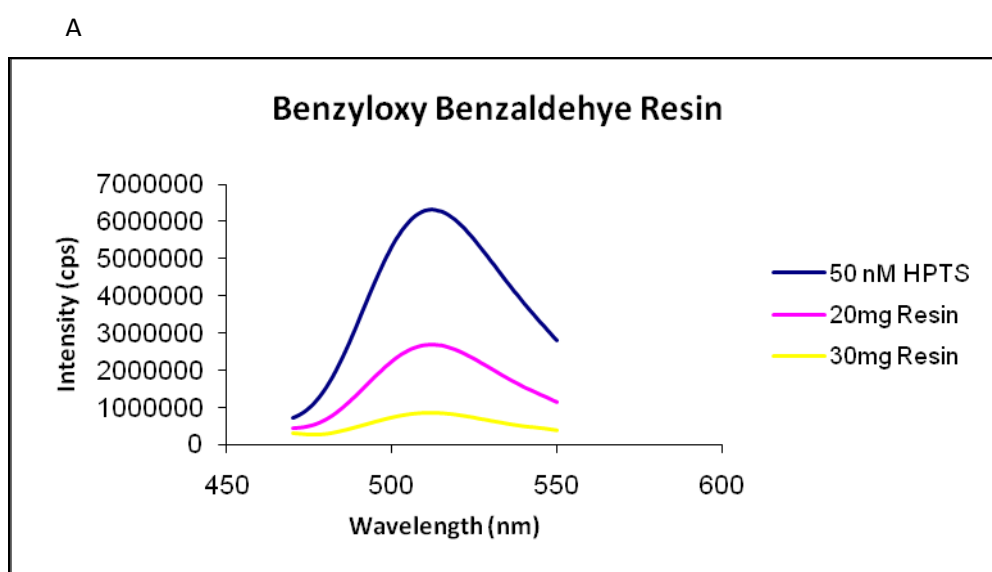
receptor **11** and the resin (fig 4.1.B, trace 4 from the bottom). This was opposite to the effect produced by the receptor **11** on the fluorescence of HPTS in the absence of the resin (fig 4.1.B, trace 1 from the bottom), where almost complete fluorescence quenching was observed. These results strongly suggest that the resin was interacting either with receptor **11** or with the receptor **11**-HPTS complex. In both cases, this made the sulfonyl chloride resin unsuitable for our purposes. The observed results with the sulfonyl chloride resin can be rationalized in the following way: Once placed under physiological conditions, the sulfonyl chloride groups were likely hydrolyzed to produce anionic sulfonic acid residues. While the anionic nature of the resin ensured the lack of interactions with the anionic HPTS dye, the cationic receptor **11** interacted with the resin via either electrostatic or electrostatic and  $\pi$ - $\pi$  stacking interactions. Therefore, this resin was not used for immobilization of the receptor **11**.

Next, we decided to look at the epoxy-functionalized resin, which can be used for immobilization of receptor **11** via nucleophilic ring opening. The hydroxide groups, formed upon the ring opening are neutral under physiological conditions, which is an ideal case for the lack of undesirable interactions between the resin and the dye or receptor. Indeed, no significant change in fluorescence was observed for the solution of HPTS in the presence of the resin (fig. 4.1.C, traces 3 and 4 from the bottom), whereas the fluorescence quenching by receptor **11** was almost identical in the presence and in the absence of the resin. A small increase in the fluorescence intensity in the presence of the resin can be explained by the light scattering caused by relatively large resin beads. We concluded that the epoxy resin could potentially serve as a solid support for immobilization of receptor **11**.

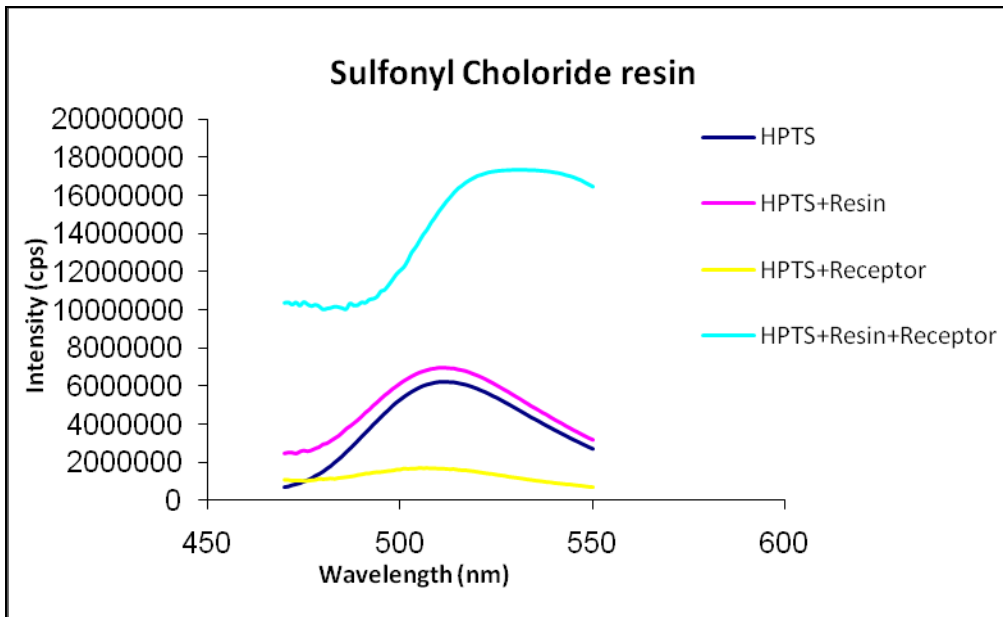
Dowex Mac-3 ion exchange resin has carboxylic acid functional groups which can be used to attach receptor **11** by forming an amide bond. Due to the inherent anionic nature, this resin was not expected to interact with HPTS dye. The fluorometric experiments for this resin (fig. 4.1.D) showed the results very similar to those observed for the epoxy resin: the Dowex Mac-

3 alone produced little effect on the fluorescence of HPTS dye (fig. 4.1.D, traces 3 and 4 from the bottom), whereas the quenching efficiency of receptor **11** was not altered by the addition of the resin to a significant extent (fig. 4.1.D, traces 1 and 2 from the bottom), suggesting that the resin did not interact with either the dye or receptor **11**.

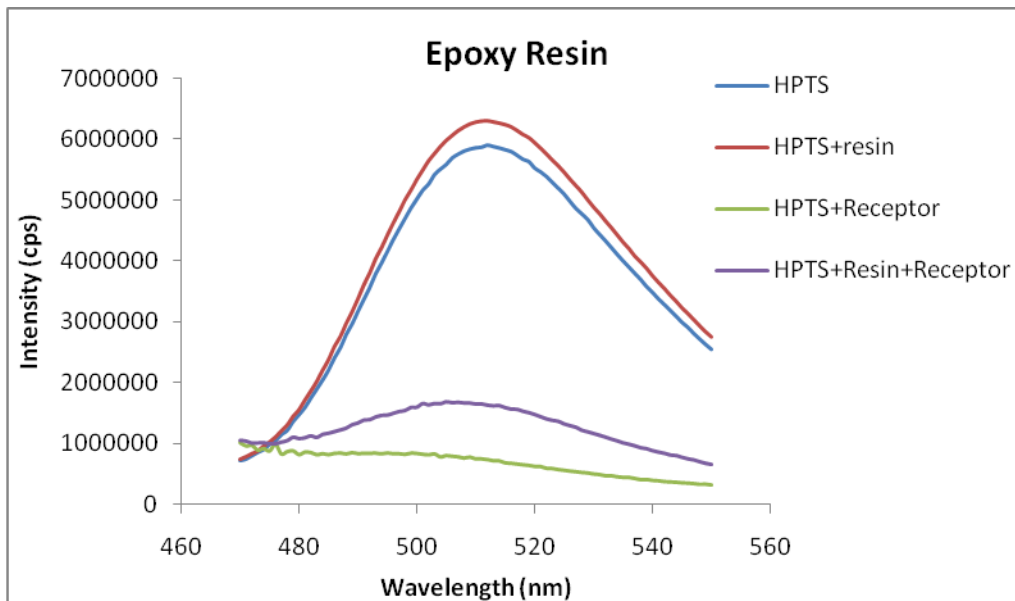
Both the epoxy- and Dowex Mac-3 resins were potentially suitable for use as solid supports, however, several attempts to immobilize the receptor **11** on these resins failed. We concluded that relatively less reactive functional groups on the resins, heterogeneous reaction conditions, less reactive aromatic amine group of the receptor and steric hindrance could be the factors causing problems in the immobilization step.



B



C



D

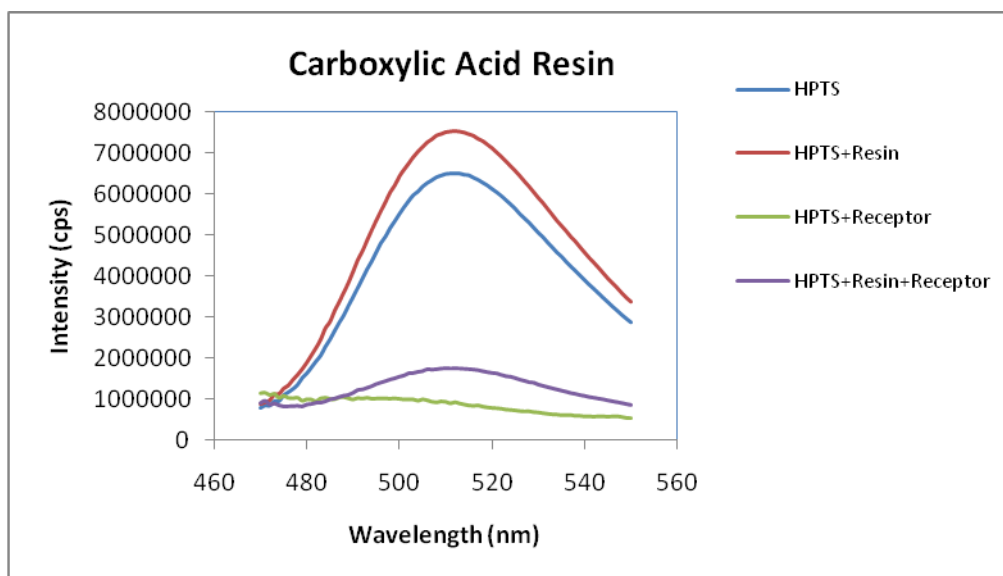


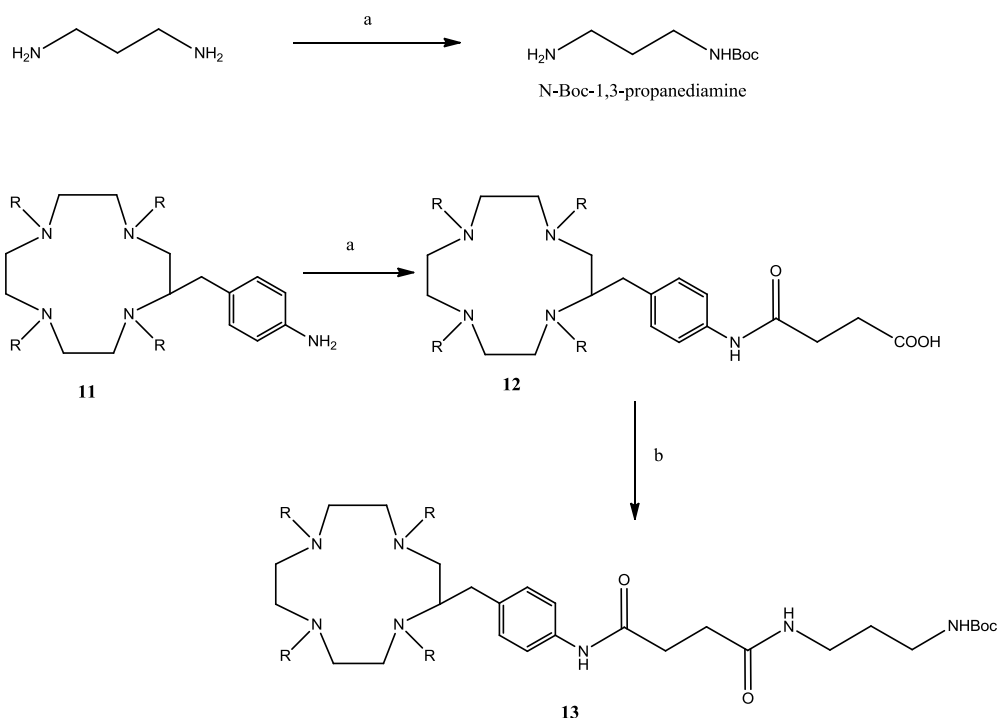
Figure 4.1. Raw fluorescence data for 50 nM solution of HPTS in the presence of the resins and (or) receptor **11**. The excitation wavelength was set at 405 nm in all experiments. A) Benzoyloxy benzaldehyde resin; B) Sulfonyl chloride resin; C) Epoxy resin; D) Carboxylic acid (Dowex Mac-3) resin.

#### 4.5 Synthesis of functionalized receptor with a spacer arm

In order to overcome the above mentioned problems likely arising from the steric hindrance at the surface of the resins, we decided to attach a spacer arm to the aromatic amine of the receptor which would have a primary amine on the free end. Such a modification of receptor **11** was expected to benefit the coupling reaction in a dual way: first, this spacer was expected to reduce the crowdedness around the reactive moiety; second, the less nucleophilic aromatic amino group would be conceptually substituted for the much more nucleophilic primary aliphatic amino group.

The spacer arm was attached by a two step synthesis (scheme 4.4.2.) In the first step, receptor **11** was reacted with succinic anhydride to give compound **12** in 80% yield. It was then reacted with N-Boc-1,3-propanediamine in the presence of 1-Ethyl-3-(3-dimethylaminopropyl)carbodiimide (EDC) and catalytic amount of DMAP (15 mol%) to

afford receptor **13** in 60% yield. N-Boc-1,3-propanediamine was synthesized by mono boc protection of propylene diamine according to scheme 4.4.1.



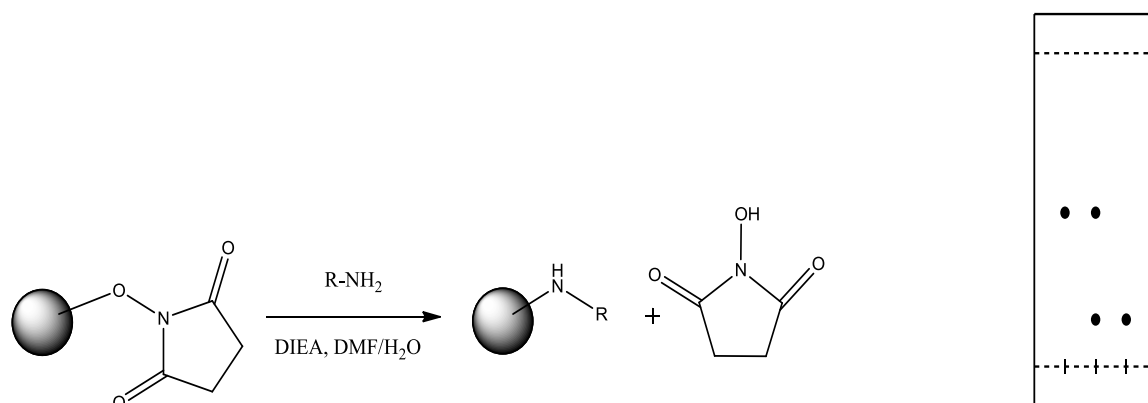
Scheme 4.4.1. Synthesis of N-Boc-1,3-propanediamine. a) Boc anhydride, rt, 6 hrs. Scheme 4.4.2. Synthesis of receptor **13**. a) Succinic anhydride, THF/CH<sub>3</sub>CN, rt, 12 hrs, 80%; b) N-Boc-1,3-propanediamine, EDC, DMAP, DMF, rt, 18 hrs.

#### 4.6 Immobilization of the receptor **13**

Receptor **13** was deprotected and subjected to immobilization reaction on the acid and epoxy functionalized resins. However, all these attempts to immobilize the receptor failed.

In addition to the resins discussed above, other functionalized solid supports are commercially available. One such support was NHS activated agarose, which was also potentially suitable for the coupling with the receptors **11** or **13**. First, we selected less nucleophilic and more sterically crowded receptor **11** for the immobilization, as the more cost-efficient precursor among these two. Immobilization was attempted according to scheme 4.5 and the reaction was monitored by thin layer chromatography (TLC). TLC showed

formation of one new spot and disappearance of the starting receptor from the reaction mixture. This new spot was due to the formation of N-hydroxysuccinimide. TLC analysis indicated that the reaction was complete in 16 hours



Scheme 4.5. Immobilization of receptor **11** on NHS activated agarose. TLC of reaction mixture at various intervals of times as visualized under UV lamp. Spot on far left, reaction at time T=0, Middle spot a co spot of reaction mixture at time T=0 and time T=16 hrs, Spot on far right, reaction at time T=16 hrs.

#### 4.7 Fluorometric titrations of receptor **11** immobilized on the solid support

We successfully immobilized the receptor **11** on the solid support. A series of fluorometric experiments (fig. 4.2) were performed in order to ascertain the effectiveness of this new affinity chromatography matrix. As discussed above, the unmodified resin produced little effect on the fluorescence of HPTS dye (fig. 4.2, traces 3 and 4 from the bottom). In contrast, the resin with immobilized receptor **11** caused almost complete fluorescence quenching upon addition to the solution of HPTS. The fluorescence quenching caused by the immobilized receptor **11** was even stronger than the fluorescence quenching caused by the same amount of the resin-free receptor **11** (traces 2 and 1 from the bottom, respectively). The residual fluorescence of HPTS in the presence of resin-free receptor **11** was due to the intrinsic fluorescence of receptor **11**-HPTS complex. Although low, this fluorescence has measurable intensity and is detectable regardless of the amount of the receptor added to the solution.



Unlike with the resin-free receptor **11**, the immobilized receptor caused a specific adsorption of the dye on the surface of the resin, thus providing its removal from the solution, which was consistent with the complete loss of fluorescence.

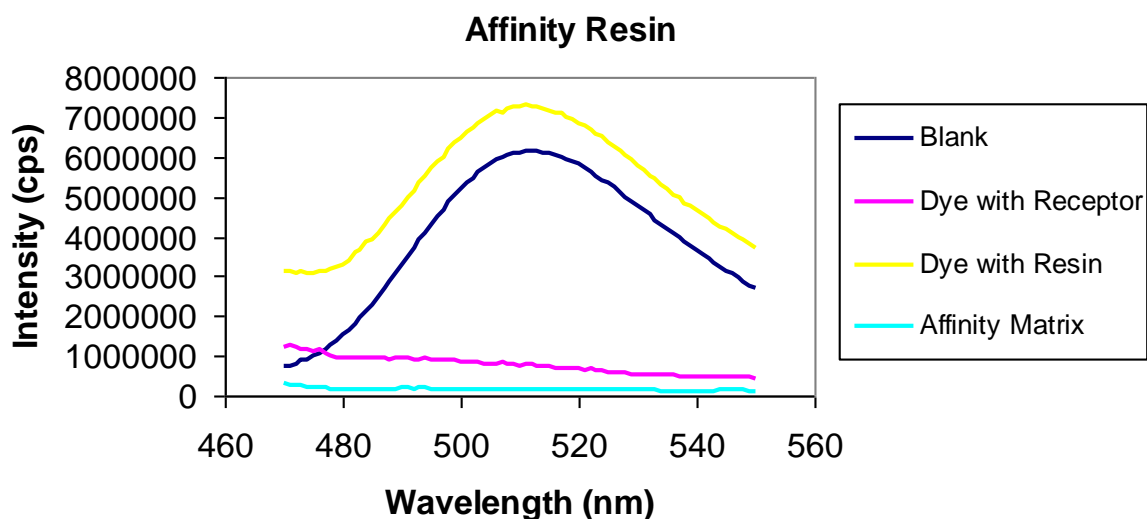


Figure 4.2. Raw fluorescence data for 50 nM solution of HPTS in the presence of the resin and (or) free or immobilized receptor **11**. The excitation wavelength was set at 405 nm in all experiments.

#### 4.8 Conclusions

We successfully synthesized cyclen receptors **11** and **13**, suitable for immobilization on the solid support for the production of the affinity chromatography matrices. We reported two different routes for the synthesis of receptor **11** while developing a simpler and more productive scheme 4.3. We reported a 2.8 fold increase in the yield by using this alternative scheme for the synthesis of receptor **10**. We have analyzed several different resins for their suitability as solid supports, and we identified NHS-activated agarose as the most appropriate candidate for these purposes. We successfully immobilized receptor **11** on NHS-activated agarose via amide coupling. The affinity matrix obtained showed specific affinity towards HPTS dye in the fluorometric experiments, which makes it suitable for the separation of HPTS-labeled biological substrates.

## Chapter 5

### Future Work

#### 5.1 Introduction

We successfully immobilized receptor **11** on NHS activated agarose. Initial results from fluorometric experiments indicated that the affinity support was very effective and a fluorescence quenching up to 95% was observed. The applicability of this matrix for the separation of various systems will be studied.

#### 5.2 Separation of a mixture of dyes

We designed this affinity support for the separation of substrates conjugated with the pyrene-based dyes (HPTS, APTS, PTA etc) (fig. 1.3). First, we will check the efficiency of the affinity matrix for the separation of the mixture of the dyes, where one dye will be a pyrene-based dye, and the other dyes will have a different nature. Anionic fluorescein-based dyes will be added to the mixture to assess the specificity of the affinity matrix, cationic dyes, such as safranin O<sup>181</sup> will be used as a negative control. The resolving efficiency of the affinity matrix will be quantified through the ratios of the retention times for the pyrene-based dyes and their nonbinding counterparts. The elution profiles and the holding capacity of the matrix will be assessed as well.

#### 5.3 Separation of low molecular weight heparin (LMWH)

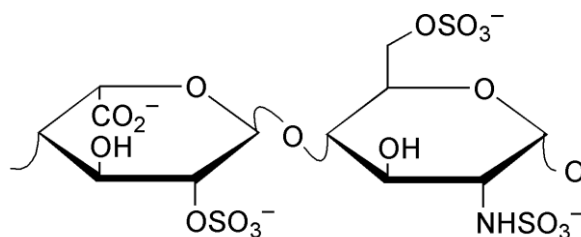
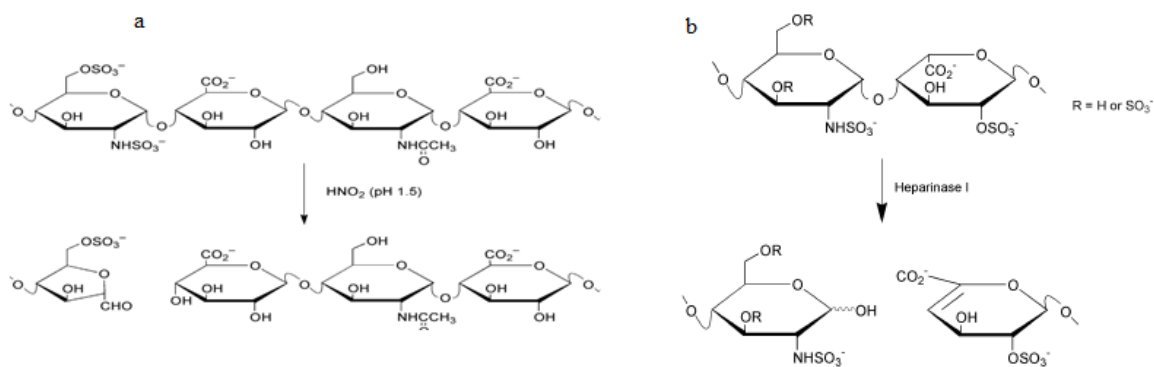


Figure 5.1 Major repeating disaccharide of heparin

Heparin is a linear polysaccharide consisting of uronic acid-(1→4)-D-glucosamine repeating disaccharide subunits (fig. 5.1) having a high degree of sulfation and acetylation.<sup>182</sup> Heparin is used as an anticoagulant. Unfractionated heparin is a heterogeneous mixture of polysaccharide chains ranging in molecular weight from 3000 to 30,000. LMWH are produced by controlled enzymatic or chemical depolymerization (scheme 5.1) of unfractionated or large molecular weight heparins, followed by size and affinity separation.<sup>183</sup> They have an average molecular weight of about 5000. Both unfractionated and LMWH are effective antithrombic therapeutics, but frequent use of unfractionated heparins can cause thrombocytopenia.<sup>184</sup> In contrast, LMWH are found safer to use. Also, outpatient treatment of conditions such as deep vein thrombosis and pulmonary embolism is possible with LMWH compared to necessary hospitalization as needed for treatment with unfractionated heparins. Therefore, use of LMWH is both safe and financially beneficial. Hence, a simple method for separation of LMWH will be of great practical interest.



Scheme 5.1. a) acid catalyzed b) enzymatic depolymerization of heparin

Since chemical and enzymatic depolymerization produce fragments having single reducing ends, APTS can be coupled with these fragments by reductive amination. These labeled fragments can be then purified using receptor immobilized affinity supports. The immobilization of receptor **11** was performed in DMF/H<sub>2</sub>O solvent system; once all the

receptor is immobilized, remaining NHS-ester groups will be hydrolyzed and carboxylic acid groups will be produced. The carboxylic acid groups produced are negatively charged and heparin itself is negatively charged due to the sulfate groups. As a result, both resin and heparin will repel each other. This repulsion will be more pronounced between the large heparin fragment and the resin and hence a differential binding will be achieved. The larger the pyrene conjugated heparin fragment is, the weaker binding to the affinity support will be expected. This variable binding affinity will be used to develop specific elution protocols for the effective separation of LMWH.

#### **5.4 Mapping of cells expressing ligand-gated ion channels**

Ligand-gated ion channels are a group of transmembrane proteins. These have specific binding sites for ligands, such as neurotransmitters.<sup>185</sup> Once bound to the ligand the ion channel opens up and influx or efflux of ions occurs which in turn plays an important role in many physiological processes. These ligand-gated ion channels are related to various diseases such as schizophrenia, depression, attention deficit, hyperactivity disorder, Alzheimer's disease and of course, tobacco addiction.<sup>186-189</sup> Thus, location of these ligand-gated ion channels and study of mechanism of ion transport is of great significance in finding a cure for these diseases.

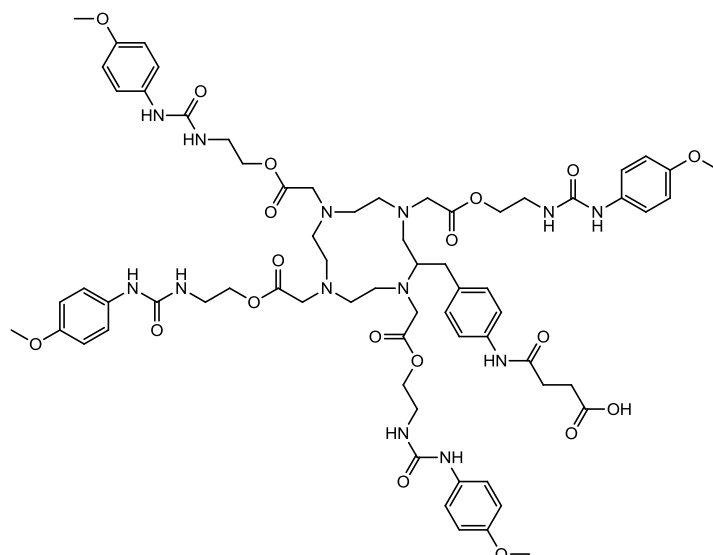
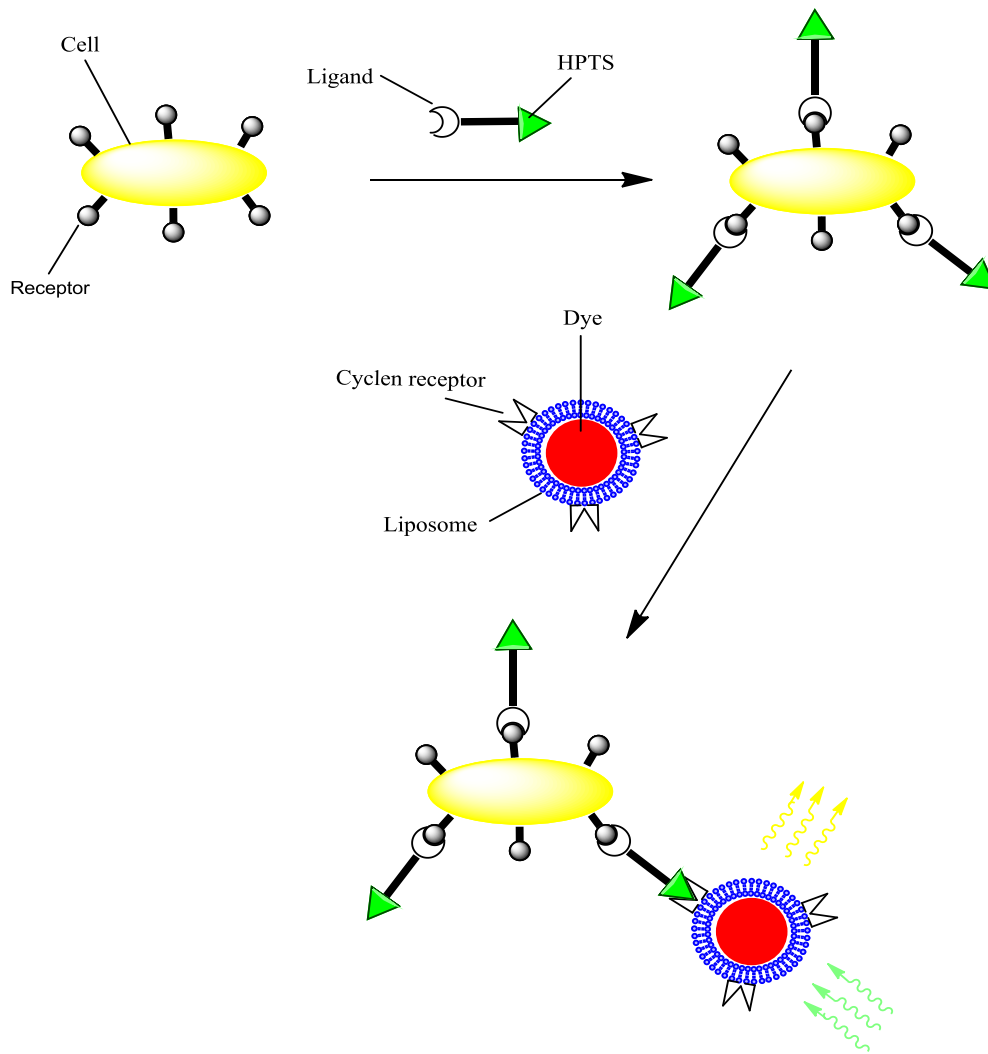


Figure 5.2. Structure of receptor **12**.

We have synthesized receptor **12** (fig. 5.2) which bears a carboxylic group attached to the cyclen core. This receptor will be reacted with 1,2-dioleoyl-*sn*-glycero-3-phosphoethanolamine (DOPE) to produce a modified lipid bearing a receptor molecule. This lipid will be then incorporated into the liposomes filled with the reporter dye. Several neurotransmitters such as acetylcholine, nicotine, GABA etc have been identified as ligands for the receptors on the ligand-gated ion channels. These ligands will be coupled with the pyrene based dyes. The effectiveness of these dye conjugated ligands will be determined by adding these into the cells bearing ligand-gated ion channels. If the dye-ligand conjugate shows effective binding then the suspension of liposomes bearing a surface-anchored receptor will be added to these cells. The receptor will bind to the pyrene portion of the ligand conjugate which in turn attaches the liposome to the ligand-gated ion channels. Since liposomes will be filled with the reporter dye, a single receptor on ligand-gated ion channels can be detected by this fluorescence amplification.



Scheme 5.2. A general scheme for the detection of ligand-gated ion channels

This work has opened several new venues and applicability of this dye-receptor pair in the fields of biochemistry, pharmacology, cell biology etc. will be explored.

## Experimental Section

### General Methods:

All the chemicals and solvents were purchased from Sigma-Aldrich (Milwaukee, WI), Acros Organics or Fisher Scientific (Pittsburgh, PA) and used without further purification. The column chromatographic separations were performed with silica gel 60 (230-400 mesh). All  $^1\text{H}$  NMR and  $^{13}\text{C}$  NMR spectra were recorded on Varian 300 and 400 MHz NMR spectrometers. All NMR chemical shifts ( $\delta$ ) were reported in parts per million (ppm) and were determined relative to the standard values for deuterated solvents. Electro spray ionization mass spectroscopy (ESI-MS) analysis was carried out using a Q-TOF2 from Micromass (Manchester, U.K.). All spectrophotometric experiments were carried out on a Fluoromax 3 (Jobin-Yvon/Horiba) spectrophotometer.

**Bromoacetic Acid 2-*t*-Butoxycarbonylaminoethyl Ester (i).** *tert*-Butyl-*N*-(2-hydroxy ethyl) carbamate (4.5 g, 28 mmol) was dissolved in dichloromethane (30 mL), and triethylamine (3.9 mL, 28 mmol) was added. The mixture was stirred for 10 min at room temperature, and bromoacetyl bromide (3.15 mL, 36 mmol) was added dropwise within 5 min. The reaction mixture was stirred for 5 h at room temperature, the solvent was removed under reduced pressure, and the crude solid was purified by column chromatography (silica gel,  $\text{CH}_2\text{Cl}_2/\text{EtOAc}$  4:6) to give 7.0 g of **i** (25 mmol, 90%).  $^1\text{H}$  NMR (300 MHz, DMSO)  $\delta$  7.03 – 6.91 (q,  $J = 6.0, 5.4$  Hz, 1H), 4.22 – 4.03 (m, 4H), 3.26 – 3.12 (p,  $J = 5.4$  Hz, 2H), 1.50 – 1.35 (d,  $J = 4.1$  Hz, 9H). ESI-MS calcd for  $\text{C}_9\text{H}_{16}\text{BrNO}_4\text{Na}$  ( $\text{M}+\text{Na}^+$ ), 304.02; found 304.02.

**tetrakis(2-((*tert*-butoxycarbonyl)amino)ethyl)2,2',2'',2'''-(1,4,7,10-**

**tetraazacyclododecane-1,4,7,10-tetrayl)tetraacetate (cyclen NH-Boc) (ii).** Cyclen (0.4 g, 2.3 mmol), sodium carbonate (2.19 g, 20.7 mmol), and bromoacetic acid 2-*tert*butoxycarbonylamino ethyl ester (3.8 g, 13.8 mmol) were suspended in 20 mL of

acetonitrile. The reaction mixture was stirred for 72 h at room temperature, and the solvent was removed under reduced pressure. The solid residue was purified by column chromatography (silica gel, CH<sub>3</sub>OH/CHCl<sub>3</sub> 5:95) to afford 1.28 g of cyclen NH-Boc **ii** (1.3 mmol, 56%). <sup>1</sup>H NMR (400 MHz, DMSO) δ 6.97 – 6.89 (t, *J* = 5.8 Hz, 1H), 4.09 – 4.04 (s, 2H), 3.22 – 3.14 (m, 3H), 1.41 – 1.33 (d, *J* = 6.8 Hz, 10H). ESI-MS calcd for C<sub>44</sub>H<sub>81</sub>BrN<sub>8</sub>O<sub>16</sub> (M+H<sup>+</sup>), 977.57, and for C<sub>44</sub>H<sub>80</sub>BrN<sub>8</sub>O<sub>16</sub>Na (M+Na<sup>+</sup>), 999.56; found 977.57 and 999.55.

**tetrakis(2-(3-(4-nitrophenyl)thioureido)ethyl)2,2',2'',2'''-(1,4,7,10-**

**tetraazacyclododecane-1,4,7,10-tetrayl)tetraacetate (4).** The precursor **ii** (25 mg, 0.025 mmol) was dissolved in 1 mL of CH<sub>2</sub>Cl<sub>2</sub>, and trifluoroacetic acid (0.19 mL of 50% v/v solution in CH<sub>2</sub>Cl<sub>2</sub>) was added dropwise. The reaction mixture was stirred for 6 h at room temperature, and the solvent and excess of trifluoroacetic acid were removed under reduced pressure to afford crude deprotected cyclen tetrafluoroacetate. Deprotected cyclen was reacted without further purification. The crude was dissolved in 1 mL of dry THF and *p*-nitrophenyl isothiocyanate (48 mg, 0.266 mmol) was added to this solution. After 15 minutes, triethylamine was added slowly to bring the pH to 9. Reaction was stirred at room temperature for 6 hours and then evaporated to dryness under reduced pressure. The crude was purified by column chromatography (silica gel, 2-6% MeOH in CHCl<sub>3</sub>) to afford 27.5 mg (0.021 mmol, 82%) of receptor **4**. <sup>1</sup>H NMR (400 MHz, DMSO) δ 8.27 – 8.10 (m, 8H), 7.94 – 7.79 (m, 8H), 4.35 – 4.28 (d, *J* = 8.5 Hz, 8H), 3.83 – 3.78 (s, 8H), 3.22 – 3.13 (dd, *J* = 5.2, 1.0 Hz, 4H). ESI-MS calcd for C<sub>52</sub>H<sub>65</sub>N<sub>16</sub>O<sub>16</sub>S<sub>4</sub> (M+H<sup>+</sup>), 1297.36; found 1297.35.

**tetrakis(2-(3-(4-methoxyphenyl)thioureido)ethyl) 2,2',2'',2'''-(1,4,7,10-**

**tetraazacyclododecane-1,4,7,10-tetrayl)tetraacetate (5).** This compound was synthesized from cyclen NH-Boc **ii** (25 mg, 0.025 mmol) and 4-Methoxyphenyl isothiocyanate (0.041 ml, 0.297 mmol) in dry THF according to the procedure described for the synthesis of receptor **4**. The isolated yield of receptor **5** was 12.3 mg (0.01 mmol, 40%). <sup>1</sup>H NMR (300 MHz,



DMSO)  $\delta$  7.27 – 7.17 (d,  $J$  = 8.4 Hz, 8H), 6.94 – 6.84 (d,  $J$  = 8.4 Hz, 8H), 4.27 – 4.20 (s, 8H), 3.77 – 3.70 (d,  $J$  = 0.6 Hz, 12H), 2.56 – 2.40 (d,  $J$  = 1.6 Hz, 6H), 2.12 – 2.06 (d,  $J$  = 0.6 Hz, 8H), 1.30 – 1.21 (d,  $J$  = 8.7 Hz, 1H). ESI-MS calcd for  $C_{56}H_{76}N_{12}O_{12}S_4Na$  ( $M+Na^+$ ), 1259.46; found 1259.51.

**tetrakis(2-(3-(4-bromophenyl)thioureido)ethyl)2,2',2'',2'''-(1,4,7,10-**

**tetraazacyclododecane-1,4,7,10-tetrayl)tetraacetate (6).** This compound was synthesized from cyclen NH-Boc **ii** (25 mg, 0.025 mmol) and 4-Bromophenyl isothiocyanate (70 mg, 0.3 mmol) in isopropyl alcohol according to the procedure described for the synthesis of receptor **4**. The isolated yield of the receptor **6** was 25.2 mg (0.017 mmol, 68.6%).  $^1H$  NMR (300 MHz, DMSO)  $\delta$  9.92 – 9.76 (s, 4H), 8.06 – 8.00 (s, 4H), 7.60 – 7.30 (m, 15H), 4.32 – 4.21 (d,  $J$  = 6.0 Hz, 8H), 3.81 – 3.74 (s, 8H), 2.61 – 2.42 (m, 8H). ESI-MS calcd for  $C_{52}H_{66}Br_4N_{12}O_8S_4$  ( $M+H^+$ ), 1429.06; found 1429.05.

**tetrakis(2-(3-butylthioureido)ethyl)2,2',2'',2'''-(1,4,7,10-tetraazacyclododecane-1,4,7,10-**

**tetrayl)tetraacetate (7).** This compound was synthesized from cyclen NH-Boc **ii** (25 mg, 0.025 mmol) and Butyl isothiocyanate (0.041 ml, 1.3 mmol) in isopropyl alcohol according to the procedure described for the synthesis of receptor **4**. The isolated yield of receptor **7** was 0.0057 mmol, 23%.  $^1H$  NMR (300 MHz, DMSO)  $\delta$  9.32 – 9.25 (s, 4H), 8.37 – 8.29, 4.27 – 4.15 (t,  $J$  = 7.5 Hz, 8H), 3.57 – 3.44 (dd,  $J$  = 7.8, 7.2 Hz, 8H), 3.43 – 3.27 (m, 11H), 2.19 – 2.03 (m, 14H), 1.66 – 1.49 (m, 8H), 1.40 – 1.17 (m, 9H), 0.96 – 0.84 (t,  $J$  = 7.3 Hz, 13H). ESI-MS calcd for  $C_{44}H_{85}N_{12}O_8S_4$  ( $M+H^+$ ), 1037.54; found 1037.35.

**tetrakis(2-benzamidoethyl)2,2',2'',2'''-(1,4,7,10-tetraazacyclododecane-1,4,7,10-**

**tetrayl)tetraacetate (8).** This compound was synthesized from cyclen NH-Boc **ii** (25 mg, 0.025 mmol) and Benzoyl chloride (0.046 ml, 0.39 mmol) in isopropyl dichloromethane according to the procedure described for the synthesis of receptor **4**. The isolated yield of

receptor **8** was 0.018 mmol, 74%.  $^1\text{H}$  NMR (400 MHz,  $\text{CDCl}_3$ )  $\delta$  7.95 – 7.81 (m, 7H), 7.53 – 7.32 (m, 12H), 7.29 – 7.16 (d,  $J = 0.7$  Hz, 5H), 4.34 – 4.24 (q,  $J = 6.3, 5.0$  Hz, 6H), 3.71 – 3.64 (m, 8H), 3.55 – 3.50 (s, 6H), 2.90 – 2.78 (d,  $J = 9.5$  Hz, 13H). ESI-MS calcd for  $\text{C}_{52}\text{H}_{65}\text{N}_8\text{O}_{12}$  ( $\text{M}+\text{H}^+$ ), 993.56; found 993.56.

**Fluorometric titration of HPTS with receptors 4-8.** In a typical experiment, an aqueous solution (2 mL) containing 50 nM HPTS, 100 mM NaCl, 10 mM  $\text{Na}_x\text{H}_{3-x}\text{PO}_4$  ( $x = 1, 2$ ; pH 6.4) was placed in a thermostated spectrophotometric cell set at  $25^\circ\text{C}$ . The solution was gently stirred during the experiment. Prior to the spectrometric recording,  $20\mu\text{L}$  of 25-5000  $\mu\text{M}$  solution of receptors **4-8** in DMSO were added to the cell giving the final concentration of the receptors in the range of 2.5-500  $\mu\text{M}$ . The emission spectra were then recorded with the excitation wavelength of 405 nm. The emission maxima at 510 nm were monitored. Binding constant and the maximum emission loss with the confidence interval values were then computed using the homemade nonlinear regression curve fitting program.

**Labeling of lactose with APTS dye via reductive amination.** 8-Aminopyrene-1,3,6-trisulfonic acid trisodium salt (APTS) (4.8 mg, 0.009 mmol) and lactose (50.6 mg, 0.140 mmol, 15 fold excess) were dissolved in 3mL of 15% aqueous acetic acid, sodium cyanoborohydride (80 mg, 1.28 mmol, 142 fold excess) was added and reaction was refluxed at  $70^\circ\text{C}$  for 5 days. The reaction was purified by ion exchange chromatography ( DEAE Sephadex A-2S anion exchange resin, 1% HCl eluent). A sample of labeled lactose (3 mg, 0.0037 mmol) was mixed with sucrose (1.3 mg, 0.0037 mmol, 1 eq) and used in the further chemoselective precipitation experiment.

Labeled lactose  $^1\text{H}$  NMR (300 MHz,  $\text{D}_2\text{O}$ )  $\delta$  9.14 (s, 1H), 9.11 (d, 1H,  $J=8.9$  Hz), 9.02 (d, 1H,  $J=11.9$  Hz), 8.92 (d, 1H,  $J=8.9$  Hz), 8.51 (d, 1H,  $J=8.9$  Hz), 8.35 (s, 1H), 4.09-3.63 (m, 13H). MS (ESI  $[\text{M}]^-$ ), monosodium salt: 804.27, calcd for  $\text{C}_{28}\text{H}_{31}\text{NNaO}_{19}\text{S}_3$ : 804.06.

Labeled lactose + sucrose  $^1\text{H}$  NMR (300 MHz,  $\text{D}_2\text{O}$ )  $\delta$  9.16 (s, 1H), 9.13 (d, 1H,  $J=8.9$  Hz), 9.07 (d, 1H,  $J=11.9$  Hz), 8.98 (d, 1H,  $J=8.9$  Hz), 8.51 (d, 1H,  $J=8.9$  Hz), 8.44 (s, 1H), 5.40 (d, 1H,  $J=2.9$  Hz), 4.20 (d, 1H,  $J=8.9$  Hz), 4.04 (t, 1H,  $J=8.9$  Hz), 3.90-3.15 (m, 23H).

**Precipitation of labeled lactose.** A solution of lactose-APTS conjugate (1 mM) in  $\text{H}_2\text{O}:\text{MeOH}$  (1:9) was mixed with equal volume of 2 mM solution of cyclen **1** in the same solvent system. An immediate precipitate formation was observed. The resulting solution was centrifuged for 15 minutes (14,000 rpm). The supernatant was removed, the precipitate was suspended in water, and extracted with chloroform. The extraction caused partitioning of lactose-APTS conjugate into the aqueous layer and partitioning of cyclen **1** into the organic layer.

Supernatant  $^1\text{H}$  NMR (300 MHz,  $\text{D}_2\text{O}$ )  $\delta$  5.40 (d, 1H,  $J=2.9$  Hz), 4.20 (d, 1H,  $J=8.9$  Hz), 4.04 (t, 1H,  $J=8.9$  Hz), 3.90-3.15 (m, 11H).

Aqueous layer (after back extraction)  $^1\text{H}$  NMR (300 MHz,  $\text{D}_2\text{O}$ )  $\delta$  9.10 (s, 1H), 9.05 (d, 1H,  $J=8.9$  Hz), 8.92 (d, 1H,  $J=11.9$  Hz), 8.80 (d, 1H,  $J=8.9$  Hz), 8.54 (d, 1H,  $J=11.9$  Hz), 8.42 (s, 1H), 3.80- 3.50 (m, 12H).

#### **Labeling of lactose with APTS in the presence of sucrose via reductive amination.**

Lactose (1mg, 0.0029 mmol), sucrose (1mg, 0.0029 mmol,) and 8-aminopyrene-1,3,6-trisulfonic acid trisodium salt (APTS) (4.4 mg, 0.0087 mmol, 3.2 fold excess) were dissolved in 2ml of 15% aqueous acetic acid, sodium cyanoborohydride (24 mg, 0.381 mmol, 141 fold excess) was added and the reaction mixture was refluxed at 70  $^\circ\text{C}$  for 2 hours. Precipitation of conjugate was carried out in the same manner as described in the previous section.

T=0 hrs  $^1\text{H}$  NMR (300 MHz,  $\text{D}_2\text{O}$ )  $\delta$  9.01 (s, 1H), 8.97 (d, 1H,  $J=11.9$  Hz), 8.85 (d, 1H,  $J=8.9$  Hz), 8.75 (d, 1H,  $J=11.9$  Hz), 8.36 (d, 1H,  $J=8.9$  Hz), 8.16 (s, 1H), 5.29 (s, 1H), 5.11 (s, 1H), 4.42 (d, 1H,  $J=8.9$  Hz), 4.11 (d, 1H,  $J=8.9$  Hz), 3.94 (t, 1H,  $J=8.9$  Hz), 3.90-3.40 (m, 23H).

T=2 hrs  $^1\text{H}$  NMR (300 MHz,  $\text{D}_2\text{O}$ )  $\delta$  9.05 (s, 1H), 8.99 (d, 1H,  $J=8.9$  Hz), 8.85 (d, 1H,  $J=8.9$  Hz), 8.75 (d, 1H,  $J=11.9$  Hz), 8.39 (d, 1H,  $J=8.9$  Hz), 8.12 (s, 1H), 5.35 (d, 1H,  $J=2.9$  Hz), 4.42 (d, 1H,  $J=8.9$  Hz), 4.18 (d, 1H,  $J=8.9$  Hz), 4.0 (t, 1H,  $J=8.9$  Hz), 3.90-3.40 (m, 23H).

Supernatant  $^1\text{H}$  NMR (300 MHz,  $\text{D}_2\text{O}$ )  $\delta$  5.40 (d, 1H,  $J=2.9$  Hz), 4.20 (d, 1H,  $J=8.9$  Hz), 4.03 (t, 1H,  $J=8.9$  Hz), 3.90-3.40 (m, 11H).

Lactose  $^1\text{H}$  NMR (300 MHz,  $\text{D}_2\text{O}$ )  $\delta$  5.19 (d, 1H,  $J=5.9$  Hz), 4.42 (d, 1H,  $J=5.9$  Hz), 3.96-3.48 (m, 12H).

Sucrose  $^1\text{H}$  NMR (300 MHz,  $\text{D}_2\text{O}$ )  $\delta$  5.38 (d, 1H,  $J=2.9$  Hz), 4.19 (d, 1H,  $J=8.9$  Hz), 4.02 (t, 1H,  $J=8.9$  Hz), 3.90-3.40 (m, 11H)

**Labeling of lactose with APTS dye via imine bond.** A mixture of lactose (2 mg, 0.0058 mmol) and APTS (2.7 mg, 0.0114 mmol) was dissolved in the minimum amount of 10% aqueous acetic acid (0.2 mL). The reaction mixture was stirred for 12 hrs at  $70^\circ\text{C}$ . Then the reaction mixture was cooled to the room temperature, the solvent was removed under reduced pressure, and  $^1\text{H}$  NMR for the solid residue was recorded in  $\text{D}_2\text{O}$ . The  $^1\text{H}$  NMR spectrum showed some conjugated as well as some free APTS present in the reaction mixture.

**Precipitation of lactose-APTS imine conjugate.** The reaction mixture described in the previous section was dissolved in 0.2 mL of 80% aqueous methanol. A saturated solution of cyclen **1** in 1 mL of the same solvent was prepared. Approximately 10 mg of cyclen **1** was dissolved. This saturated solution of cyclen **1** was added to the solution of lactose-APTS imine conjugate in small aliquotes. Instantaneous precipitation was observed. The solution of

cyclen **1** was added until green fluorescence of reaction mixture disappeared. This precipitate was collected by centrifugation.

**Hydrolysis of lactose-APTS imine conjugate.** The collected solid was suspended in 10 mL of 20% aqueous acetic acid and stirred at 70 °C for 12 hours. A gradual dissolution of precipitate was observed during the reaction. Then, the solution was evaporated to dryness under reduced pressure and the residual solid was suspended in 10 mL of water. The pH of solution was raised to 9 by addition of 1M aqueous ammonia. Then, the solution was extracted with chloroform (5 x 25 mL) to remove cyclen **1**. The <sup>1</sup>H NMR spectrum of the aqueous layer showed only free APTS dye and free lactose peaks, indicating that hydrolysis was successful.

**Recovery of unlabeled lactose and APTS dye.** The aqueous layer from the previous experiment was evaporated and the residue was dissolved in 0.2 mL of 80% aqueous methanol. APTS dye was precipitated by application of saturated solution of cyclen **1** in the same solvent. The precipitate was removed by centrifugation, and the supernatant was evaporated to dryness under reduced pressure. <sup>1</sup>H NMR analysis of the solid residue revealed only peaks consistent with label-free lactose. The remaining precipitate was dissolved in 10 mL of water, and back extracted with chloroform (5 x 25 mL). This extraction caused partitioning of APTS-free cyclen **1** into the organic layer. Both organic and aqueous layers were evaporated to dryness, and analyzed by <sup>1</sup>H NMR. A solid residue from the aqueous layer revealed only peaks consistent with APTS, and organic layer revealed only peaks consistent with cyclen **1**. Overall, 0.4 mg of lactose, 0.9 mg of APTS and 7.2 mg of cyclen **1** was recovered.

Synthesis of functionalized cyclen receptor following scheme 4.1

**Bromoacetic Acid 2-*t*-Butoxycarbonylaminoethyl Ester i.** *tert*-Butyl-*N*-(2-hydroxy ethyl) carbamate (4.5 g, 28 mmol) was dissolved in dichloromethane (30 mL), and triethylamine (3.9 mL, 28 mmol) was added. The mixture was stirred for 10 min at room temperature, and bromoacetyl bromide (3.15 mL, 36 mmol) was added dropwise within 5 min. The reaction mixture was stirred for 5 h at room temperature, the solvent was removed under reduced pressure, and the crude solid was purified by column chromatography (silica gel, CH<sub>2</sub>Cl<sub>2</sub>/EtOAc 4:6) to give 7.0 g of **i** (25 mmol, 90%). <sup>1</sup>H NMR (300 MHz, DMSO) δ 7.03 – 6.91 (q, *J* = 6.0, 5.4 Hz, 1H), 4.22 – 4.03 (m, 4H), 3.26 – 3.12 (p, *J* = 5.4 Hz, 2H), 1.50 – 1.35 (d, *J* = 4.1 Hz, 9H). ESI-MS calcd for C<sub>9</sub>H<sub>16</sub>BrNO<sub>4</sub>Na (M+Na<sup>+</sup>), 304.01; found 304.02.

**tetrakis(2-((*tert*-butoxycarbonyl)amino)ethyl)2,2',2'',2'''-(2-(4-nitrobenzyl)-1,4,7,10-tetraazacyclododecane-1,4,7,10-tetrayl)tetraacetate (9).** To a solution of p-NO<sub>2</sub>-Bn-Cyclen (40mg, 0.13 mmol) in 10 ml of dry DMF was added Na<sub>2</sub>CO<sub>3</sub> (110mg, 1.04mmol), followed by addition of Bromoacetic Acid 2-*t*-Butoxycarbonylaminoethyl Ester arm **i** ( 230mg, 1.04 mmol). The reaction solution was first stirred at 60<sup>0</sup>C for 6hrs followed by overnight stirring at room temperature. The solvent was removed under reduced pressure and the crude solid was purified by column chromatography (silica gel, 2-6% MeOH in CHCl<sub>3</sub>) to afford 79.65 mg (0.072 mmol, 55%) of precursor **9**. <sup>1</sup>H NMR (300 MHz, CDCl<sub>3</sub>) δ 8.22 – 8.10 (t, *J* = 9.2 Hz, 2H), 7.66 – 7.47 (dd, *J* = 26.7, 8.2 Hz, 2H), 4.39 – 4.04 (s, 8H), 3.58 – 3.43 (s, 10H), 3.40 – 3.34 (s, 10H), 3.03 – 2.91 (m, 2H), 2.20 – 2.08 (s, 4H), 1.48 – 1.38 (q, *J* = 3.5 Hz, 38H), 1.30 – 1.18 (m, 4H). ESI-MS calcd for C<sub>51</sub>H<sub>85</sub>N<sub>9</sub>O<sub>18</sub>Na (M+Na<sup>+</sup>), 1111.6; found 1134.6.

**tetrakis(2-(3-(4-methoxyphenyl)ureido)ethyl)2,2',2'',2'''-(2-(4-nitrobenzyl)-1,4,7,10-tetraazacyclododecane-1,4,7,10-tetrayl)tetraacetate (10).** The precursor **9** (170 mg, 0.152 mmol) was dissolved in 5 mL of CH<sub>2</sub>Cl<sub>2</sub>, and trifluoroacetic acid (2.4 mL of 50% v/v

solution in  $\text{CH}_2\text{Cl}_2$ ) was added dropwise. The reaction mixture was stirred for 6 h at room temperature, and the solvent and excess of trifluoroacetic acid were removed under reduced pressure to afford crude deprotected cyclen tetrafluoroacetate. Deprotected cyclen was reacted without further purification. The crude was dissolved in 10 ml of isopropyl alcohol and 4-Methoxyphenyl isocyanate (182.4 mg, 1.22 mmol) was added to this solution. After 15 minutes, triethylamine was added slowly to bring the pH to 9. White precipitate produced with the addition of triethylamine and acetonitrile was added to dissolve all the solid. Reaction was stirred at room temperature for 16 hours and then evaporated to dryness under reduced pressure. The crude was purified by column chromatography (silica gel, 2-6% MeOH in  $\text{CHCl}_3$ ) to afford 79.95 mg (0.061 mmol, 40%) of functionalized OMe receptor **10**.  $^1\text{H}$  NMR (400 MHz, DMSO)  $\delta$  8.45 – 8.39 (d,  $J = 3.4$  Hz, 4H), 8.21 – 8.15 (d,  $J = 8.4$  Hz, 1H), 7.65 – 7.55 (d,  $J = 8.3$  Hz, 2H), 7.32 – 7.23 (m, 8H), 6.85 – 6.75 (m, 8H), 6.22 – 6.14 (q,  $J = 5.0$  Hz, 4H), 4.15 – 4.00 (q,  $J = 5.2$  Hz, 8H), 3.72 – 3.63 (dd,  $J = 1.4, 0.8$  Hz, 12H), 3.62 – 3.44 (ddd,  $J = 29.0, 14.2, 5.5$  Hz, 6H), 3.22 – 3.03 (m, 37H), 2.94 – 2.87 (m, 6H). ESI-MS calcd for  $\text{C}_{63}\text{H}_{82}\text{N}_{13}\text{O}_{18}$  ( $\text{M}+\text{H}^+$ ), 1308.58; found 1308.50.

Alternative scheme for the synthesis of functionalized OMe receptor:

**1-(2-hydroxyethyl)-3-(4-methoxyphenyl)urea (partial arm).** To a solution of 4-Methoxyphenyl isocyanate ( 1.0 g, 6.7 mmol) in 15 mL of ethylacetate was added ethanolamine (0.404 ml, 6.7 mmol). A white precipitate formed with the addition of ethanolamine. The reaction mixture was stirred for two hours at room temperature and then evaporated to dryness under reduced pressure to afford (1.365 g, 6.5 mmol) “partial arm” in 98% yield.  $^1\text{H}$  NMR (300 MHz, DMSO)  $\delta$  8.36 – 8.29 (s, 1H), 7.33 – 7.20 (m, 2H), 6.92 – 6.73 (m, 2H), 6.11 – 6.00 (t,  $J = 5.5$  Hz, 1H), 4.78 – 4.66 (qd,  $J = 3.8, 2.8, 1.4$  Hz, 1H), 3.76 – 3.63 (m, 3H), 3.51 – 3.25 (m, 2H), 3.23 – 3.05 (dtd,  $J = 6.7, 5.5, 1.2$  Hz, 2H).  $^{13}\text{C}$  NMR (75

MHz, DMSO)  $\delta$  156.33 – 156.07 (s), 154.65 – 154.39 (s), 134.50 – 134.23 (s), 120.08 – 119.82 (s), 114.69 – 114.42 (s), 61.29 – 61.03 (s), 55.93 – 55.66 (s), 42.63 – 42.37 (s). ESI-MS calcd for C<sub>10</sub>H<sub>15</sub>N<sub>2</sub>O<sub>3</sub> (M+H<sup>+</sup>), 211.1; found 211.15.

**2-(3-(4-methoxyphenyl)ureido)ethyl 2-bromoacetate (complete arm).** To the partial arm (1.4097 g, 6.7 mmol) dissolved in 100 ml of CH<sub>2</sub>Cl<sub>2</sub> was added triethylamine (1.0311 ml, 7.39 mmol). The mixture was stirred for 10 min at room temperature, and bromoacetyl bromide (1.033 mL, 11.97 mmol) was added dropwise within 5 min. The reaction mixture was stirred for 5 h at room temperature, the solvent was removed under reduced pressure, and the crude solid was purified by column chromatography (silica gel, 2-5% MeOH in CHCl<sub>3</sub>) to give 1.99 g of “complete arm” (6.02 mmol, 90%). <sup>1</sup>H NMR (300 MHz, DMSO)  $\delta$  8.39 – 8.33 (s, 1H), 7.34 – 7.17 (m, 2H), 6.87 – 6.73 (m, 2H), 6.21 – 6.10 (t, *J* = 5.9 Hz, 1H), 4.20 – 3.95 (m, 4H), 3.73 – 3.65 (d, *J* = 0.9 Hz, 3H), 3.40 – 3.22 (m, 2H). <sup>13</sup>C NMR (75 MHz, DMSO)  $\delta$  168.01 – 167.75 (s), 156.26 – 155.99 (s), 154.85 – 154.58 (s), 134.25 – 133.98 (s), 120.39 – 120.13 (s), 114.67 – 114.41 (s), 65.93 – 65.67 (s), 55.91 – 55.65 (s), 38.88 – 38.61 (s), 28.01 – 27.75 (s). ESI-MS calcd for C<sub>12</sub>H<sub>15</sub>BrN<sub>2</sub>O<sub>4</sub>Na (M+Na<sup>+</sup>), 353.02; found 353.05.

**tetrakis(2-(3-(4-methoxyphenyl)ureido)ethyl)2,2',2'',2'''-(2-(4-nitrobenzyl)-1,4,7,10-tetraazacyclododecane-1,4,7,10-tetrayl)tetraacetate (10).** To a solution of p-NO<sub>2</sub>-Bn-Cyclen (40 mg, 0.13 mmol) in 15 ml of dry DMF was added K<sub>2</sub>CO<sub>3</sub> (160 mg, 1.15 mmol). The reaction was stirred for 15 min and a solution of complete arm (400 mg, 1.2 mmol) in 10 ml of dry DMF was added over a period of 30 min. The reaction was then stirred for 6 h at room temp. Excess solvent was removed under reduced pressure and crude was purified by column chromatography (silica, 2-5% MeOH in CHCl<sub>3</sub>) to afford 105.6 mg (0.08 mmol, 62%) of functionalized OMe receptor **10**. <sup>1</sup>H NMR (400 MHz, DMSO)  $\delta$  8.45 – 8.39 (d, *J* = 3.4 Hz, 4H), 8.21 – 8.15 (d, *J* = 8.4 Hz, 1H), 7.65 – 7.55 (d, *J* = 8.3 Hz, 2H), 7.32 – 7.23 (m,



8H), 6.85 – 6.75 (m, 8H), 6.22 – 6.14 (q,  $J = 5.0$  Hz, 4H), 4.15 – 4.00 (q,  $J = 5.2$  Hz, 8H), 3.72 – 3.63 (dd,  $J = 1.4, 0.8$  Hz, 12H), 3.62 – 3.44 (ddd,  $J = 29.0, 14.2, 5.5$  Hz, 6H), 3.22 – 3.03 (m, 37H), 2.94 – 2.87 (m, 6H).  $^{13}\text{C}$  NMR (75 MHz,  $\text{CDCl}_3$ )  $\delta$  174.45 – 173.69 (m), 157.25 – 156.88 (d,  $J = 7.4$  Hz), 155.55 – 155.17 (d,  $J = 8.6$  Hz), 147.27 – 147.00 (s), 146.85 – 146.50 (d,  $J = 6.0$  Hz), 132.69 – 132.12 (dt,  $J = 12.5, 6.5$  Hz), 130.15 – 129.76 (s), 124.27 – 123.92 (d,  $J = 6.7$  Hz), 121.65 – 120.62 (h,  $J = 10.2, 7.9$  Hz), 114.31 – 113.99 (s), 64.99 – 64.32 (m), 55.63 – 55.37 (s), 55.10 – 54.58 (m), 52.99 – 52.72 (s), 49.74 – 49.48 (s), 49.15 – 48.79 (d,  $J = 7.2$  Hz), 48.44 – 48.17 (s), 48.12 – 47.85 (s), 38.76 – 38.50 (s), 32.17 – 31.91 (s). ESI-MS calcd for  $\text{C}_{63}\text{H}_{82}\text{N}_{13}\text{O}_{18}$  ( $\text{M}+\text{H}^+$ ), 1308.58; found 1308.50.

**tetrakis(2-(3-(4-methoxyphenyl)ureido)ethyl)2,2',2'',2'''-(2-(4-aminobenzyl)-1,4,7,10-tetraazacyclododecane-1,4,7,10-tetrayl)tetraacetate (11).** To the solution of **10** (105 mg, 0.08 mmol) in 25 ml of dry THF was added Sn (170 mg, 1.44 mmol). The reaction was stirred and HCl gas was passed through this solution. The solution became turbid with the passage of HCl gas. Continued passing HCl gas and after two h solution became clear. Passed HCl gas for another two h and then solvent was removed under reduced pressure to afford a colorless, viscous liquid. An ammonical ethylacetate solution was added to this viscous liquid to make pH 10. A white solid was formed with the addition of ammonical ethylacetate, which was then centrifuged and solid was separated. Solid was then sonicated with 20 ml of 10% MeOH in  $\text{CHCl}_3$  for 15 min. This solution was then centrifuged and clear solution was collected. It was then dried under reduced pressure to give a crude solid, which was purified by column chromatography (silica, 2-6% MeOH in  $\text{CHCl}_3$ ) to afford 64.63 mg (0.051 mmol, 63%) of reduced functionalize OMe receptor **11**.  $^1\text{H}$  NMR (300 MHz, DMSO)  $\delta$  8.51 – 8.40 (q,  $J = 5.1, 4.4$  Hz, 4H), 7.36 – 7.21 (m, 8H), 6.90 – 6.74 (t,  $J = 9.7$  Hz, 10H), 6.52 – 6.43 (d,  $J = 7.8$  Hz, 2H), 6.32 – 6.21 (m, 4H), 4.33 – 3.91 (m, 8H), 3.71 – 3.51 (m, 16H), 3.50 – 3.37 (m, 2H), 3.28 – 3.20 (m, 14H), 2.99 – 2.92 (s, 4H), 2.77 – 2.70 (s, 8H).  $^{13}\text{C}$  NMR (75 MHz,

CDCl<sub>3</sub>)  $\delta$  174.25 – 173.90 (d,  $J = 6.1$  Hz), 157.29 – 157.03 (s), 155.47 – 155.20 (s), 132.74 – 132.35 (d,  $J = 9.7$  Hz), 121.58 – 120.77 (m), 116.04 – 115.78 (s), 114.29 – 114.03 (s), 64.85 – 64.39 (d,  $J = 11.8$  Hz), 55.66 – 55.40 (s), 55.10 – 54.80 (m), 50.21 – 49.95 (s), 49.90 – 49.63 (s), 48.65 – 48.30 (m), 38.76 – 38.50 (s), 32.81 – 29.58 (s). ESI-MS calcd for C<sub>63</sub>H<sub>83</sub>N<sub>13</sub>O<sub>16</sub>Na (M+Na<sup>+</sup>), 1300.61; found 1300.72.

**4-oxo-4-((4-((1,4,7,10-tetrakis(2-(2-(3-(4-methoxyphenyl)ureido)ethoxy)-2-oxoethyl)-1,4,7,10-tetraazacyclododecan-2-yl)methyl)phenyl)amino)butanoic acid (12).** To a solution of compound 11 (35 mg, 0.027 mmol) in 6 ml of CH<sub>2</sub>Cl<sub>2</sub> was added succinic anhydride (8 mg, 0.08 mmol), followed by an addition of 3 ml of dry THF. The reaction was stirred at room temperature for 12 h. The reaction mixture was dried under reduced pressure and the crude was purified by column chromatography (silica, 10% MeOH in CHCl<sub>3</sub>) to afford 29.74 mg (0.021 mmol, 80%) of compound 12. <sup>1</sup>H NMR (300 MHz, DMSO)  $\delta$  8.51 – 8.41 (d,  $J = 6.8$  Hz, 4H), 7.54 – 7.45 (m, 2H), 7.36 – 7.20 (m, 8H), 7.18 – 7.06 (t,  $J = 8.1$  Hz, 2H), 6.84 – 6.72 (m, 8H), 6.30 – 6.21 (d,  $J = 8.0$  Hz, 4H), 4.33 – 3.89 (hept,  $J = 11.8, 9.7$  Hz, 12H), 3.71 – 3.57 (d,  $J = 3.2$  Hz, 12H), 3.21 – 3.13 (d,  $J = 5.1$  Hz, 8H), 2.98 – 2.86 (m, 2H). <sup>13</sup>C NMR (75 MHz, CDCl<sub>3</sub>)  $\delta$  155.50 – 155.24 (s), 132.59 – 132.32 (s), 121.35 – 121.09 (s), 114.31 – 114.05 (s), 68.23 – 67.97 (s), 64.89 – 64.41 (d,  $J = 15.9$  Hz), 55.68 – 55.41 (s), 50.54 – 50.27 (s), 50.19 – 49.92 (s), 48.53 – 48.27 (s), 38.83 – 38.57 (s). ESI-MS calcd for C<sub>67</sub>H<sub>88</sub>N<sub>13</sub>O<sub>19</sub> (M+H<sup>+</sup>), 1378.62; found 1378.60.

**tetrakis(2-(3-(4-methoxyphenyl)ureido)ethyl)2,2',2'',2'''-(2-(4-(4-((3-((tert-butoxycarbonyl)amino)propyl)amino)-4-oxobutanamido)benzyl)-1,4,7,10-tetraazacyclododecane-1,4,7,10-tetrayl)tetraacetate (13).** To a solution of 12 (25 mg, 0.018 mmol) in 10 ml of dry DMF was added EDC (3.6 mg, 0.024 mmol), followed by addition of N-Boc-1,3-propanediamine (4.18 mg, 0.024 mmol). A catalytic amount of DMAP was added. Reaction was stirred for 18 h at room temperature, the solvent was removed under

reduced pressure to give a crude mixture. This crude mixture was purified by column chromatography (silica, 2-6% MeOH in CHCl<sub>3</sub>) to afford 10.8mg (0.007 mmol, 40%) of compound **13**. <sup>1</sup>H NMR (400 MHz, DMSO) δ 8.59 – 8.54 (s, 2H), 7.35 – 7.23 (tdd, *J* = 9.2, 7.0, 2.4 Hz, 7H), 7.15 – 7.06 (t, *J* = 6.9 Hz, 1H), 6.99 – 6.91 (t, *J* = 5.9 Hz, 3H), 6.84 – 6.73 (tt, *J* = 5.9, 1.8 Hz, 8H), 6.41 – 6.32 (m, 3H), 4.30 – 3.95 (m, 10H), 3.70 – 3.64 (d, *J* = 2.8 Hz, 10H), 3.46 – 3.38 (d, *J* = 8.2 Hz, 2H), 3.20 – 3.15 (s, 9H), 3.04 – 2.86 (m, 12H), 2.80 – 2.69 (dd, *J* = 8.6, 6.5 Hz, 9H), 1.25 – 1.17 (s, 10H). ESI-MS calcd for C<sub>75</sub>H<sub>103</sub>N<sub>15</sub>O<sub>20</sub>Na (M+Na<sup>+</sup>), 1533.75; found 1556.60.

**tert-butyl (3-aminopropyl)carbamate.** To a solution of propylenediamine (0.675 ml, 8.1 mmol) in 40 ml of chloroform, a solution of Boc anhydride (353.3 mg, 1.6 mmol) in 10 ml of chloroform was added dropwise over a period of 3hrs. Reaction was stirred for another 3hrs at room temperature. Reaction was dried under reduced pressure and crude was purified by column chromatography (silica, 4-8% MeOH in CHCl<sub>3</sub>) to yield 220 mg (1.2 mmol, 78.5%) of the product. <sup>1</sup>H NMR (300 MHz, CDCl<sub>3</sub>) δ 5.08 – 5.01 (s, 1H), 3.21 – 3.07 (q, *J* = 8.4, 7.0 Hz, 2H), 2.78 – 2.61 (q, *J* = 6.2, 5.8 Hz, 2H), 1.63 – 1.40 (m, 2H), 1.40 – 1.21 (s, 11H). <sup>13</sup>C NMR (75 MHz, CDCl<sub>3</sub>) δ 156.49 – 156.22 (s), 79.25 – 78.99 (s), 39.90 – 39.63 (s), 38.66 – 38.39 (s), 33.63 – 33.37 (s), 28.73 – 28.46 (s). ESI-MS calcd for C<sub>8</sub>H<sub>19</sub>N<sub>2</sub>O<sub>2</sub> (M+H<sup>+</sup>), 175.14; found 175.20.

## List of References

## References

1. Komatsu N. Separation of nanocarbons by molecular recognition. *J. Inclusion Phenom. Macrocyclic Chem.* 2008;61(3-4):195-216.
2. Nerurkar J, Beach JW, Park MO, Jun HW. Solubility of (+/-)-ibuprofen and S (+/-)-ibuprofen in the presence of cosolvents and cyclodextrins. *Pharm. Dev. Technol.* 2005;10(3):413-21.
3. Atwood JL, Koutsantonis GA, Raston CL. Purification of C-60 and C-70 by selective complexation with calixarenes. *Nature* 1994;368(6468):229-31.
4. Atwood JL, Barnes MJ, Gardiner MG, Raston CL. Cyclotrimeratrylene polarisation assisted aggregation of C-60. *Chem. Commun.* 1996;(12):1449-50.
5. Bosanac T, Yang J, Wilcox CS. Precipitons-functional protecting groups to facilitate product separation: Applications in isoxazoline synthesis. *Angew. Chem. Int. Ed. Engl.* 2001;40(10):1875-9.
6. Bosanac T, Wilcox CS. Precipiton strategies applied to the isolation of alpha-substituted beta-ketoesters. *Tetrahedron Lett.* 2001;42(26):4309-12.
7. Bosanac T, Wilcox CS. A novel precipitating auxiliary approach to the purification of baylis-hillman adducts. *Chem. Commun.* 2001;(17):1618-9.
8. Fletcher KA, McHale MER, Coym KS, Acree WE. Solubility of trans-stilbene in organic nonelectrolyte solvents. comparison of observed versus predicted values based upon mobile order theory. *Canadian Journal of Chemistry-Revue Canadienne De Chimie* 1997;75(3):258-61.
9. Winschel CA, Kalidindi A, Zgani I, Magruder JL, Sidorov V. Receptor for anionic pyrene derivatives provides the basis for new biomembrane assays. *J. Am. Chem. Soc.* 2005;127(42):14704-13.
10. Kaushik V, Cook N, Liang AY, Desai UR, Sidorov V. Chemoselective precipitation of lactose from a lactose/sucrose mixture: Proof of concept for a new separation methodology. *Supramol. Chem.* 2010;22(11-12):751-7.
11. Yarmush ML, Weiss AM, Antonsen KP, Odde DJ, Yarmush DM. Immunoaffinity purification: Basic principles and operational considerations. *Biotechnol. Adv.* 1992;10(3):413-46.
12. Campbell DH, Luescher E, Lerman LS. Immunologic adsorbents: I. isolation of antibody by means of a cellulose-protein antigen. *Proc. Natl. Acad. Sci. U S A* 1951;37(9):575-8.
13. Hirata AA, Campbell DH. The use of a specific antibody adsorbent for estimation of total antibody against bovine serum albumin. *Immunochemistry* 1965;2(2):195-205.

14. Terman DS, Tavel T, Petty D, Racic MR, Buffaloe G. Specific removal of antibody by extracorporeal circulation over antigen immobilized in collodion-charcoal. *Clin. Exp. Immunol.* 1977;28(1):180-8.
15. Wang R, Merrill B, Maggio ET. A simplified solid-phase immunofluorescence assay for measurement of serum immunoglobulins. *Clin. Chim. Acta.* 1980;102(2-3):169-77.
16. Chase HA. Affinity separations utilizing immobilized monoclonal-antibodies - a new tool for the biochemical engineer. *Chem. Eng. Sci.* 1984;39(7-8):1099-125.
17. Bigio M, Rossi R, Borri MG, Casagli MC, Nucci D, Baldari C, Volpini G, Boraschi D. One-step immunoaffinity purification of bioactive human recombinant il-1-beta with a monoclonal-antibody directed to a well-exposed domain of the protein. *J. Immunol. Methods* 1989;123(1):1-8.
18. Jack GW, Wade HE. Immunoaffinity chromatography of clinical-products. *Trends Biotechnol.* 1987;5(4):91-5.
19. Janson JC. Large-scale affinity purification - state of the art and future-prospects. *Trends Biotechnol.* 1984;2(2):31-8.
20. Muller HP, Vantilburg NH, Derks J, Kleinbreteler E, Bertina RM. A monoclonal-antibody to viii-C produced by a mouse hybridoma. *Blood* 1981;58(5):1000-6.
21. Davis GC, Hein MB, Chapman DA. Evaluation of immunosorbents for the analysis of small molecules. isolation and purification of cytokinins. *J. Chromatogr.* 1986;366:171-89.
22. Ueda EKM, Gout PW, Morganti L. Current and prospective applications of metal ion-protein binding. *J. Chromatogr.* 2003;988(1):1-23.
23. Suen SY, Liu YC, Chang CS. Exploiting immobilized metal affinity membranes for the isolation or purification of therapeutically relevant species. *J. Chromatogr. B Analyt. Technol. Biomed. Life Sci.* 2003;797(1-2):305-19.
24. Denizli A, Piskin E. Dye-ligand affinity systems. *J. Biochem. Biophys. Methods* 2001;49(1-3):391-416.
25. Cuatrecasas P, Wilchek M, Anfinsen CB. Selective enzyme purification by affinity chromatography. *Proc. Natl. Acad. Sci. U S A* 1968;61(2):636,&.
26. Porath J, Janson JC, Laas T. Agar derivatives for chromatography, electrophoresis and gel-bound enzymes .1. desulphated and reduced cross-linked agar and agarose in spherical bead form. *J. Chromatogr.* 1971;60(2):167,&.
27. Borchert A, Larsson PO, Mosbach K. High-performance liquid affinity-chromatography on silica-bound concanavalin-a. *J. Chromatogr.* 1982;244(1):49-56.
28. Wang W, Singh S, Zeng DL, King K, Nema S. Antibody structure, instability, and formulation. *J. Pharm. Sci.* 2007;96(1):1-26.

29. Chase HA. Scale-up of immunoaffinity separation processes. *J. Biotechnol.* 1984;1(2):67-80.
30. Axen R, Porath J, Ernback S. Chemical coupling of peptides and proteins to polysaccharides by means of cyanogen halides. *Nature* 1967;214(5095):1302-4.
31. March SC, Parikh I, Cuatrecasas P. A simplified method for cyanogen bromide activation of agarose for affinity chromatography. *Anal. Biochem.* 1974;60(1):149-52.
32. Kohn J, Wilchek M. The use of cyanogen-bromide and other novel cyanylating agents for the activation of polysaccharide resins. *Appl. Biochem. Biotechnol.* 1984;9(3):285-305.
33. Tesser GI, Fisch HU, Schwyzer R. Limitations of affinity chromatography - solvolytic detachment of ligands from polymeric supports. *Helv. Chim. Acta.* 1974;57(6):1718-30.
34. Nilsson K, Mosbach K. Immobilization of enzymes and affinity ligands to various hydroxyl group carrying supports using highly reactive sulfonyl chlorides. *Biochem. Biophys. Res. Commun.* 1981;102(1):449-57.
35. Bethell GS, Ayers JS, Hancock WS, Hearn MTW. Novel method of activation of cross-linked agaroses with 1,1'-carbonyldiimidazole which gives a matrix for affinity chromatography devoid of additional charged groups. *J. Biol. Chem.* 1979;254(8):2572-4.
36. Bethell GS, Ayers JS, Hearn MTW, Hancock WS. Investigation of the activation of cross-linked agarose with carbonylating reagents and the preparation of matrices for affinity-chromatography purifications. *J. Chromatogr.* 1981;219(3):353-9.
37. Gersten DM, Marchalonis JJ. A rapid, novel method for the solid-phase derivatization of IgG antibodies for immune-affinity chromatography. *J. Immunol. Methods* 1978;24(3-4):305-9.
38. Sisson TH, Castor CW. An improved method for immobilizing IgG antibodies on protein A-agarose. *J. Immunol. Methods* 1990;127(2):215-20.
39. Matson RS, Little MC. Strategy for the immobilization of monoclonal antibodies on solid-phase supports. *J. Chromatogr.* 1988;458:67-77.
40. O'Shannessy DJ, Hoffman WL. Site-directed immobilization of glycoproteins on hydrazide-containing solid supports. *Biotechnol. Appl. Biochem.* 1987;9(6):488-96.
41. Prisyazhnoy VS, Fusek M, Alakhov YB. Synthesis of high-capacity immunoaffinity sorbents with oriented immobilized immunoglobulins or their fab' fragments for isolation of proteins. *J. Chromatogr.-Biomed. Appli.* 1988;424(2):243-53.
42. Margel S, Offarim M. Novel effective immunoadsorbents based on agarose-polyaldehyde microsphere beads: Synthesis and affinity chromatography. *Anal. Biochem.* 1983;128(2):342-50.
43. Lim PL. Isolation of specific IgM monoclonal antibodies by affinity chromatography using alkaline buffers. *Mol. Immunol.* 1987;24(1):11-5.

44. Vetterlein D, Calton GJ. Purification of urokinase from complex mixtures using immobilized monoclonal antibody against urokinase light chain. *Thromb. Haemost.* 1983;49(1):24-7.
45. Church WR, Mann KG. A simple purification of human factor-X using a high-affinity monoclonal-antibody immunoabsorbant. *Thromb. Res.* 1985;38(4):417-24.
46. Andersson KK, Benyamin Y, Douzou P, Balny C. The effects of organic solvents and temperature on the desorption of yeast 3-phosphoglycerate kinase from immunoabsorbent. *J. Immunol. Methods* 1979;25(4):375-81.
47. Massaglia A, Roller E, Barbieri U, Rosa U. Fractionation of antibodies to testosterone. *J. Clin. Endocrinol. Metab.* 1974;38(5):820-7.
48. Hodgkinson SC, Lowry PJ. Selective elution of immunoabsorbed anti-(human prolactin) immunoglobulins with enhanced immunochemical properties. *Biochem. J.* 1982;205(3):535-41.
49. Cobbs CS, Gaur PK, Russo AJ, Warnick JE, Calton GJ, Burnett JW. Immunosorbent chromatography of sea nettle (*chrysaora quinquecirrha*) venom and characterization of toxins. *Toxicon.* 1983;21(3):385-91.
50. Bureau D, Daussant J. Desorption following immunoaffinity chromatography; generalization of a gentle procedure for desorbing antigen. *J. Immunol. Methods* 1983;57(1-3):205-13.
51. Danielsen EM, Sjostrom H, Noren O. Hypotonic elution, a new desorption principle in immunoabsorbent chromatography. *J. Immunol. Methods* 1982;52(2):223-32.
52. Korpela TK, Makinen E. Temperature effects in affinity chromatography of alanine aminotransferase. *J. Chromatogr.* 1979;174(2):361-8.
53. Yarmush ML, Olson WC. Electrophoretic elution from biospecific adsorbents: Principles, methodology, and applications. *Electrophoresis* 1988;9(3):111-20.
54. Olson WC, Leung SK, Yarmush ML. Recovery of antigens from immunoabsorbents using high-pressure. *Bio-Technology* 1989;7(4):369-73.
55. Gutierrez R, del Valle EMM, Galan MA. Immobilized metal-ion affinity chromatography: Status and trends. *Sep. and Purif. Rev.* 2007;36(1):71-111.
56. Everson RJ, Parker HE. Zinc binding and synthesis eight-hydroxy-quinoline-agarose. *Bioinorg. Chem.* 1974;4(1):15-20.
57. Hemdan ES, Zhao YJ, Sulkowski E, Porath J. Surface topography of histidine residues: A facile probe by immobilized metal ion affinity chromatography. *Proc. Natl. Acad. Sci. U S A* 1989;86(6):1811-5.



58. Porath J, Olin B. Immobilized metal ion affinity adsorption and immobilized metal ion affinity chromatography of biomaterials. serum protein affinities for gel-immobilized iron and nickel ions. *Biochemistry* 1983;22(7):1621-30.
59. Ramadan N, Porath J. Fe<sup>3+</sup>-hydroxamate as immobilized metal affinity-adsorbent for protein chromatography. *J. Chromatogr.* 1985;321(1):93-104.
60. Sulkowski E. The saga of IMAC and MIT. *Bioessays* 1989;10(5):170-5.
61. Sulkowski E. Immobilized metal-ion affinity chromatography: Imidazole proton pump and chromatographic sequelae. I. proton pump. *J. Mol. Recognit.* 1996;9(5-6):389-93.
62. Sulkowski E. Immobilized metal-ion affinity chromatography: Imidazole proton pump and chromatographic sequelae. II. chromatographic sequelae. *J. Mol. Recognit.* 1996;(5-6):494-8.
63. Porath J, Carlsson J, Olsson I, Belfrage G. Metal chelate affinity chromatography, a new approach to protein fractionation. *Nature* 1975;258(5536):598-9.
64. Chaga GS. Twenty-five years of immobilized metal ion affinity chromatography: Past, present and future. *J. Biochem. Biophys. Methods* 2001;49(1-3):313-34.
65. Gaberc-Porekar V, Menart V. Perspectives of immobilized-metal affinity chromatography. *J. Biochem. Biophys. Methods* 2001;49(1-3):335-60.
66. Pearson RG, Songstad J. Application of principle of hard and soft acids and bases to organic chemistry. *J. Am. Chem. Soc.* 1967;89(8):1827,&.
67. Akgol S, Denizli A. Novel metal-chelate affinity sorbents for reversible use in catalase adsorption. *J. Mol. Catal. B-Enzy.* 2004;28(1):7-14.
68. Arica MY, Testereci HN, Denizli A. Dye-ligand and metal chelate poly(2-hydroxyethylmethacrylate) membranes for affinity separation of proteins. *J. Chromatogr. A* 1998;799(1-2):83-91.
69. Bayramoglu G, Kaya B, Arica MY. Procion brown MX-5BR attached and lewis metals ion-immobilized poly(hydroxyethyl methacrylate)/chitosan IPNs membranes: Their lysozyme adsorption equilibria and kinetics characterization. *Chem. Eng. Sci.* 2002;57(13):2323-34.
70. Denizli A, Senel S, Arica MY. Cibacron blue F3GA and cu(II) derived poly(2-hydroxyethylmethacrylate) membranes for lysozyme adsorption. *Colloids and Surfaces B-Biointerfaces* 1998;11(3):113-22.
71. Angal S, Dean PDG. Effect of matrix on binding of albumin to immobilized cibacron blue. *Biochem. J.* 1977;167(1):301-3.
72. Baird JK, Sherwood RF, Carr RJG, Atkinson A. Enzyme-purification by substrate elution chromatography from procion dye polysaccharide matrices. *FEBS Lett.* 1976;70(1):61-6.

73. Shi QH, Tian Y, Dong XY, Bai S, Sun Y. Chitosan-coated silica beads as immobilized metal affinity support for protein adsorption. *Biochem. Eng. J.* 2003;16(3):317-22.
74. Zhou FL, Muller D, Santarelli X, Jozefonvicz J. Coated silica supports for high-performance affinity-chromatography of proteins. *J. Chromatogr.* 1989;476:195-203.
75. Zhou FL, Muller D, Jozefonvicz J. Double-coated silica supports for high-performance affinity-chromatography of proteins. *J. Chromatogr.* 1990;510:71-81.
76. Santarelli X, Muller D, Jozefonvicz J. Dextran-coated silica packings for high-performance size-exclusion chromatography of proteins. *J. Chromatogr.* 1988;443:55-62.
77. Lakhiari H, Muller D. Insulin adsorption on coated silica based supports grafted with N-acetylglucosamine by liquid affinity chromatography. *J. Chromatogr. B Analyt. Technol. Biomed. Life Sci.* 2004;808(1):35-41.
78. Xi FN, Wu JM, Jia ZS, Lin XF. Preparation and characterization of trypsin immobilized on silica gel supported macroporous chitosan bead. *Process Biochemistry* 2005;40(8):2833-40.
79. Xi FN, Wu JM, Luan MM. Silica-supported macroporous chitosan bead for affinity purification of trypsin inhibitor. *Chin. Chem. Lett.* 2005;16(8):1089-92.
80. Zou HF, Luo QZ, Zhou DM. Affinity membrane chromatography for the analysis and purification of proteins. *J. Biochem. Biophys. Methods* 2001;49(1-3):199-240.
81. Sharma S, Agarwal GP. Interactions of proteins with immobilized metal ions - role of ionic strength and pH. *J. Colloid. Interface Sci.* 2001;243(1):61-72.
82. Wu CY, Suen SY, Chen SC, Tzeng JH. Analysis of protein adsorption on regenerated cellulose-based immobilized copper ion affinity membranes. *J. Chromatogr. A* 2003;996(1-2):53-70.
83. Tsai YH, Wang MY, Suen SY. Purification of hepatocyte growth factor using polyvinylidene fluoride-based immobilized metal affinity membranes: Equilibrium adsorption study. *J. Chromatogr. B Analyt. Technol. Biomed. Life Sci.* 2002;766(1):133-43.
84. Yip TT, Nakagawa Y, Porath J. Evaluation of the interaction of peptides with Cu(II), Ni(II), and Zn(II) by high-performance immobilized metal ion affinity chromatography. *Anal. Biochem.* 1989;183(1):159-71.
85. Jiang W, Graham B, Spiccia L, Hearn MT. Protein selectivity with immobilized metal ion-tacn sorbents: Chromatographic studies with human serum proteins and several other globular proteins. *Anal. Biochem.* 1998;255(1):47-58.
86. Zachariou M, Hearn MTW. Adsorption and selectivity characteristics of several human serum proteins with immobilised hard Lewis metal ion-chelate adsorbents. *J. Chromatogr. a* 2000;890(1):95-116.

87. Johnson RD, Todd RJ, Arnold FH. Multipoint binding in metal-affinity chromatography II. effect of pH and imidazole on chromatographic retention of engineered histidine-containing cytochromes c. *J. Chromatogr. A* 1996;725(2):225-35.
88. Akgol S, Denizli A. Novel metal-chelate affinity sorbents for reversible use in catalase adsorption. *Journal of Molecular Catalysis B-Enzymatic* 2004;28(1):7-14.
89. Hochuli E, Bannwarth W, Dobeli H, Gentz R, Stuber D. Genetic approach to facilitate purification of recombinant proteins with a novel metal chelate adsorbent. *Bio-Technology* 1988;6(11):1321-5.
90. Zeng Q, Xu J, Fu R, Ye Q. Functional polymer affinity matrix for purifying hexahistidine-tagged recombinant protein. *J. Chromatogr. A* 2001;921(2):197-205.
91. Cha HJ, Wu CF, Valdes JJ, Rao G, Bentley WE. Observations of green fluorescent protein as a fusion partner in genetically engineered escherichia coli: Monitoring protein expression and solubility. *Biotechnol. Bioeng.* 2000;67(5):565-74.
92. Clemmitt RH, Chase HA. Facilitated downstream processing of a histidine-tagged protein from unclarified E-coli homogenates using immobilized metal affinity expanded-bed adsorption. *Biotechnol. Bioeng.* 2000;67(2):206-16.
93. Delcarte J, Fauconnier ML, Jacques P, Matsui K, Thonart P, Marlier M. Optimisation of expression and immobilized metal ion affinity chromatographic purification of recombinant (His)<sub>6</sub>-tagged cytochrome P450 hydroperoxide lyase in escherichia coli. *J. Chromatogr. B-Analyt. Technol. in Biomed. Life Sci.* 2003;786(1-2):229-36.
94. Hefti MH, Van Vugt-Van der Toorn CJG, Dixon R, Vervoort J. A novel purification method for histidine-tagged proteins containing a thrombin cleavage site. *Anal. Biochem.* 2001;295(2):180-5.
95. Ichikawa N, Mizuno M. Functional expression of hexahistidine-tagged beta-subunit of yeast F1-ATPase and isolation of the enzyme by immobilized metal affinity chromatography. *Protein Expr. Purif.* 2004;37(1):97-101.
96. Kumar A, Wahlund PO, Kepka C, Galaev IY, Mattiasson B. Purification of histidine-tagged single-chain fv-antibody fragments by metal chelate affinity precipitation using thermoresponsive copolymers. *Biotechnol. Bioeng.* 2003;84(4):494-503.
97. Singh SM, Panda AK. Solubilization and refolding of bacterial inclusion body proteins. *J. Biosci. Bioeng.* 2005;99(4):303-10.
98. Lemercier G, Bakalara N, Santarelli X. On-column refolding of an insoluble histidine tag recombinant exopolyphosphatase from trypanosoma brucei overexpressed in escherichia coli. *J. Chromatogr. B Analyt. Technol. Biomed. Life Sci.* 2003;786(1-2):305-9.
99. Glynou K, Ioannou PC, Christopoulos TK. One-step purification and refolding of recombinant photoprotein aequorin by immobilized metal-ion affinity chromatography. *Protein Expr. Purif.* 2003;27(2):384-90.

100. Rehm BH, Qi Q, Beermann BB, Hinz HJ, Steinbuchel A. Matrix-assisted in vitro refolding of pseudomonas aeruginosa class II polyhydroxyalkanoate synthase from inclusion bodies produced in recombinant escherichia coli. *Biochem. J.* 2001;358(Pt 1):263-8.
101. Schauer S, Luer C, Moser J. Large scale production of biologically active escherichia coli glutamyl-tRNA reductase from inclusion bodies. *Protein Expr. Purif.* 2003;31(2):271-5.
102. Vincent P, Dieryck W, Maneta-Peyret L, Moreau P, Cassagne C, Santarelli X. Chromatographic purification of an insoluble histidine tag recombinant Ykt6p SNARE from arabidopsis thaliana over-expressed in E-coli. *J. Chromatogr. B Analyt. Technol. Biomed. Life Sci.* 2004;808(1):83-9.
103. Yin SM, Zheng Y, Tien P. On-column purification and refolding of recombinant bovine prion protein: Using its octarepeat sequences as a natural affinity tag. *Protein Expr. Purif.* 2003;32(1):104-9.
104. Zahn R, von Schroetter C, Wuthrich K. Human prion proteins expressed in escherichia coli and purified by high-affinity column refolding. *FEBS Lett.* 1997;417(3):400-4.
105. Zhu XQ, Li SX, He HJ, Yuan QS. On-column refolding of an insoluble his(6)-tagged recombinant EGSOD overexpressed in escherichia coli. *Acta Biochim. Biophys. Sin.* 2005;37(4):265-9.
106. Zouhar J, Nanak E, Brzobohaty B. Expression, single-step purification, and matrix-assisted refolding of a maize cytokinin glucoside-specific beta-glucosidase. *Protein Expr. Purif.* 1999;17(1):153-62.
107. Feuerstein I, Morandell S, Stecher G, Huck CW, Stasyk T, Huang HL, Huber LA, Bonn GK. Phosphoproteomic analysis using immobilized metal ion affinity chromatography on the basis of cellulose powder. *Proteomics* 2005;5(1):46-54.
108. Urh M, Simpson D, Zhao K. Affinity chromatography: General methods. *Guide to Protein Purification, Second Edition* 2009;463:417-38.
109. Labrou NE. Design and selection of ligands for affinity chromatography. *Journal of J. Chromatogr. B Analyt. Technol. Biomed. Life Sci.* 2003;790(1-2):67-78.
110. Owen RO, McCreath GE, Chase HA. A new approach to continuous counter-current protein chromatography: Direct purification of malate dehydrogenase from a saccharomyces cerevisiae homogenate as a model system. *Biotechnol. Bioeng.* 1997;53(4):427-41.
111. Sherwood RF, Melton RG, Alwan SM, Hughes P. Purification and properties of carboxypeptidase G2 from pseudomonas sp strain rs-16 - use of a novel triazine dye affinity method. *Eur. J. Biochem.* 1985;148(3):447-53.
112. Andrews P. Gel-filtration behaviour of proteins related to their molecular weights over a wide range. *Biochem. J.* 1965;96(3):595,&.

113. Ashton AR, Polya GM. Specific interaction of cibacron and related dyes with cyclic nucleotide phosphodiesterase and lactate-dehydrogenase. *Biochem. J.* 1978;175(2):501-6.
114. Alderton WK, Lowe CR, Thatcher DR. Purification of recombinant ricin-a chain with immobilized triazine dyes. *J. Chromatogr. a* 1994;677(2):289-99.
115. Clonis YD, Labrou NE, Kotsira VP, Mazitsos C, Melissis S, Gogolas G. Biomimetic dyes as affinity chromatography tools in enzyme purification. *J. Chromatogr. a* 2000;891(1):33-44.
116. Lindner NM, Jeffcoat R, Lowe CR. Design and applications of biomimetic anthraquinone dyes. purification of calf intestinal alkaline phosphatase with immobilised terminal ring analogues of C.I. reactive blue 2. *J. Chromatogr.* 1989;473(1):227-40.
117. Bode W, Schwager P. Refined crystal-structure of bovine beta-trypsin at 1.8 a resolution .2. crystallographic refinement, calcium-binding site, benzamidine binding-site and active-site at ph 7.0. *J. Mol. Biol.* 1975;98(4):693-717.
118. Clonis YD, Goldfinch MJ, Lowe CR. The interaction of yeast hexokinase with procion green H-4g. *Biochem. J.* 1981;197(1):203-11.
119. Burton SJ, Mcloughlin SB, Stead CV, Lowe CR. Design and applications of biomimetic anthraquinone dyes .1. synthesis and characterization of terminal ring isomers of ci reactive blue-2. *J. Chromatogr.* 1988;435(1):127-37.
120. Hey Y, Dean PDG. Dyes - a colorful addition to protein-purification. *Chem. Ind.* 1981(20):726-32.
121. Clonis YD. Matrix evaluation for preparative high-performance affinity-chromatography. *J. Chromatogr.* 1987;407:179-87.
122. Clonis YD, Jones K, Lowe CR. Process scale high-performance liquid affinity-chromatography. *J. Chromatogr.* 1986;363(1):31-6.
123. Bresolin IT, Borsoi-Ribeiro M, Caro JR, dos Santos FP, de Castro MP, Bueno SM. Adsorption of human serum proteins onto TREN-agarose: Purification of human IgG by negative chromatography. *J. Chromatogr. B Analyt. Technol. Biomed. Life Sci.* 2009;877(1-2):17-23.
124. Bresolin IT, de Souza MC, Bueno SM. A new process of IgG purification by negative chromatography: Adsorption aspects of human serum proteins onto omega-aminodecyl-agarose. *J. Chromatogr. B Analyt. Technol. Biomed. Life Sci.* 2010;878(23):2087-93.
125. Hughes P, Lowe C, Sherwood R. Metal ion-promoted binding of proteins to immobilized triazine dye affinity adsorbents. *Biochim. Biophys. Acta* 1982;700(1):90-100.
126. Rajgopal S, Vijayalakshmi M. Purification of luciferase by affinity elution chromatography on blue dextran columns - comparison of sepharose and silica as support matrices. *J. Chromatogr.* 1982;243(1):164-7.

127. Bosanac T, Wilcox CS. A photoactivated precipiton for reagent sequestration in solution-phase synthesis. *J. Am. Chem. Soc.* 2002;124(16):4194-5.
128. Bosanac T, Wilcox CS. A novel precipitating auxiliary approach to the purification of baylis-hillman adducts. *Chem. Commun. (Camb)* 2001;(17)(17):1618-9.
129. Bosanac T, Wilcox CS. Precipiton strategies applied to the isolation of alpha-substituted beta-ketoesters. *Tetrahedron Lett.* 2001;42(26):4309-12.
130. Herkstro.Wg, Hammond GS. Mechanisms of photochemical reactions in solution .39. study of energy transfer by kinetic spectrophotometry. *J. Am. Chem. Soc.* 1966;88(21):4769,&.
131. Ali MA, Tsuda Y. New method for isomerization of (Z)-stilbenes into the (E)-isomers catalyzed by diaryl disulfide. *Chem. Pharm. Bull.* 1992;40(10):2842-4.
132. Shankar BB, Yang DY, Girton S, Ganguly AK. One pot solid phase synthesis of isoxazolines. *Tetrahedron Lett.* 1998;39(17):2447-8.
133. Savage GP, Wernert GT. Nitrile oxide cycloaddition chemistry using benzotriazole as a steric auxiliary. *Aust J Chem* 2005;58(12):877-81.
134. Kellogg RM, Vanbergen TJ, Vandoren H, Hedstrand D, Kooi J, Kruizinga WH, Troostwijk CB. The hantzsch 1,4-dihydropyridine synthesis as a route to bridged pyridine and dihydropyridine crown ethers. *J. Org. Chem.* 1980;45(14):2854-61.
135. Kawai Y, Hida K, Dao DH, Ohno A. Asymmetric synthesis of beta-hydroxy esters having three consecutive chiral centers with a reductase from bakers' yeast. *Tetrahedron Lett.* 1998;39(50):9219-22.
136. Basavaiah D, Rao PD, Hyma RS. The Baylis-Hillman reaction: A novel carbon-carbon bond forming reaction. *Tetrahedron* 1996;52(24):8001-62.
137. Fort Y, Berthe MC, Caubere P. The Baylis-Hillman reaction-mechanism and applications revisited. *Tetrahedron* 1992;48(31):6371-84.
138. Brzezinski LJ, Rafel S, Leahy JW. The asymmetric Baylis-Hillman reaction as a template in organic synthesis. *Tetrahedron* 1997;53(48):16423-34.
139. Matile S, Som A, Sorde N. Recent synthetic ion channels and pores. *Tetrahedron* 2004;60(31):6405-35.
140. FYLES T, JAMES T, KAYE K. Biomimetic ion-transport - on the mechanism of ion-transport by an artificial ion channel mimic rid B-5125-2009. *Canadian Journal of Chemistry-Revue Canadienne De Chimie* 1990;68(6):976-8.
141. Fyles T, Kaye K, James T, Smiley D. Biomimetic ion-transport - synthesis and activity of an amphotericin mimic rid B-5125-2009. *Tetrahedron Lett.* 1990;31(9):1233-6.

142. Kano K, Fendler J. Pyranine as a sensitive ph probe for liposome interiors and surfaces - ph gradients across phospholipid vesicles. *Biochim. Biophys. Acta* 1978;509(2):289-99.
143. Iwaszko E, Wardak A, Krupa Z, Gruszecki W. Ion transport across model lipid membranes containing light-harvesting complex II: An effect of light. *J. Photochem. Photobiol. B-Biol.* 2004;74(1):13-21.
144. Coutinho A, Silva L, Fedorov A, Prieto M. Cholesterol and ergosterol influence nystatin surface aggregation: Relation to pore formation. *Biophys J.* 2004;87(5):3264-76.
145. Carmichael V, Dutton P, Fyles T, James T, Swan J, Zojaji M. Biomimetic ion-transport - a functional-model of a unimolecular ion channel. *J. Am. Chem. Soc.* 1989;111(2):767-9.
146. Gokel G, Schlesinger P, Djedovic N, Ferdani R, Harder E, Hu J, Leevy W, Pajewska J, Pajewski R, Weber M. Functional, synthetic organic chemical models of cellular ion channels. *Bioorg. Med. Chem.* 2004;12(6):1291-304.
147. Rex S. Pore formation induced by the peptide melittin in different lipid vesicle membranes. *Biophys. Chem.* 1996;58(1-2):75-85.
148. Barbet J, Machy P, Truneh A, Leserman L. Weak acid-induced release of liposome-encapsulated carboxyfluorescein. *Biochim. Biophys. Acta.* 1984;772(3):347-56.
149. Tedesco M, Matile S. Spectroscopic detection of endovesiculation by large unilamellar phosphatidylcholine vesicles: Effects of chlorpromazine, dibucaine, and safinolol. *Bioorg. Med. Chem.* 1999;7(7):1373-9.
150. Walter A, Siegel D. Divalent cation-induced lipid mixing between phosphatidylserine liposomes studied by stopped-flow fluorescence measurements - effects of temperature, comparison of barium and calcium, and perturbation by dpx. *Biochemistry (N Y)* 1993;32(13):3271-81.
151. Lin F, Chen W, Hearn M. Microcalorimetric studies on the interaction mechanism between proteins and hydrophobic solid surfaces in hydrophobic interaction chromatography: Effects of salts, hydrophobicity of the sorbent, and structure of the protein. *Anal. Chem.* 2001;73(16):3875-83.
152. Shinoda S, Nishimura T, Tadokoro M, Tsukube H. Ester-armed cyclens having quadruplicated helical geometry: Remarkably stable and selective encapsulation of  $\text{Na}^+$  ion. *J. Org. Chem.* 2001;66(18):6104-8.
153. Nishimura T, Shinoda S, Tsukube H. Chirality induction in supramolecular aggregate: Chiral recognition between armed cyclen- $\text{Na}^+$  complexes having quadruplicated helical geometry. *Chirality* 2002;14(7):555-7.
154. Hinze WL, Pramauro E. A critical-review of surfactant-mediated phase separations (cloud-point extractions) - theory and applications. *Crit. Rev. Anal. Chem.* 1993;24(2):133-77.

155. Cuatrecasas P, Anfinsen CB. Affinity chromatography. *Annu. Rev. Biochem.* 1971;40:259-&.
156. Diamandis EP, Christopoulos TK. The biotin (strept)avidin system - principles and applications in biotechnology. *Clin. Chem.* 1991;37(5):625-36.
157. Lee WC, Lee KH. Applications of affinity chromatography in proteomics. *Anal. Biochem.* 2004;324(1):1-10.
158. Anderson DJ, Blobel G. Immunoprecipitation of proteins from cell-free translations. *Meth Enzymol* 1983;96:111-20.
159. Bjerrum OJ. Immunochemical investigation of membrane proteins - a methodological survey with emphasis placed on immunoprecipitation in gels. *Biochim. Biophys. Acta.* 1977;472(2):135-95.
160. Hirabayashi J, Hashidate T, Arata Y, Nishi N, Nakamura T, Hirashima M, Urashima T, Oka T, Futai M, Muller WEG, Yagi F, Kasai K. Oligosaccharide specificity of galectins: A search by frontal affinity chromatography. *Biochimica. Et Biophysica. Acta.-General Subjects* 2002;1572(2-3):232-54.
161. Monnig CA, Kennedy RT. Capillary electrophoresis. *Anal. Chem.* 1994;66(12):R280-314.
162. Krylov SN, Dovichi NJ. Capillary electrophoresis for the analysis of biopolymers. *Anal. Chem.* 2000;72(12):111R-28R.
163. Righetti PG, Bossi A. Isoelectric focusing of proteins and peptides in gel slabs and in capillaries. *Anal. Chim. Acta.* 1998;372(1-2):1-19.
164. Clonis YD. Affinity chromatography matures as bioinformatic and combinatorial tools develop. *J. Chromatogr. a* 2006;1101(1-2):1-24.
165. Righetti PG. Bioanalysis: Its past, present, and some future. *Electrophoresis* 2004;25(14):2111-27.
166. Saleh A, Alvarez-Venegas R, Avramova Z. An efficient chromatin immunoprecipitation (ChIP) protocol for studying histone modifications in arabidopsis plants. *Nat. Protoc.* 2008;3(6):1018-25.
167. Arakawa T, Timasheff SN. Preferential interactions of proteins with salts in concentrated-solutions. *Biochemistry (N Y )* 1982;21(25):6545-52.
168. Baldwin RL. How Hofmeister ion interactions affect protein stability. *Biophys J.* 1996;71(4):2056-63.
169. Goodwin GH, Nicolas RH, Johns EW. Improved large-scale fractionation of high mobility group non-histone chromatin proteins. *Biochim. Biophys. Acta.* 1975;405(2):280-91.



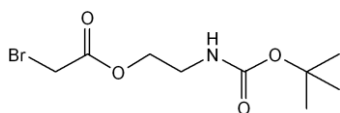
170. Winschel CA, Kaushik V, Abdrakhmanova G, Aris SM, Sidorov V. New noninvasive methodology for real-time monitoring of lipid flip. *Bioconjug. Chem.* 2007;18(5):1507-15.
171. Vente JA, Bosch H, de Haan AB, Bussmann PJT. Comparison of sorption isotherms of mono- and disaccharides relevant to oligosaccharide separations for Na, K, and Ca loaded cation exchange resins. *Chem. Eng. Commun.* 2005;192(1):23-33.
172. Bhushan R, Kaur S. TLC separation of some common sugars on silica gel plates impregnated with transition metal ions. *Biomed. Chromatogr.* 1997;11(1):59-60.
173. Chavez-Servin JL, Castellote AI, Lopez-Sabater MC. Analysis of mono- and disaccharides in milk-based formulae by high-performance liquid chromatography with refractive index detection. *J. Chromatogr. A* 2004;1043(2):211-5.
174. Evangelista RA, Liu MS, Chen FTA. Characterization of 9-aminopyrene-1,4,6-trisulfonate-derivatized sugars by capillary electrophoresis with laser-induced fluorescence detection. *Anal. Chem.* 1995;67(13):2239-45.
175. Jin LJ, Li SFY. Screening of carbohydrates in urine by capillary electrophoresis. *Electrophoresis* 1999;20(17):3450-4.
176. Hong Q, Rogero C, Lakey JH, Connolly BA, Houlton A, Horrocks BR. Immobilisation of proteins at silicon surfaces using undecenylaldehyde: Demonstration of the retention of protein functionality and detection strategies. *Analyst* 2009;134(3):593-601.
177. Hirsh J, Warkentin TE, Shaughnessy SG, Anand SS, Halperin JL, Raschke R, Granger C, Ohman EM, Dalen JE. Heparin and low-molecular-weight heparin - mechanisms of action, pharmacokinetics, dosing, monitoring, efficacy, and safety. *Chest* 2001;119(1):64S-94S.
178. Gemma E, Meyer O, Uhrin D, Hulme AN. Enabling methodology for the end functionalisation of glycosaminoglycan oligosaccharides. *Mol. Biosyst.* 2008;4(6):481-95.
179. Lehrer S. Intramolecular pyrene excimer fluorescence: A probe of proximity and protein conformational change. *Fluoresc. Spectrosc.* 1997;278:286-95.
180. Marti AA, Jockusch S, Stevens N, Ju J, Turro NJ. Fluorescent hybridization probes for sensitive and selective DNA and RNA detection. *Acc. Chem. Res.* 2007;40(6):402-9.
181. Baumgartner C, Richtol H, Aikens D. Transient photochemistry of safranin-O. *Photochem. Photobiol.* 1981;34(1):17-22.
182. Rabenstein D. Heparin and heparan sulfate: Structure and function. *Nat. Prod. Rep.* 2002;19(3):312-31.
183. Olson S, Bjork I, Sheffer R, Craig P, Shore J, Choay J. Role of the antithrombin-binding pentasaccharide in heparin acceleration of antithrombin-proteinase reactions - resolution

- of the antithrombin conformational change contribution to heparin rate enhancement. *J. Biol. Chem.* 1992;267(18):12528-38.
184. Warkentin T, Levine M, Hirsh J, Horsewood P, Roberts R, Gent M, Kelton J. Heparin-induced thrombocytopenia in patients treated with low-molecular-weight heparin or unfractionated heparin. *N. Engl. J. Med.* 1995;332(20):1330-5.
185. Improgo MRD, Scofield MD, Tapper AR, Gardner PD. The nicotinic acetylcholine receptor CHRNA5/A3/B4 gene cluster: Dual role in nicotine addiction and lung cancer. *Prog. Neurobiol.* 2010;92(2):212-26.
186. Arneric SP, Holladay M, Williams M. Neuronal nicotinic receptors: A perspective on two decades of drug discovery research. *Biochem. Pharmacol.* 2007;74(8):1092-101.
187. Levin ED, Rezvani AH. Nicotinic interactions with antipsychotic drugs, models of schizophrenia and impacts on cognitive function. *Biochem. Pharmacol.* 2007;74(8):1182-91.
188. Romanelli MN, Gratteri P, Guandalini L, Martini E, Bonaccini C, Gualtieri F. Central nicotinic receptors: Structure, function, ligands, and therapeutic potential. *Chemmedchem.* 2007;2(6):746-67.
189. Taly A, Corringer P, Guedin D, Lestage P, Changeux J. Nicotinic receptors: Allosteric transitions and therapeutic targets in the nervous system. *Nat. Rev. Drug Discovery* 2009;8(9):733-50.
190. <http://www.inflammation.dk/iir/30arthritis/abig.htm>
191. Renn O, Meares CF. Large scale synthesis of the bifunctional chelating agent 2-(*p*-Nitrobenzyl)-1,4,7,10-tetraazacyclododecane-*N,N',N'',N'''*-tetraacetic Acid, and determination of its enantiomeric purity by chiral chromatography. *Bioconjugate Chem.* 1992;3(6):563-569.

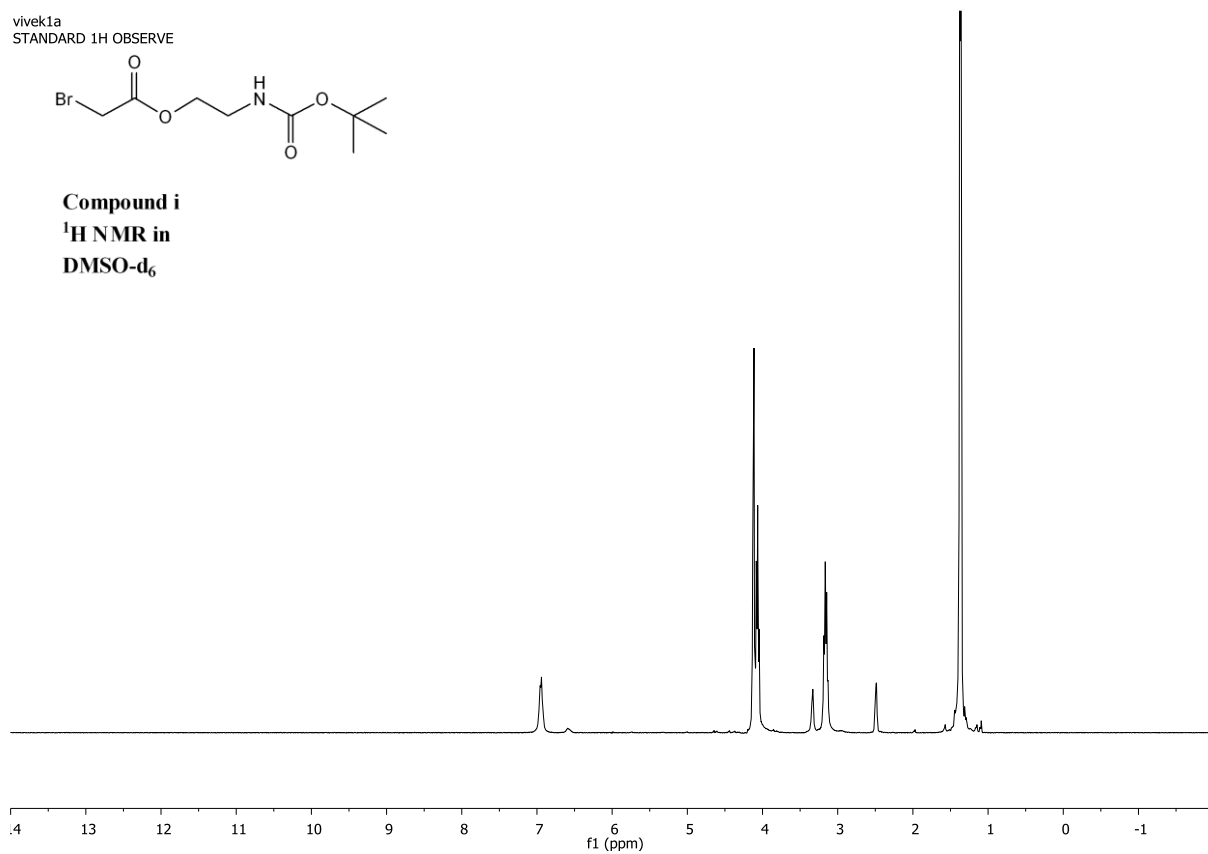
## APPENDIX

### $^1\text{H}$ and $^{13}\text{C}$ NMR

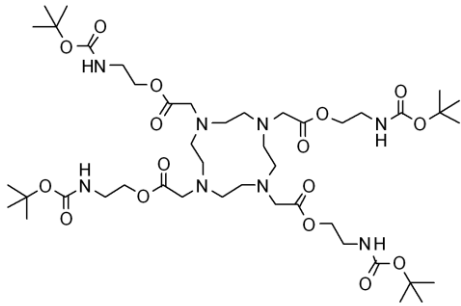
vivek1a  
STANDARD 1H OBSERVE



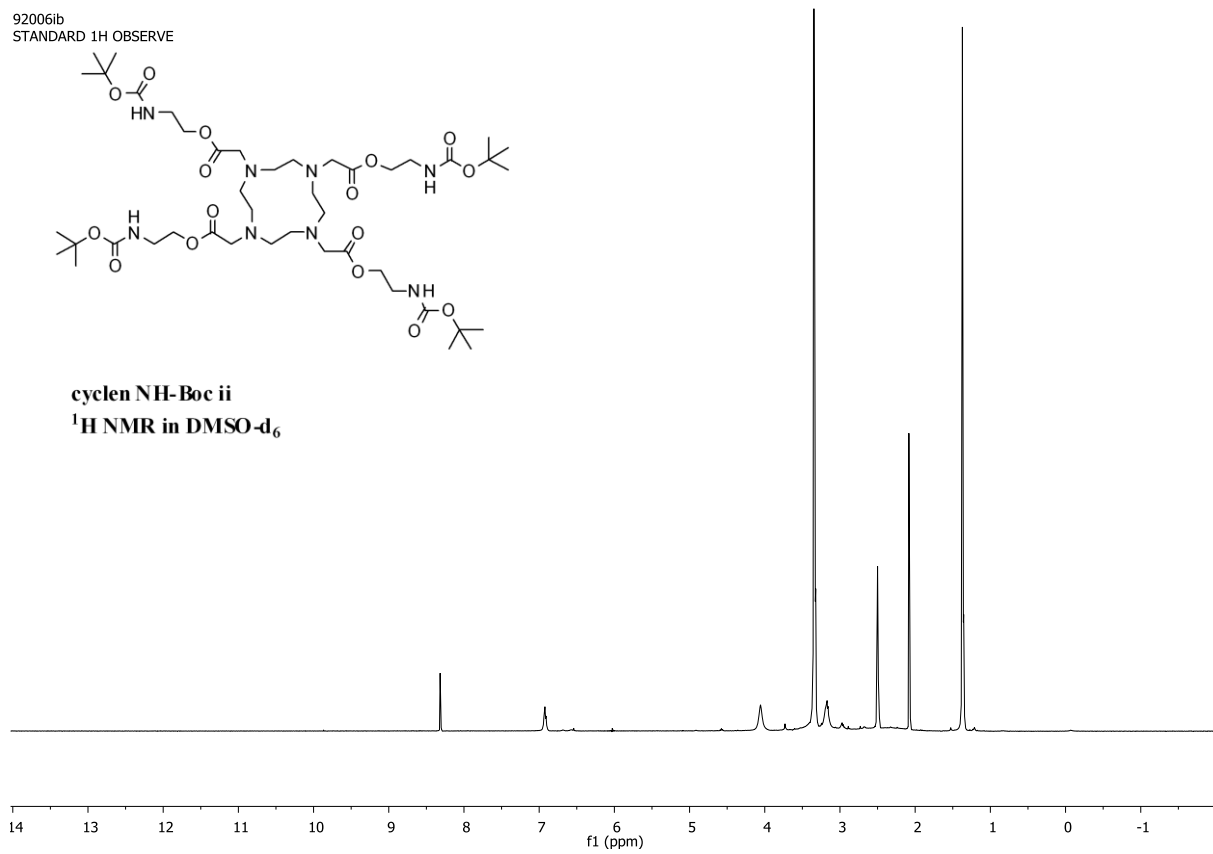
**Compound i**  
**<sup>1</sup>H NMR in**  
**DMSO-d<sub>6</sub>**



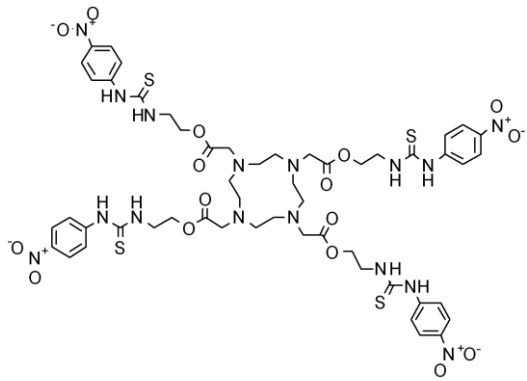
92006ib  
STANDARD 1H OBSERVE



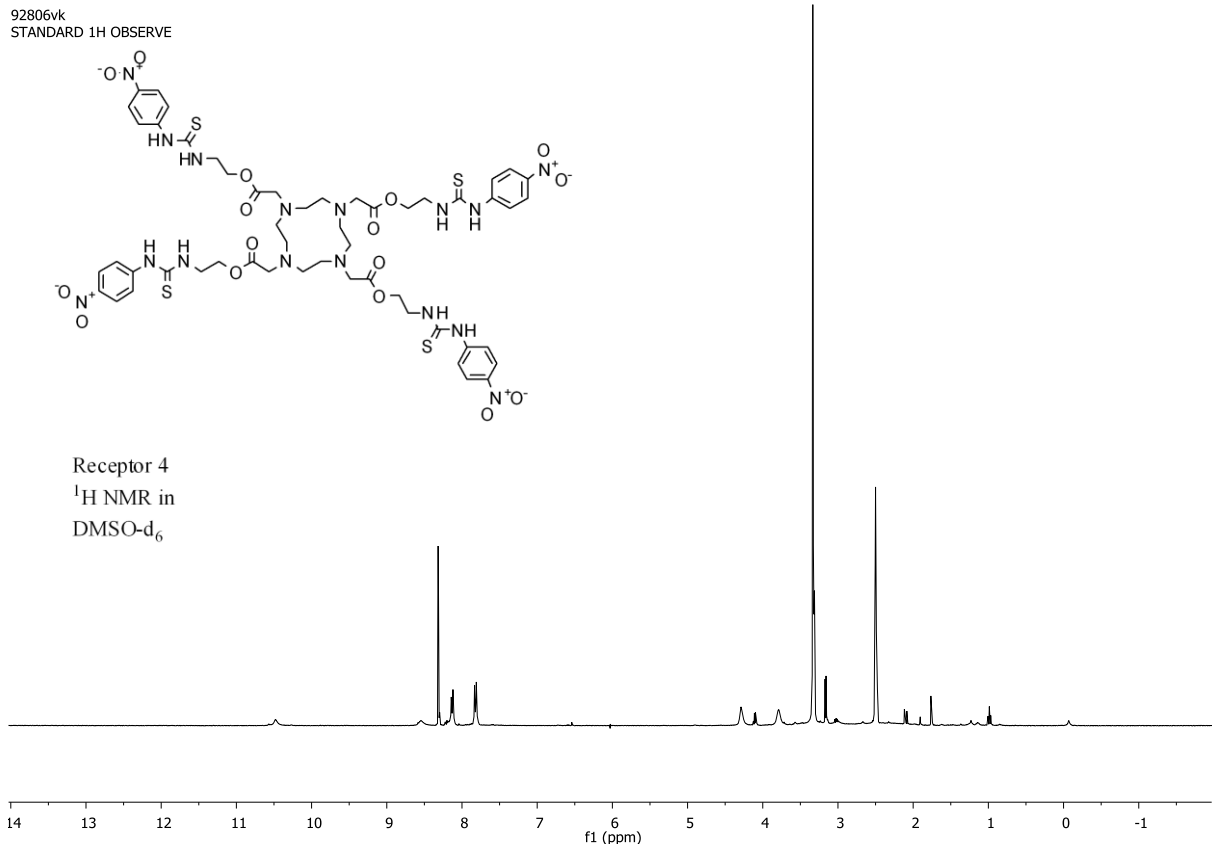
**cyclen NH-Boc ii**  
<sup>1</sup>H NMR in DMSO-d<sub>6</sub>



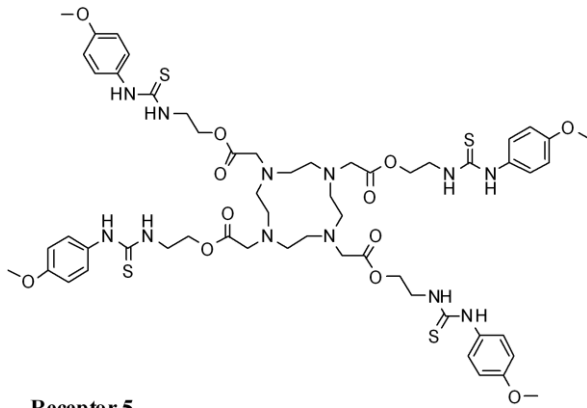
92806vk  
STANDARD 1H OBSERVE



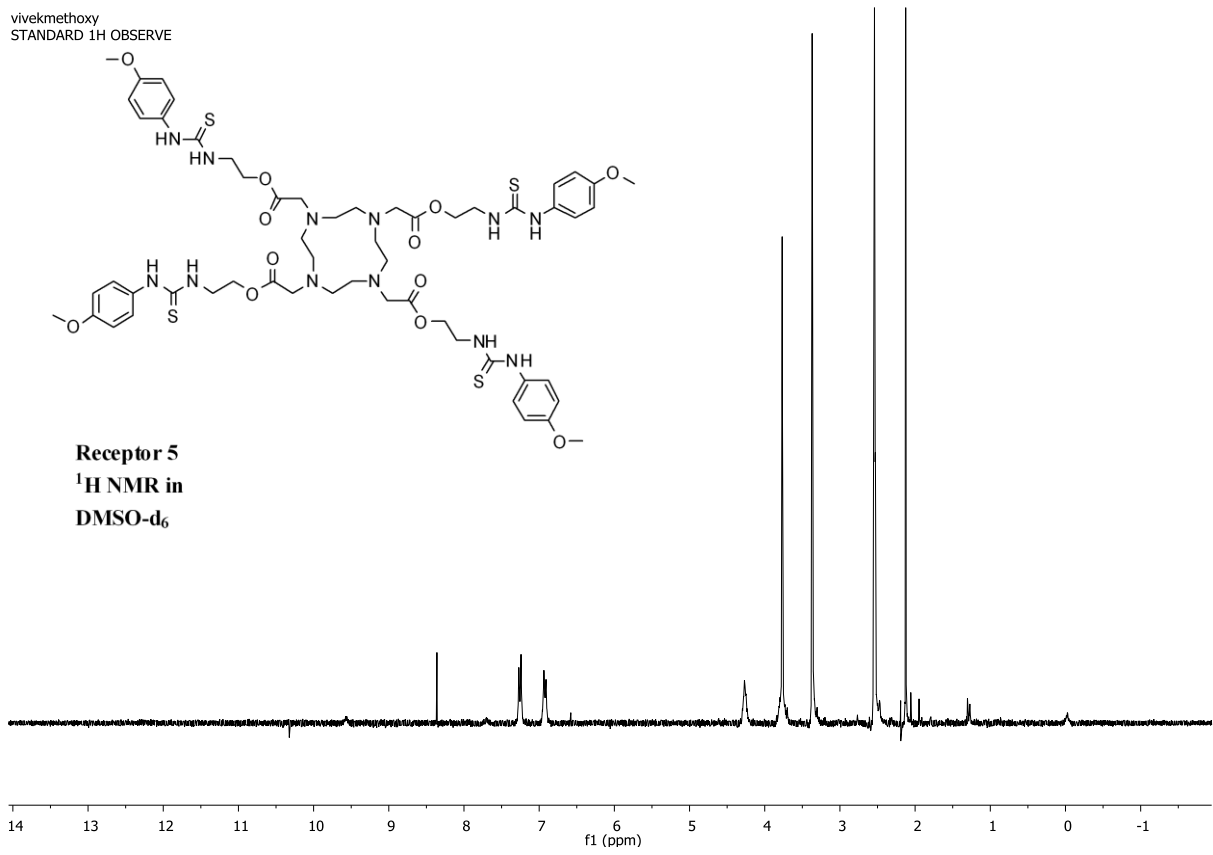
Receptor 4  
<sup>1</sup>H NMR in  
DMSO-d<sub>6</sub>



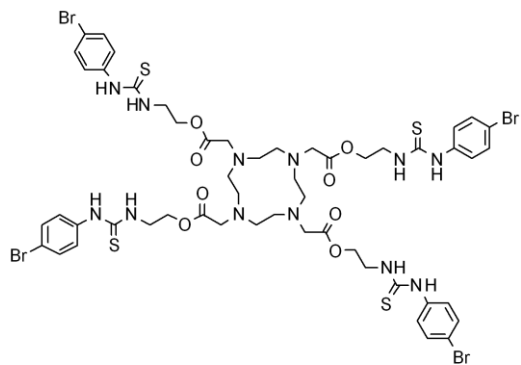
vivekmethoxy  
STANDARD 1H OBSERVE



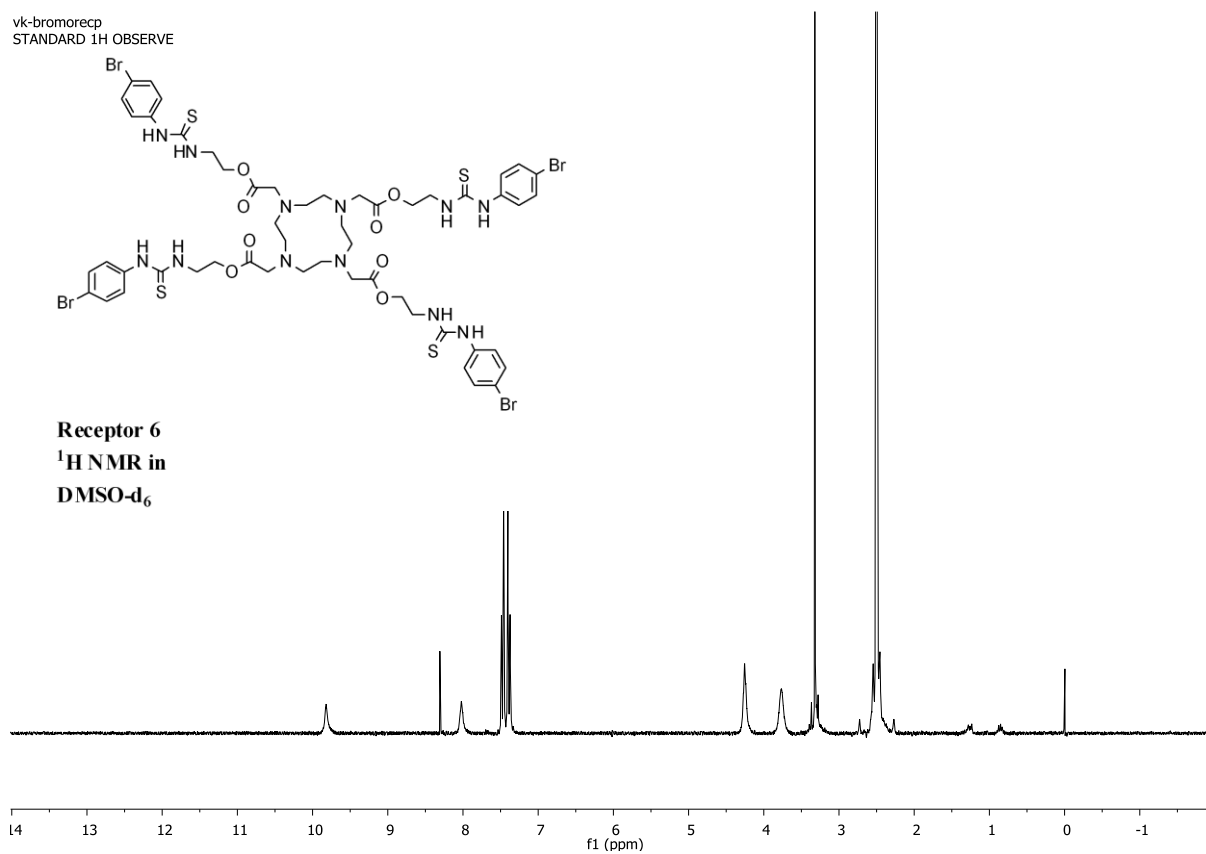
**Receptor 5**  
**<sup>1</sup>H NMR in**  
**DMSO-d<sub>6</sub>**



vk-bromorecp  
STANDARD 1H OBSERVE

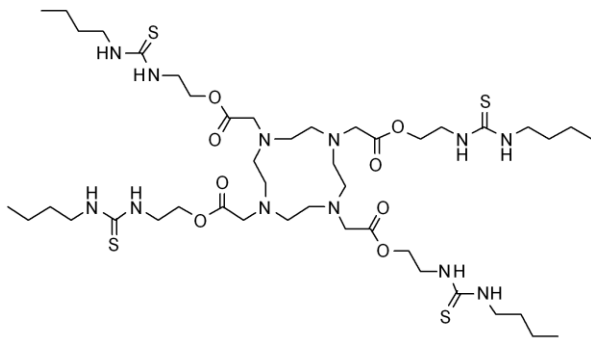


**Receptor 6**  
**<sup>1</sup>H NMR in**  
**DMSO-d<sub>6</sub>**

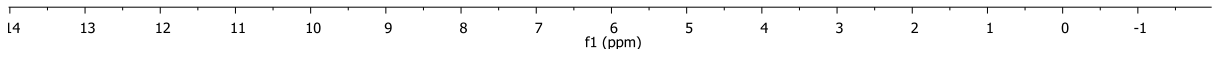
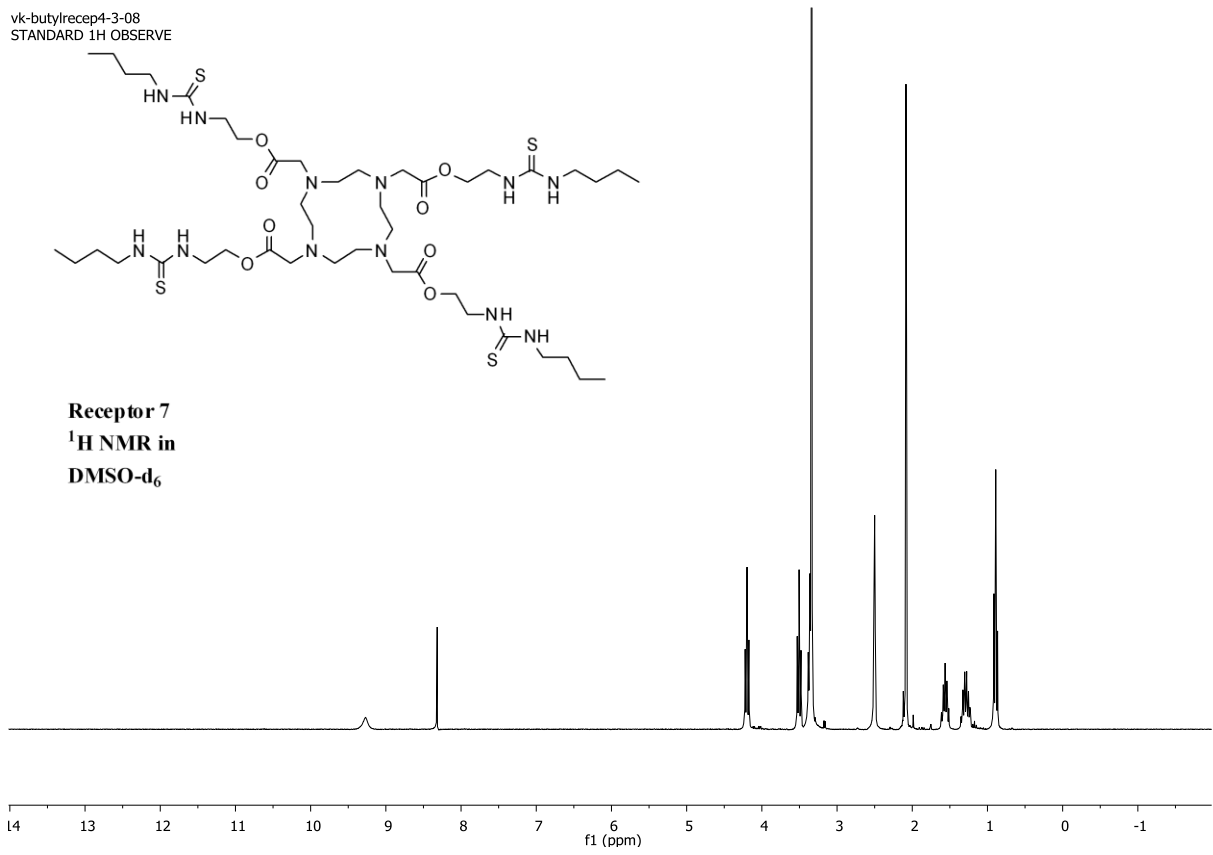




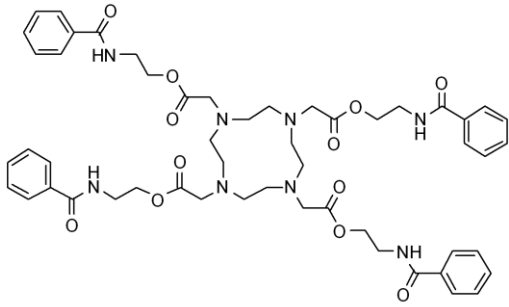
vk-butylrecep4-3-08  
STANDARD 1H OBSERVE



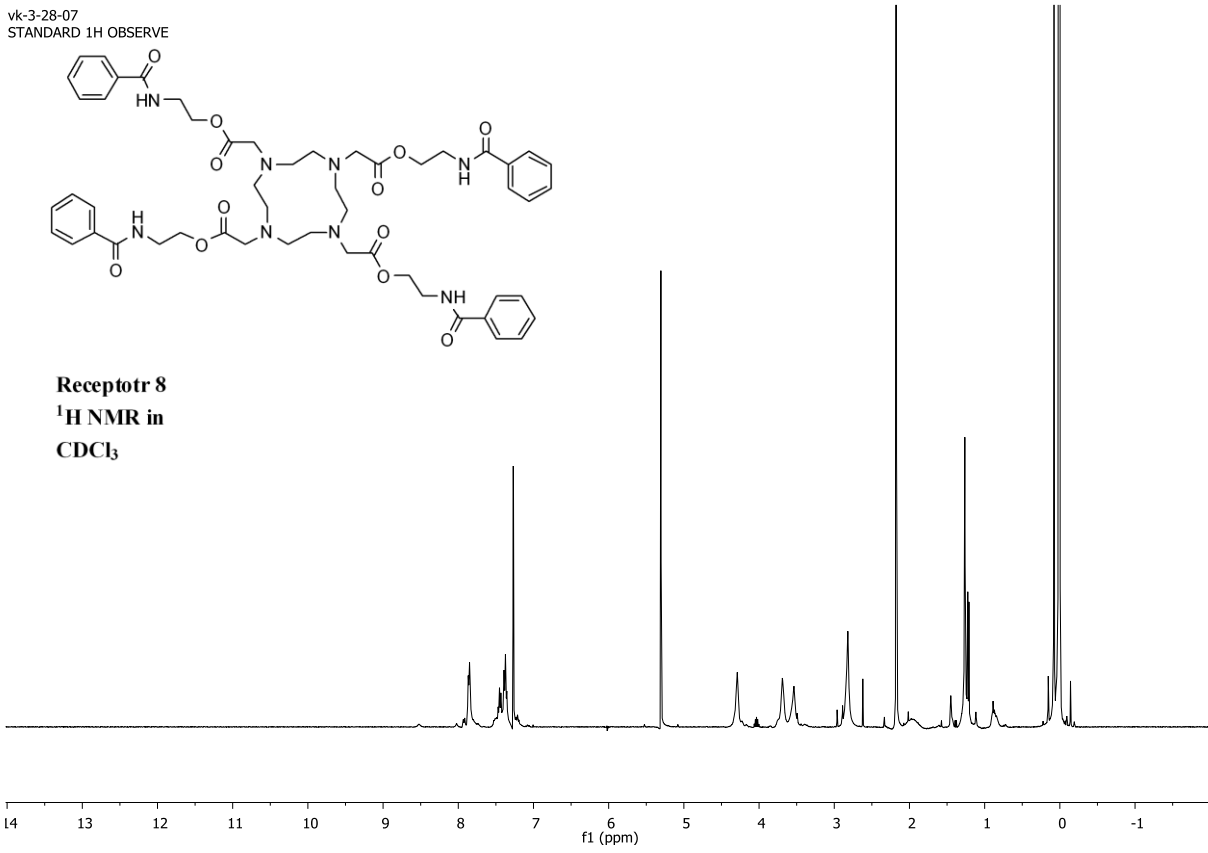
**Receptor 7**  
**<sup>1</sup>H NMR in**  
**DMSO-d<sub>6</sub>**



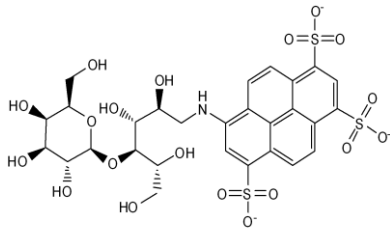
vk-3-28-07  
STANDARD 1H OBSERVE



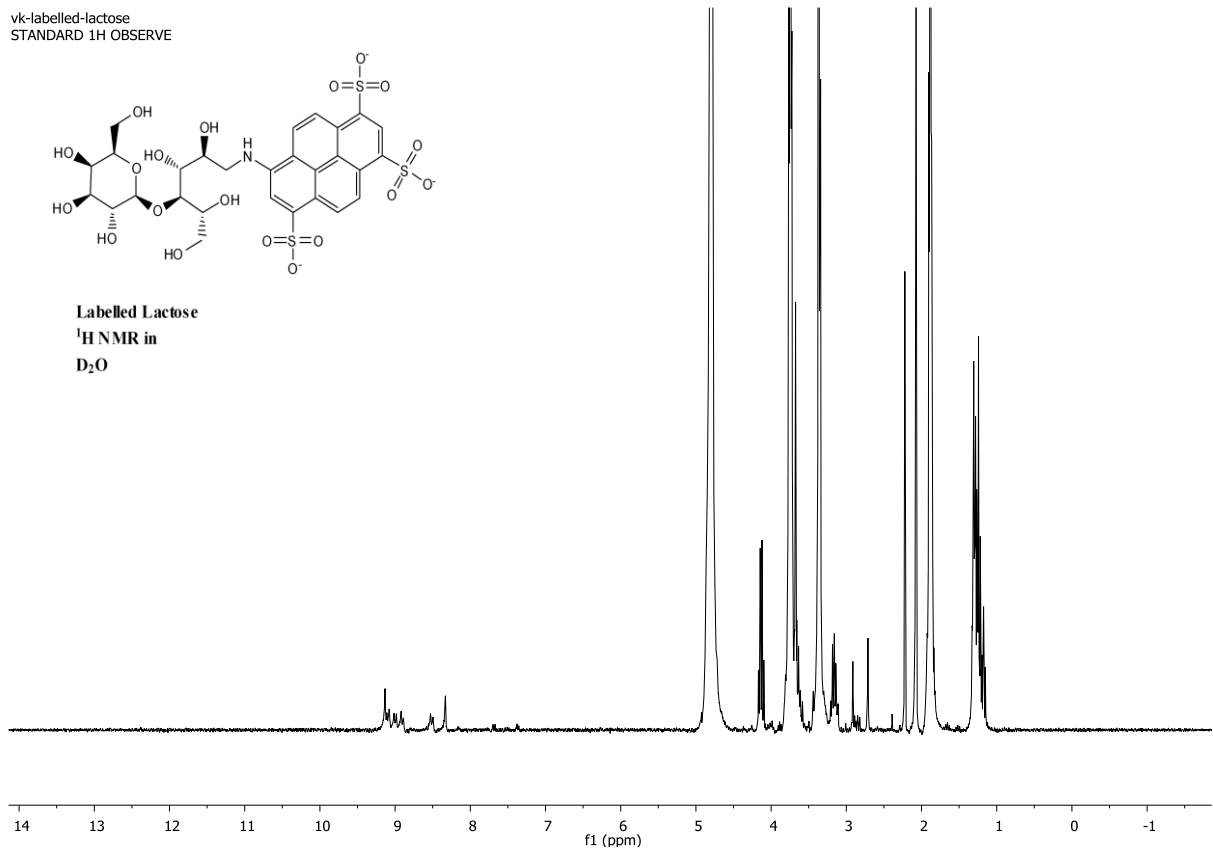
**Receptotr 8**  
**<sup>1</sup>H NMR in**  
**CDCl<sub>3</sub>**



vk-labelled-lactose  
STANDARD 1H OBSERVE



Labelled Lactose  
<sup>1</sup>H NMR in  
D<sub>2</sub>O

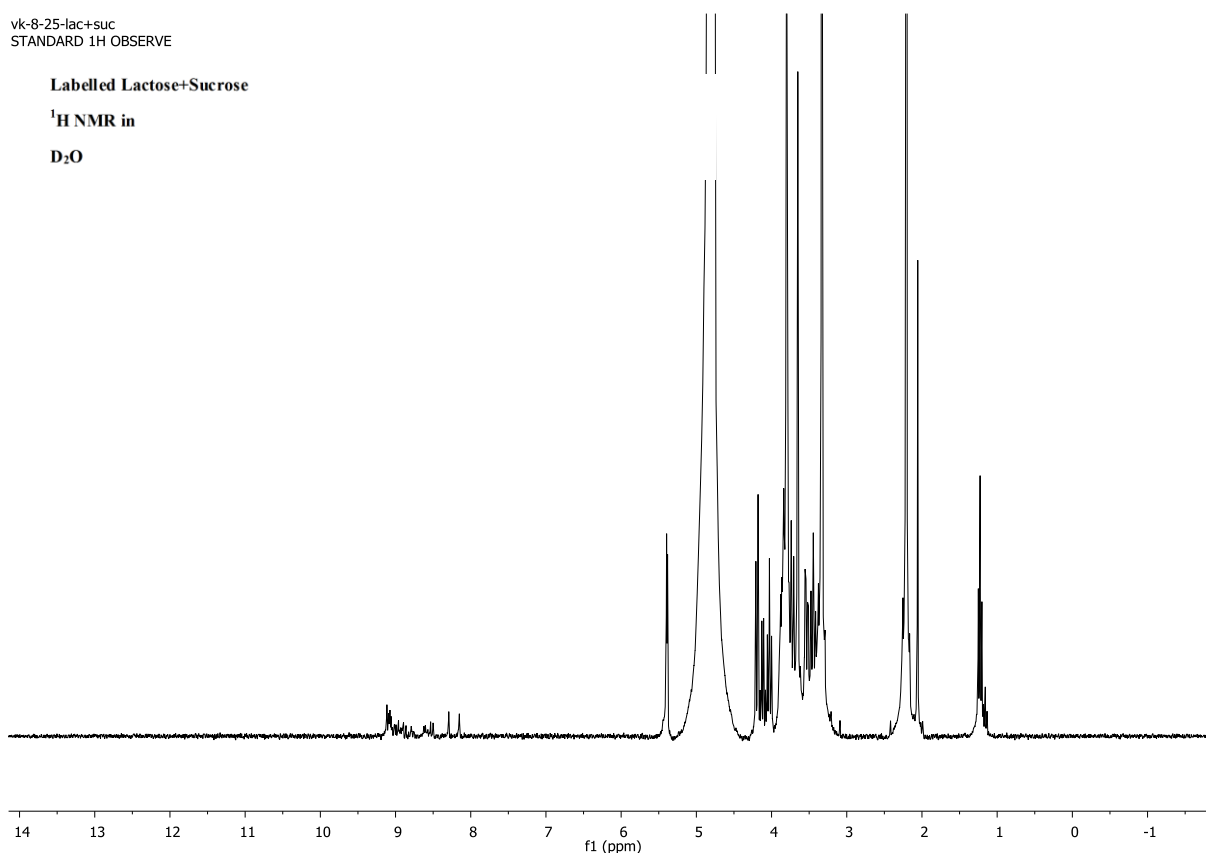


vk-8-25-lac+suc  
STANDARD 1H OBSERVE

Labelled Lactose+Sucrose

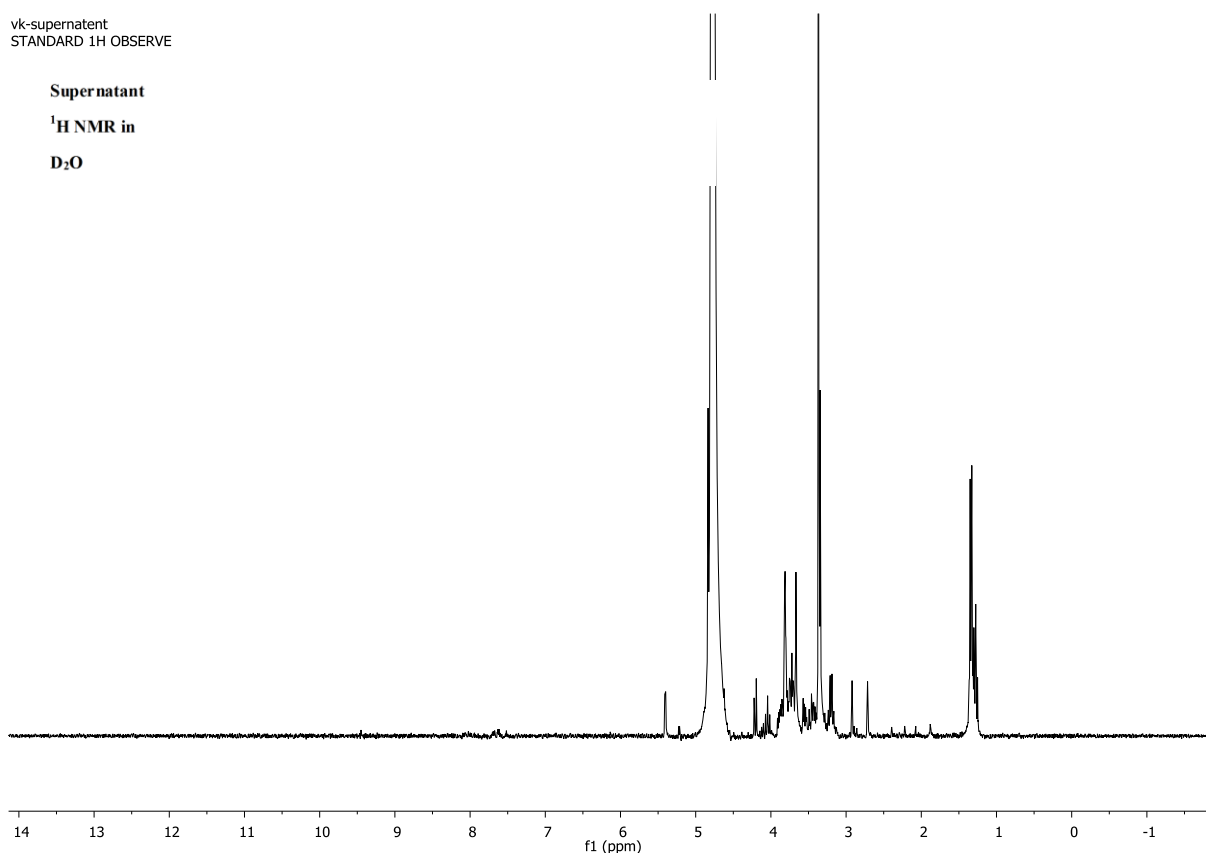
$^1\text{H}$  NMR in

$\text{D}_2\text{O}$



vk-supernatant  
STANDARD 1H OBSERVE

Supernatant  
<sup>1</sup>H NMR in  
D<sub>2</sub>O

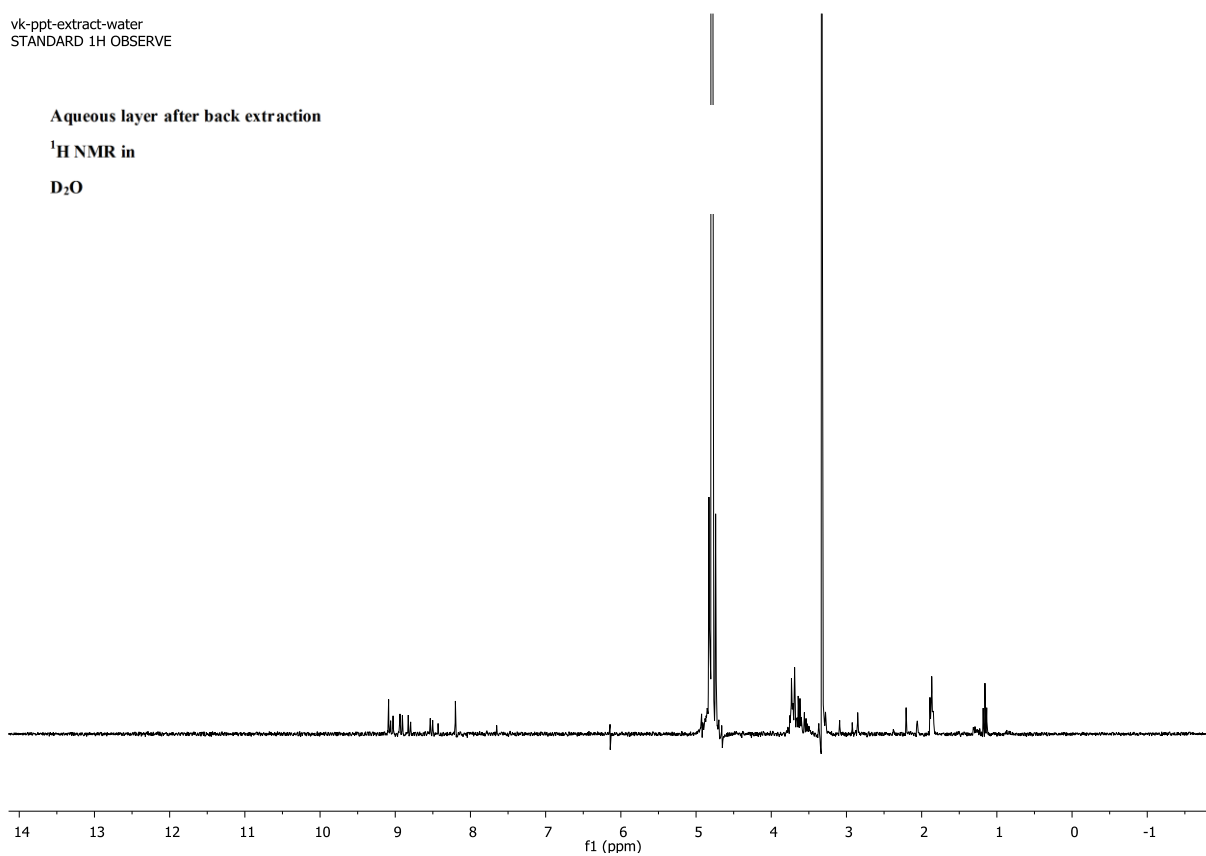


vk-ppt-extract-water  
STANDARD 1H OBSERVE

Aqueous layer after back extraction

$^1\text{H}$  NMR in

$\text{D}_2\text{O}$

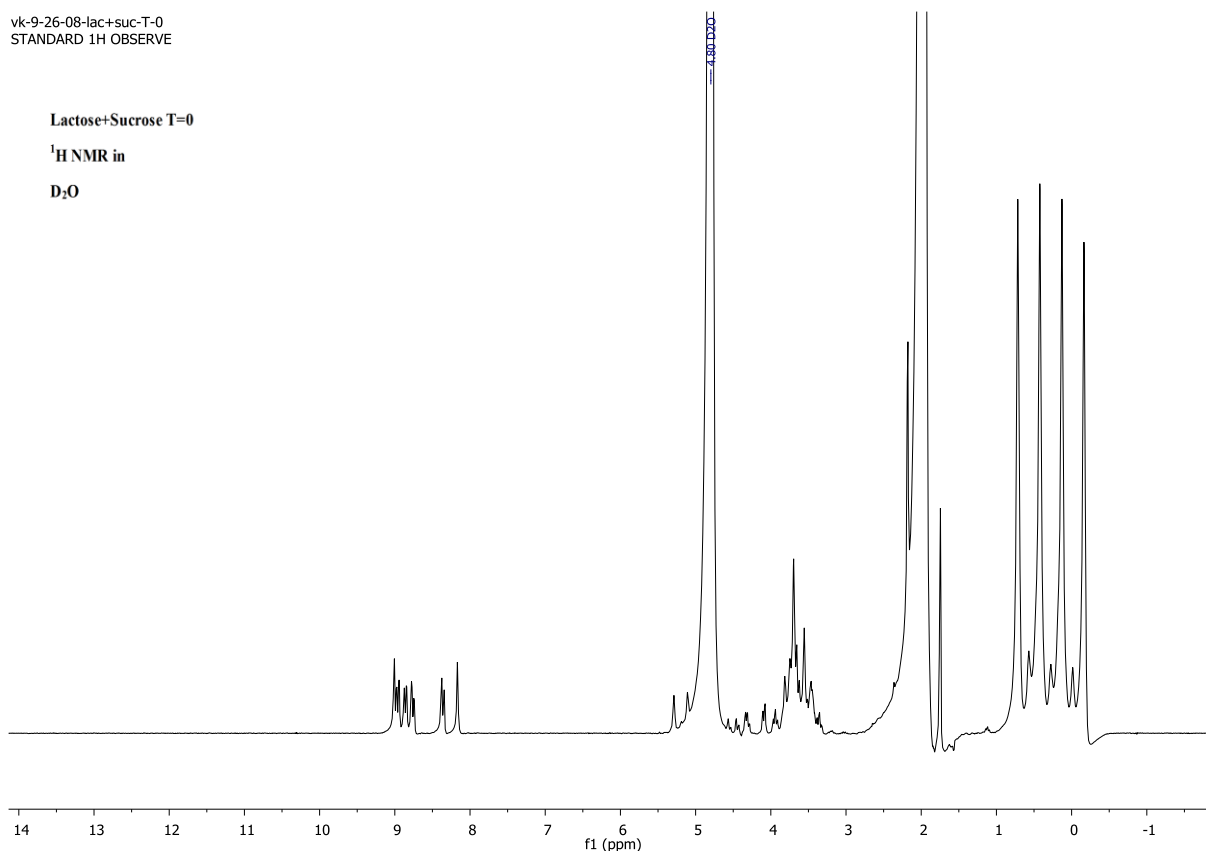


vk-9-26-08-lac+suc-T-0  
STANDARD 1H OBSERVE

Lactose+Sucrose T=0

<sup>1</sup>H NMR in

D<sub>2</sub>O

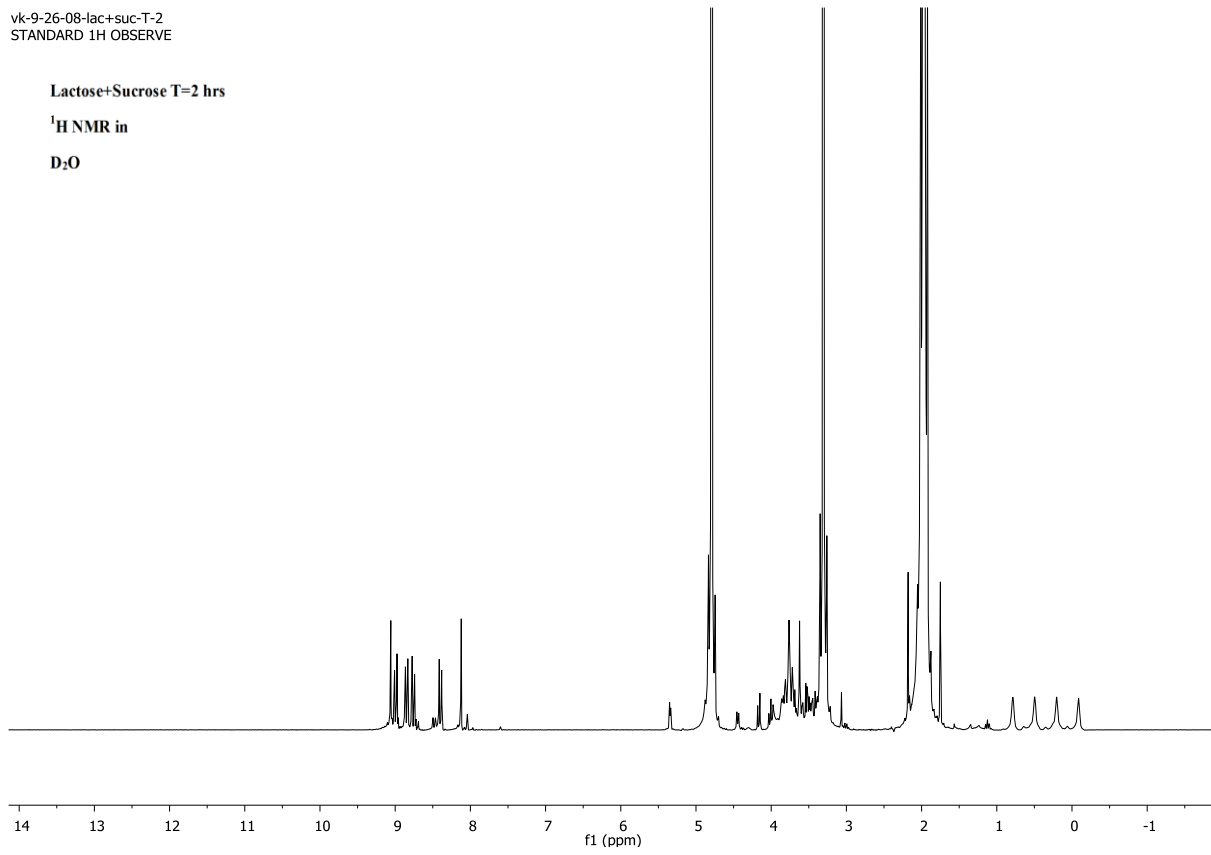


vk-9-26-08-lac+suc-T-2  
STANDARD 1H OBSERVE

Lactose+Sucrose T=2 hrs

$^1\text{H}$  NMR in

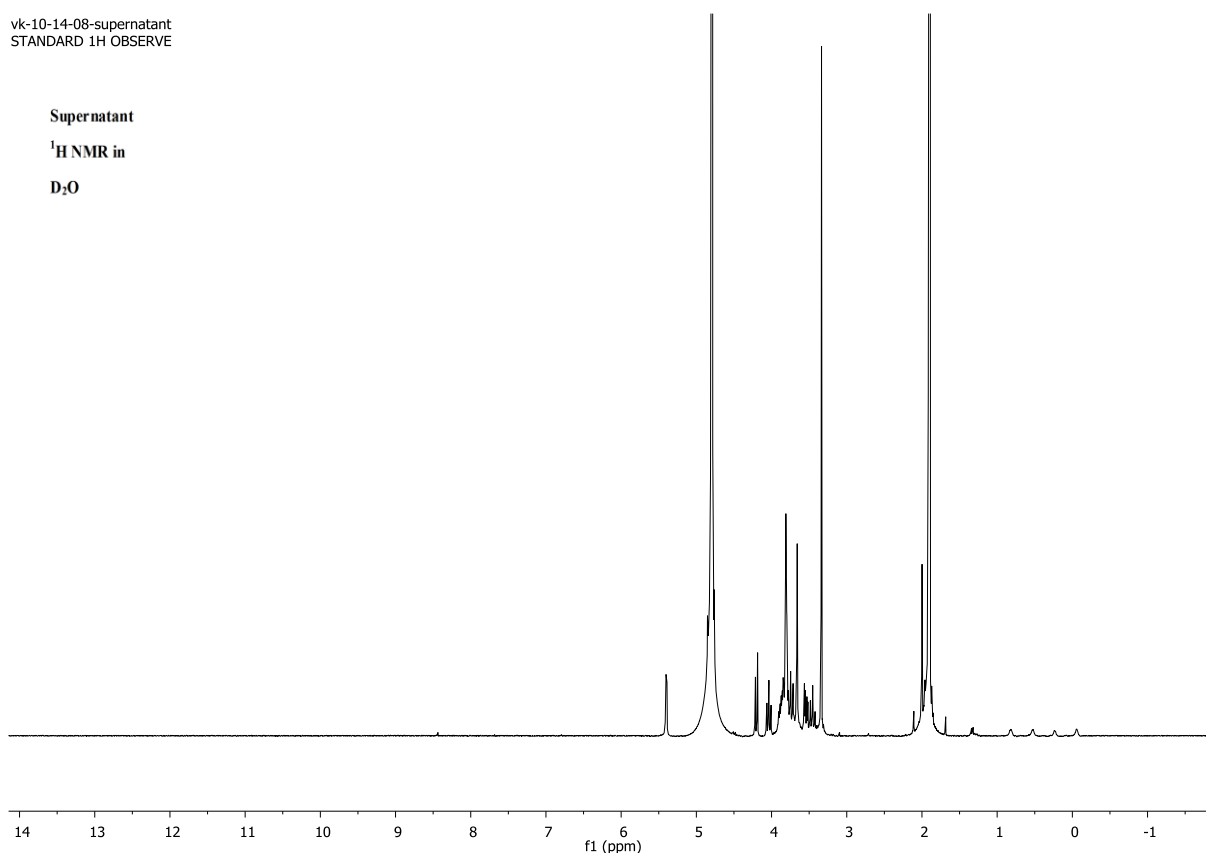
$\text{D}_2\text{O}$



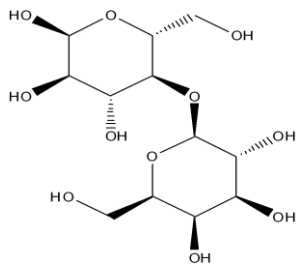


vk-10-14-08-supernatant  
STANDARD 1H OBSERVE

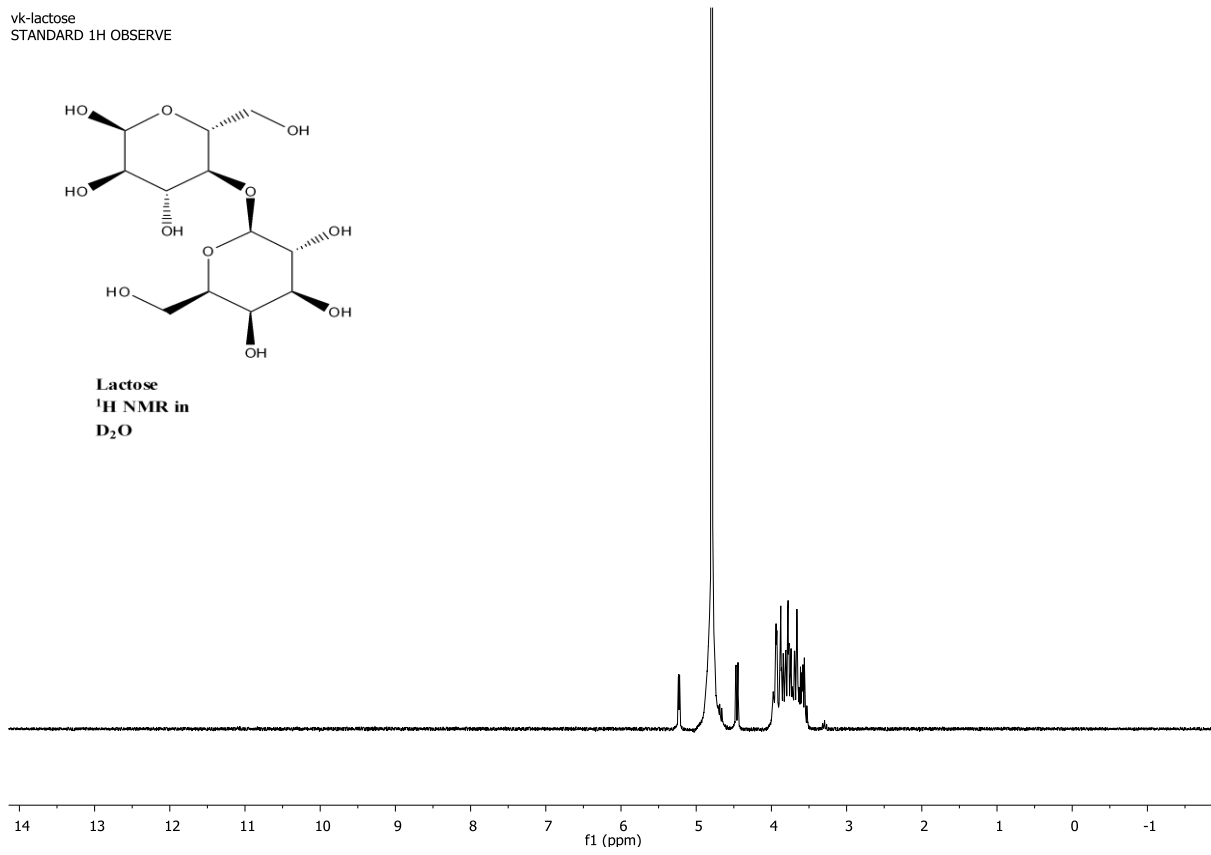
Supernatant  
<sup>1</sup>H NMR in  
D<sub>2</sub>O



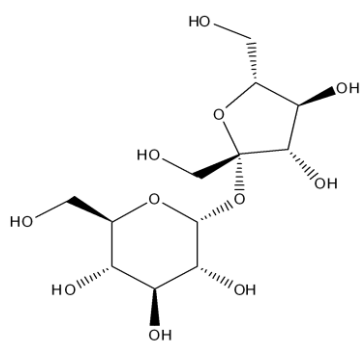
vk-lactose  
STANDARD 1H OBSERVE



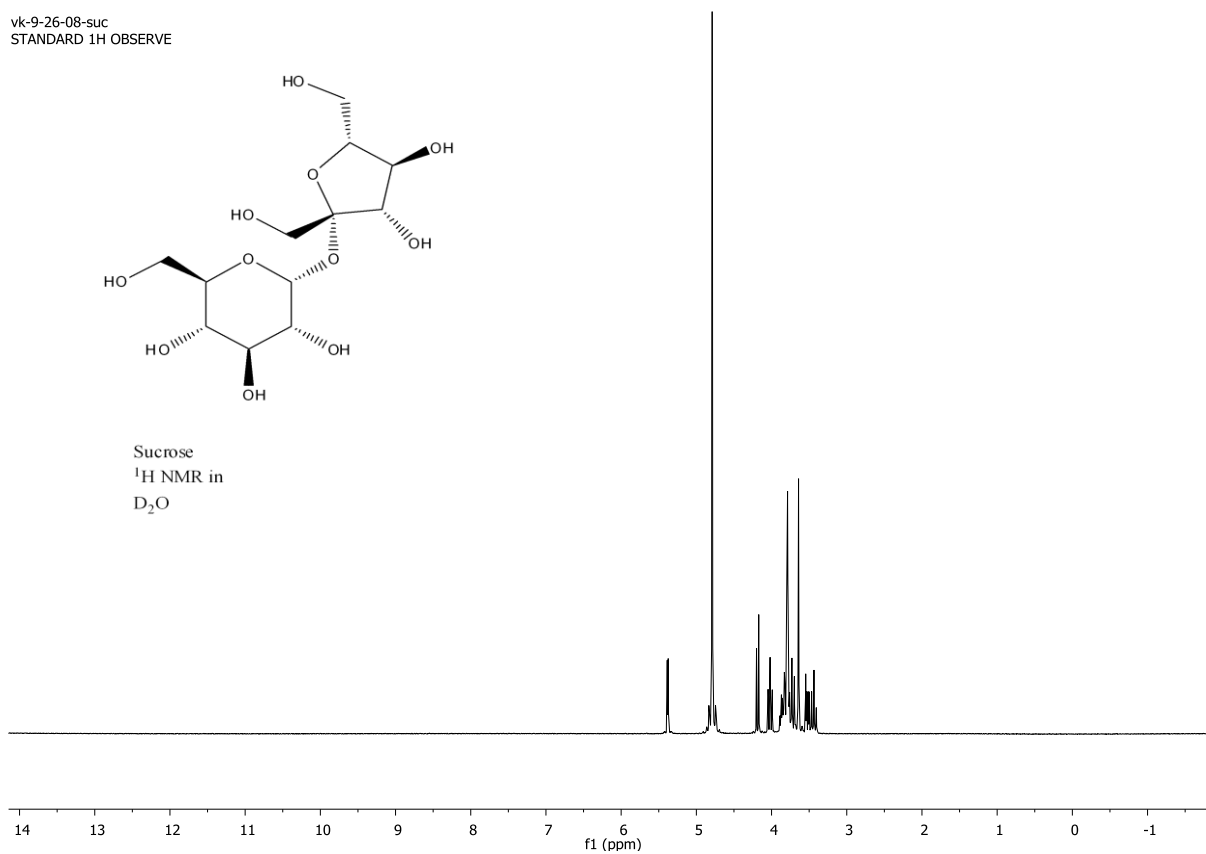
**Lactose**  
**<sup>1</sup>H NMR in**  
**D<sub>2</sub>O**



vk-9-26-08-suc  
STANDARD 1H OBSERVE



Sucrose  
 $^1\text{H}$  NMR in  
 $\text{D}_2\text{O}$

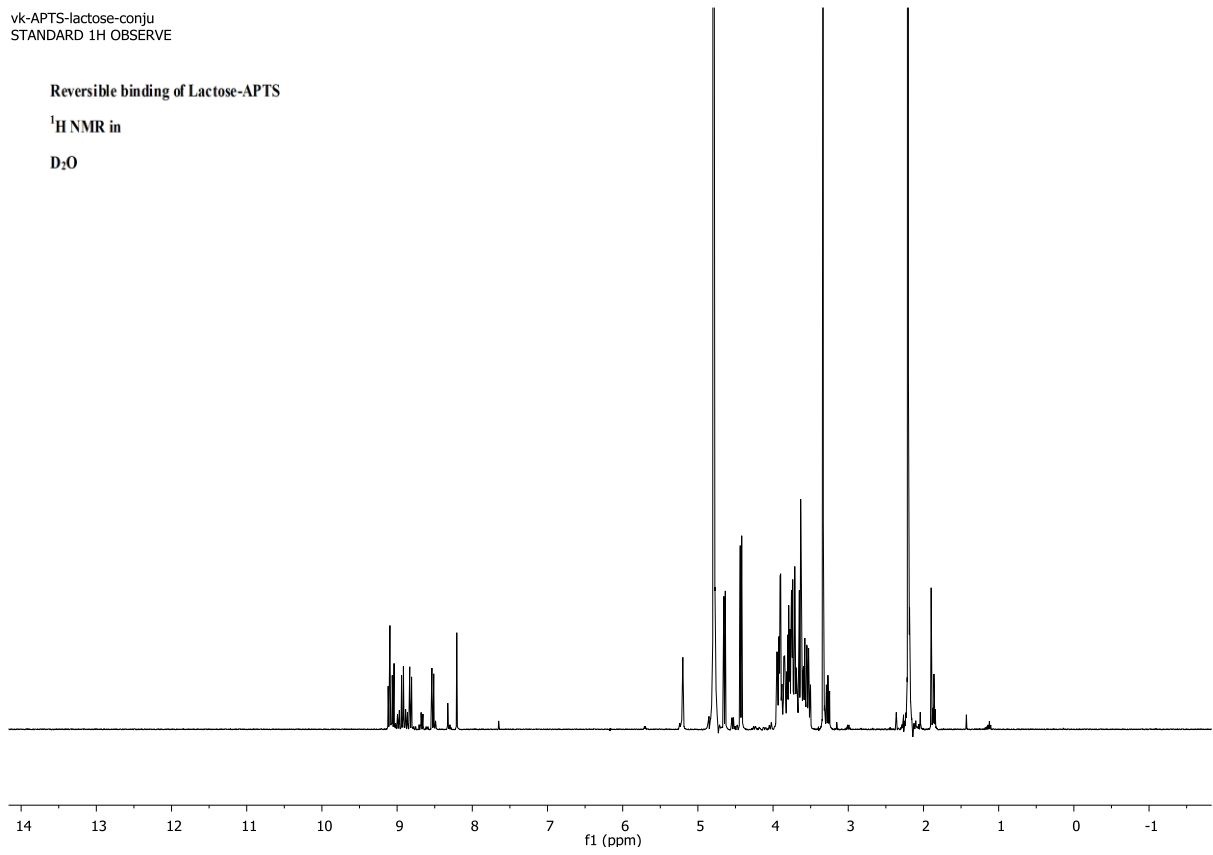


vk-APTS-lactose-conju  
STANDARD 1H OBSERVE

Reversible binding of Lactose-APTS

$^1\text{H}$  NMR in

$\text{D}_2\text{O}$

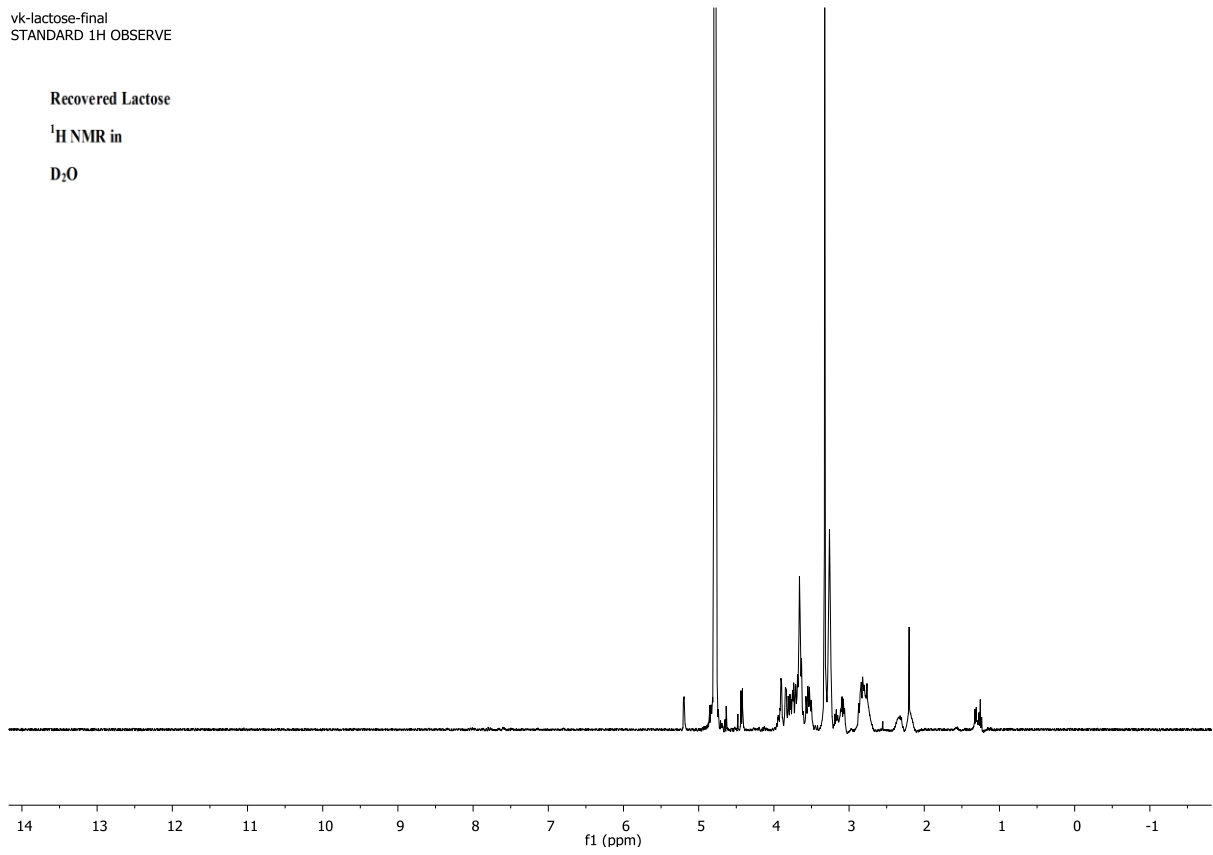


vk-lactose-final  
STANDARD 1H OBSERVE

Recovered Lactose

$^1\text{H}$  NMR in

$\text{D}_2\text{O}$

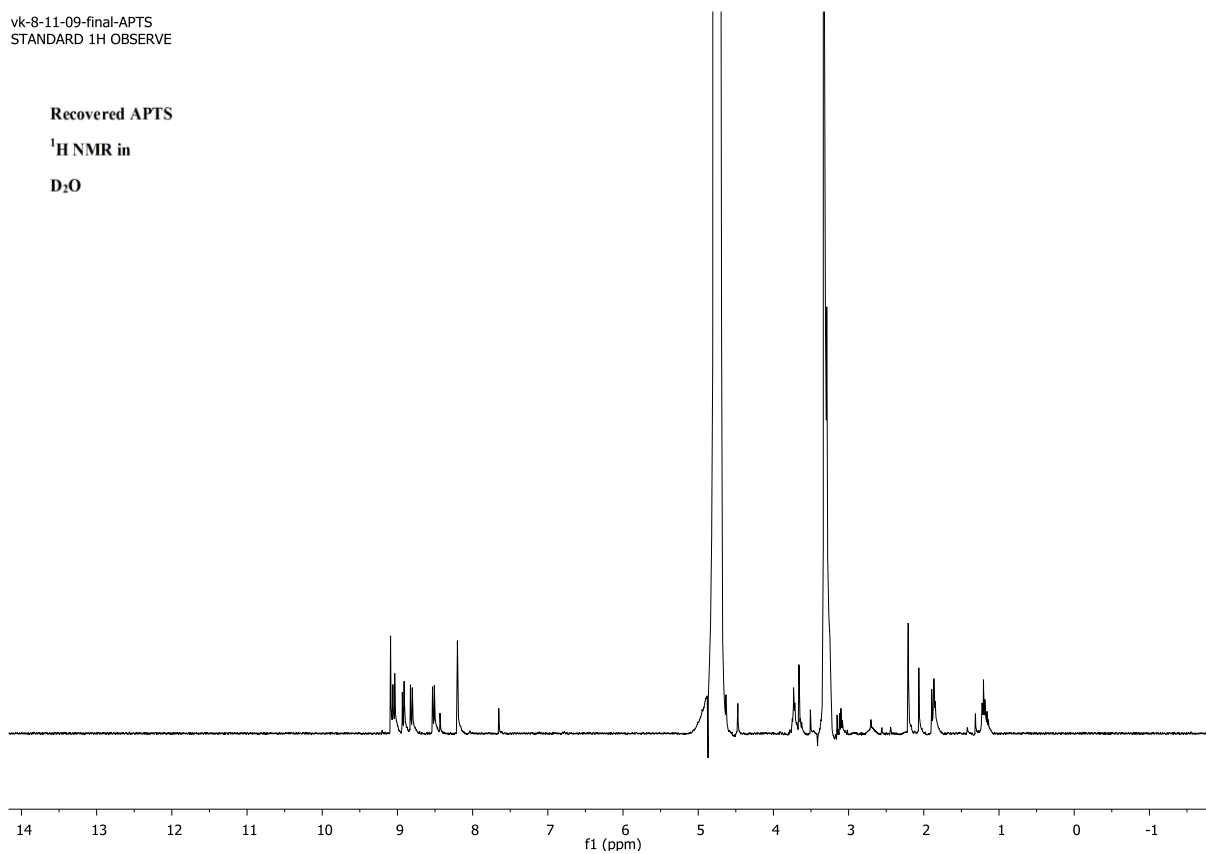


vk-8-11-09-final-APTS  
STANDARD 1H OBSERVE

Recovered APTS

$^1\text{H}$  NMR in

$\text{D}_2\text{O}$

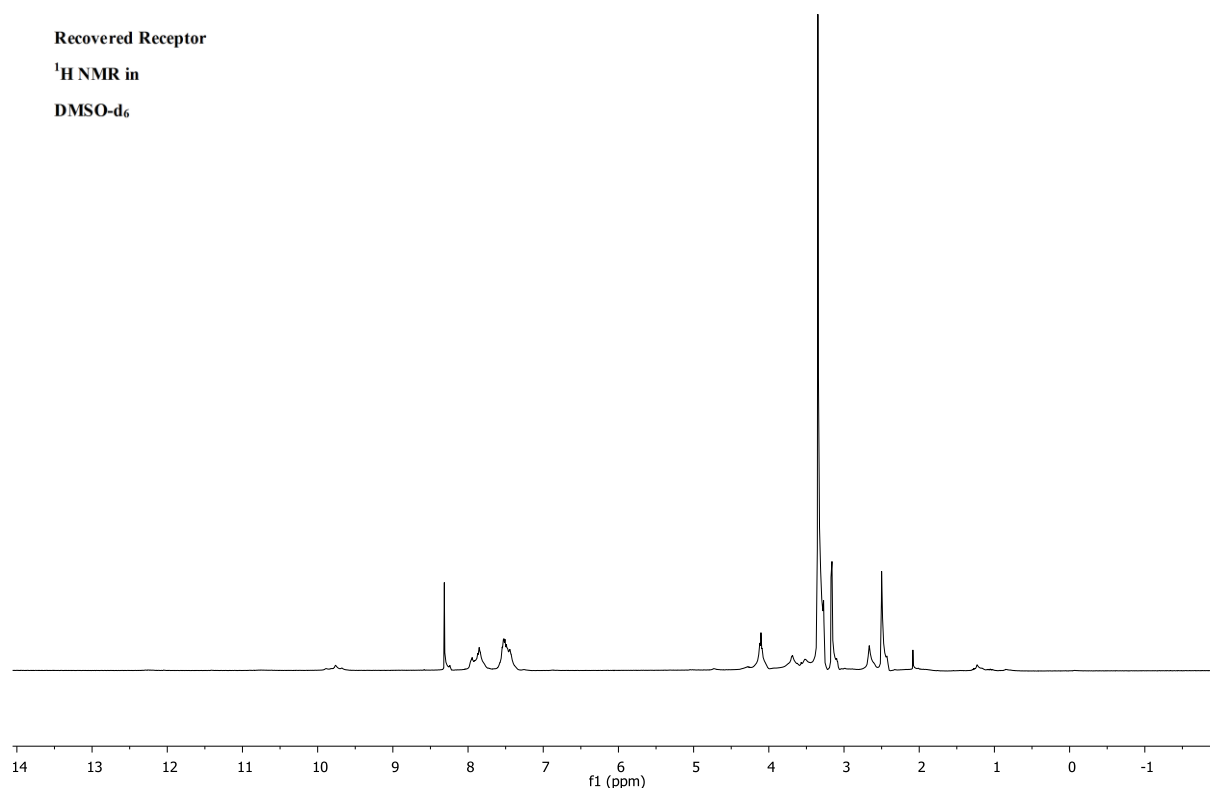


vk-receptor-8-14-09  
STANDARD 1H OBSERVE

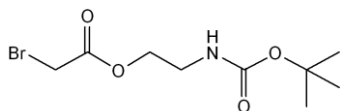
Recovered Receptor

<sup>1</sup>H NMR in

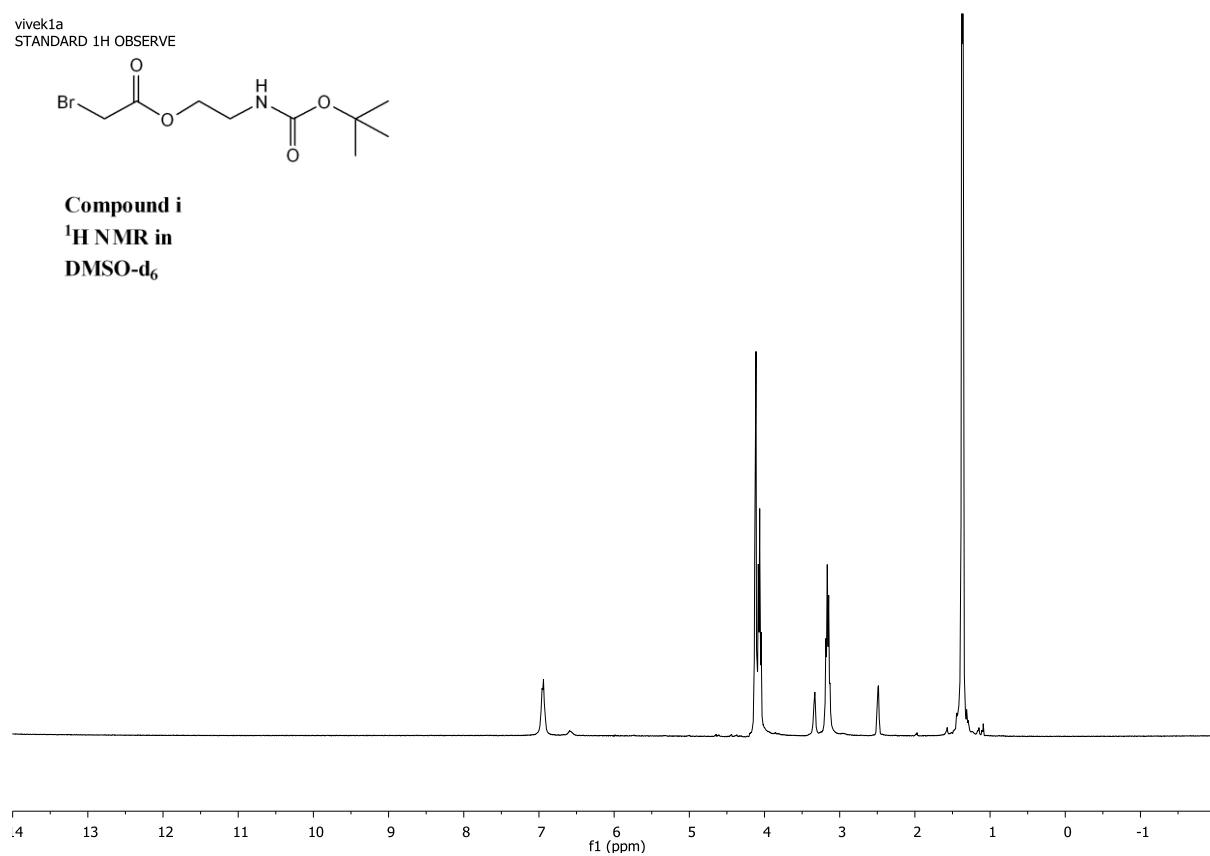
DMSO-d<sub>6</sub>



vivek1a  
STANDARD 1H OBSERVE



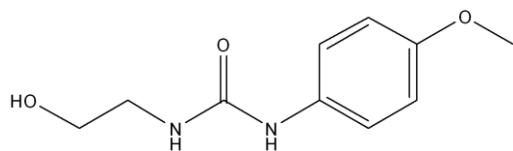
**Compound i**  
**<sup>1</sup>H NMR in**  
**DMSO-d<sub>6</sub>**



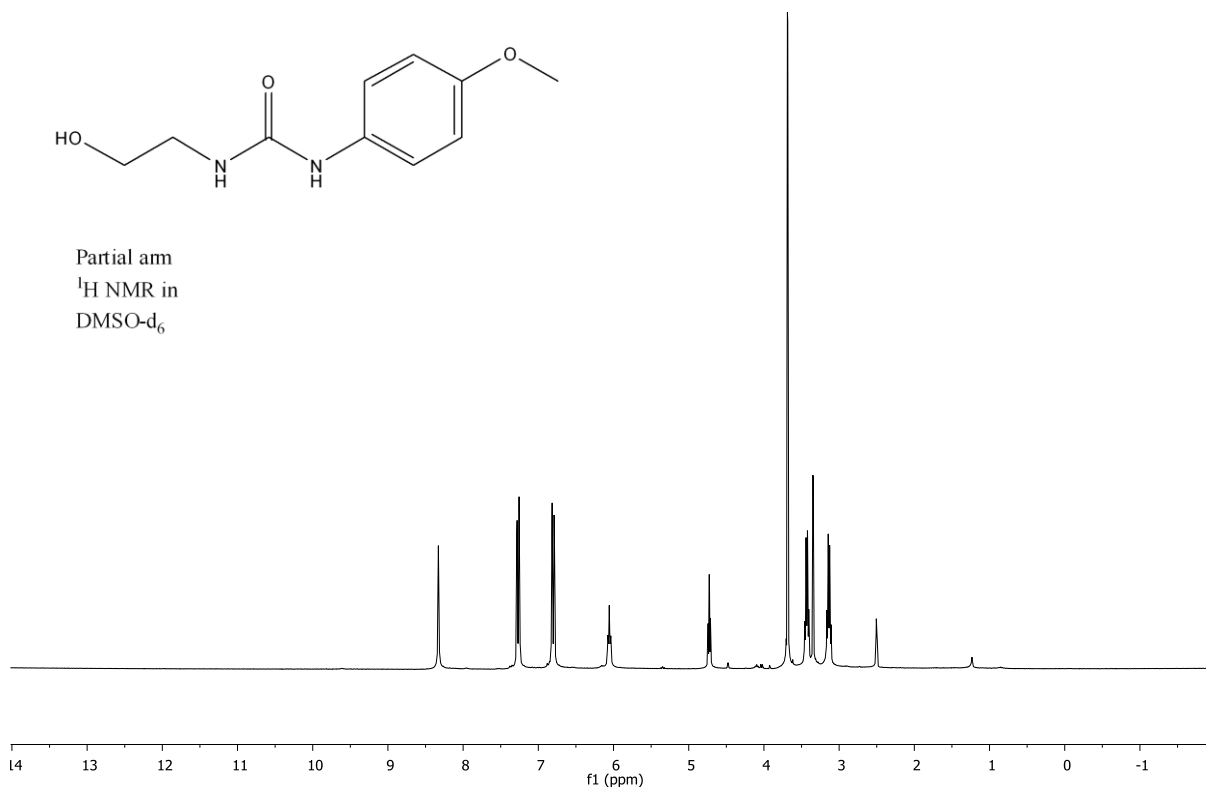




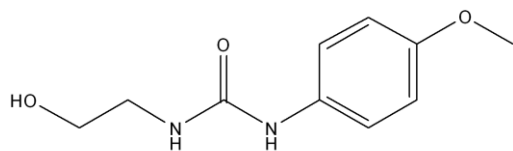
vk-7-27-11-partial\_arm  
STANDARD 1H OBSERVE



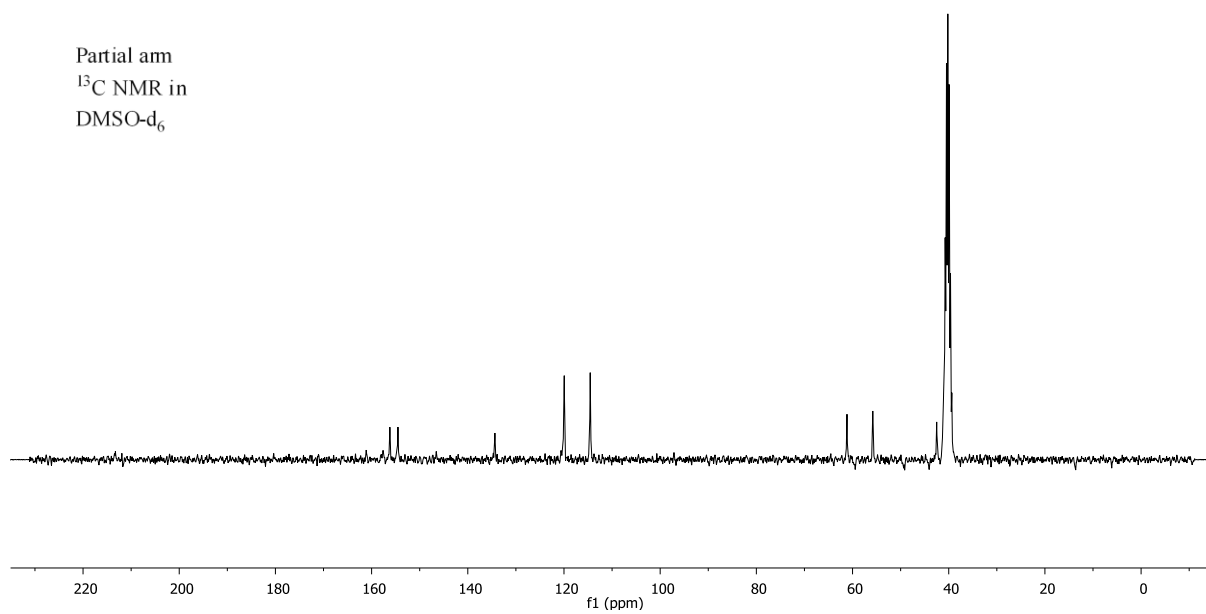
Partial arm  
 $^1\text{H}$  NMR in  
 $\text{DMSO-d}_6$



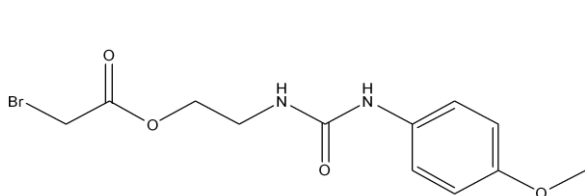
vk-7-27-11-partial\_armC13  
13C OBSERVE



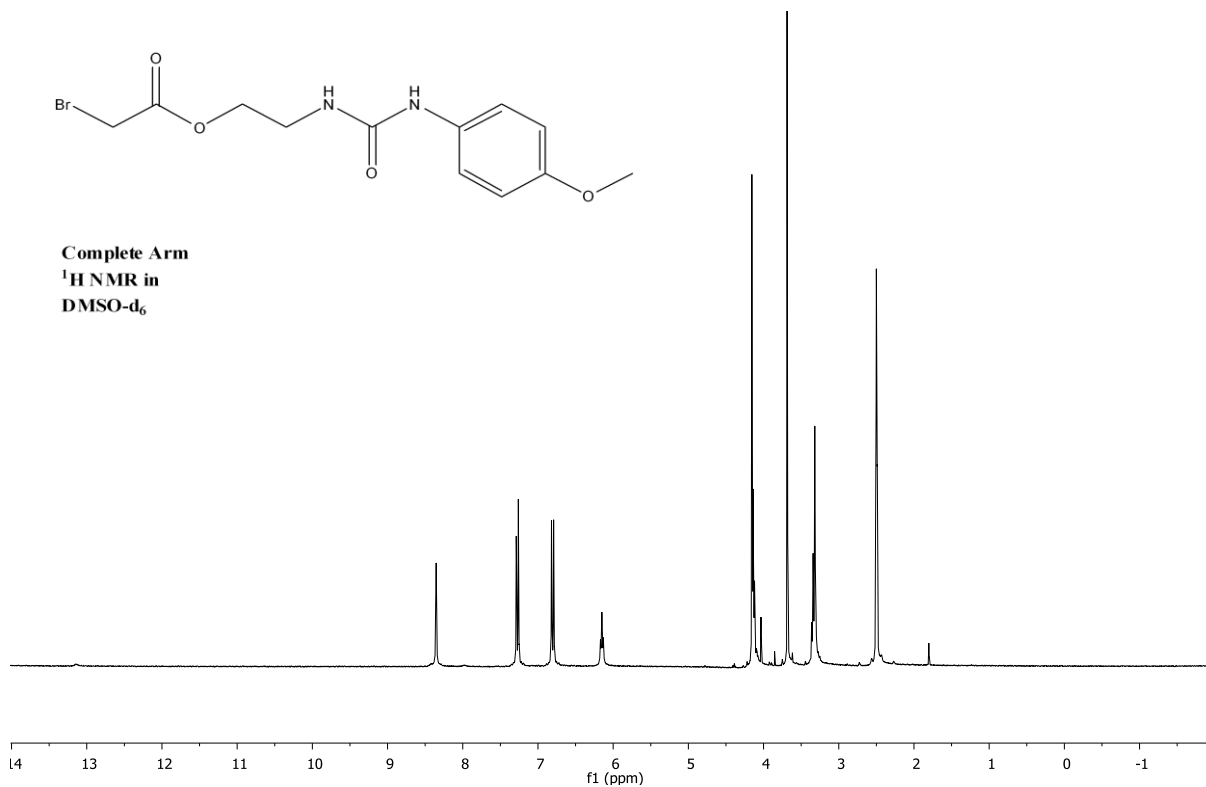
Partial arm  
 $^{13}\text{C}$  NMR in  
 $\text{DMSO-d}_6$



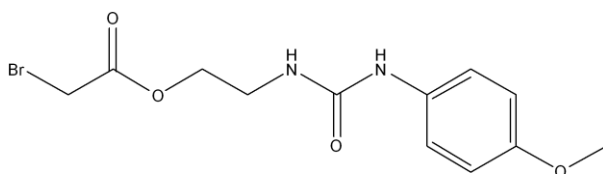
vk-5-13-11-full-arm  
STANDARD 1H OBSERVE



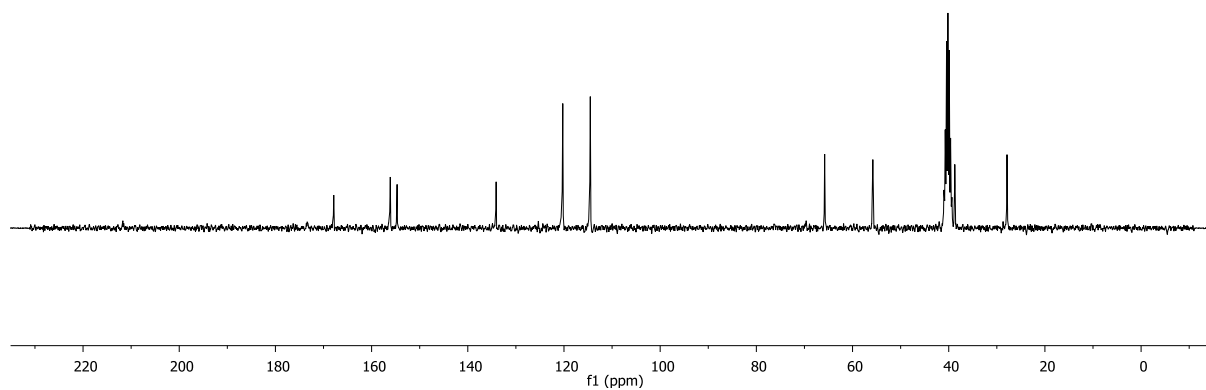
Complete Arm  
<sup>1</sup>H NMR in  
DMSO-d<sub>6</sub>



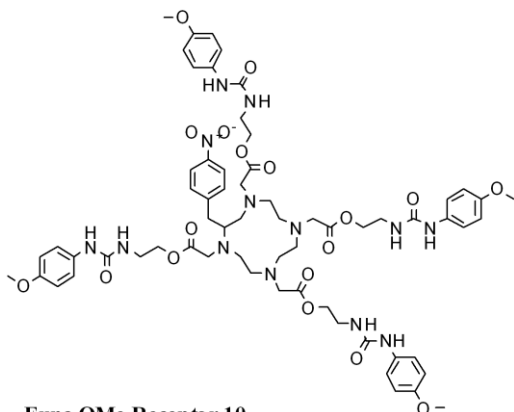
vk-7-27-11-complete\_armC13  
13C OBSERVE



Complete Arm  
<sup>13</sup>C NMR in  
DMSO-d<sub>6</sub>

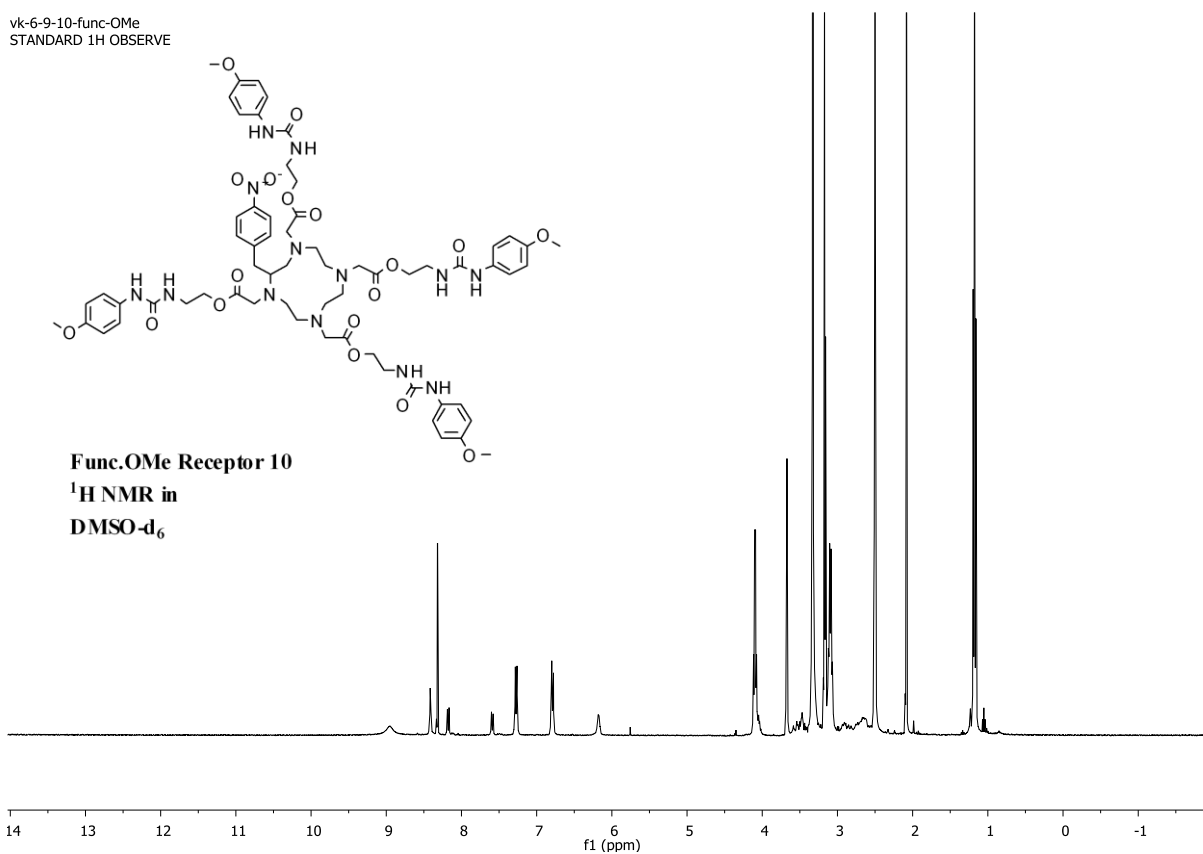


vk-6-9-10-func-OMe  
STANDARD 1H OBSERVE

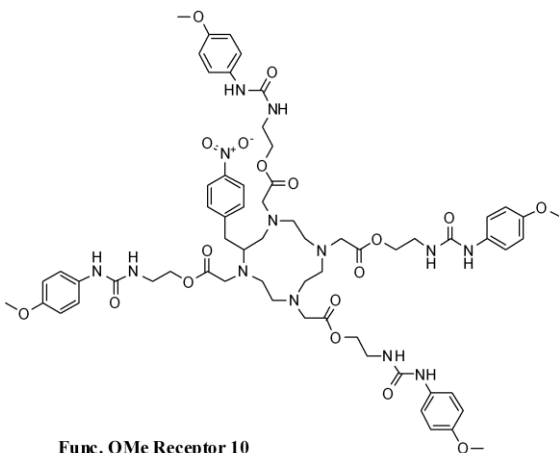


Func. OMe Receptor 10

$^1\text{H}$  NMR in  
DMSO- $\text{d}_6$

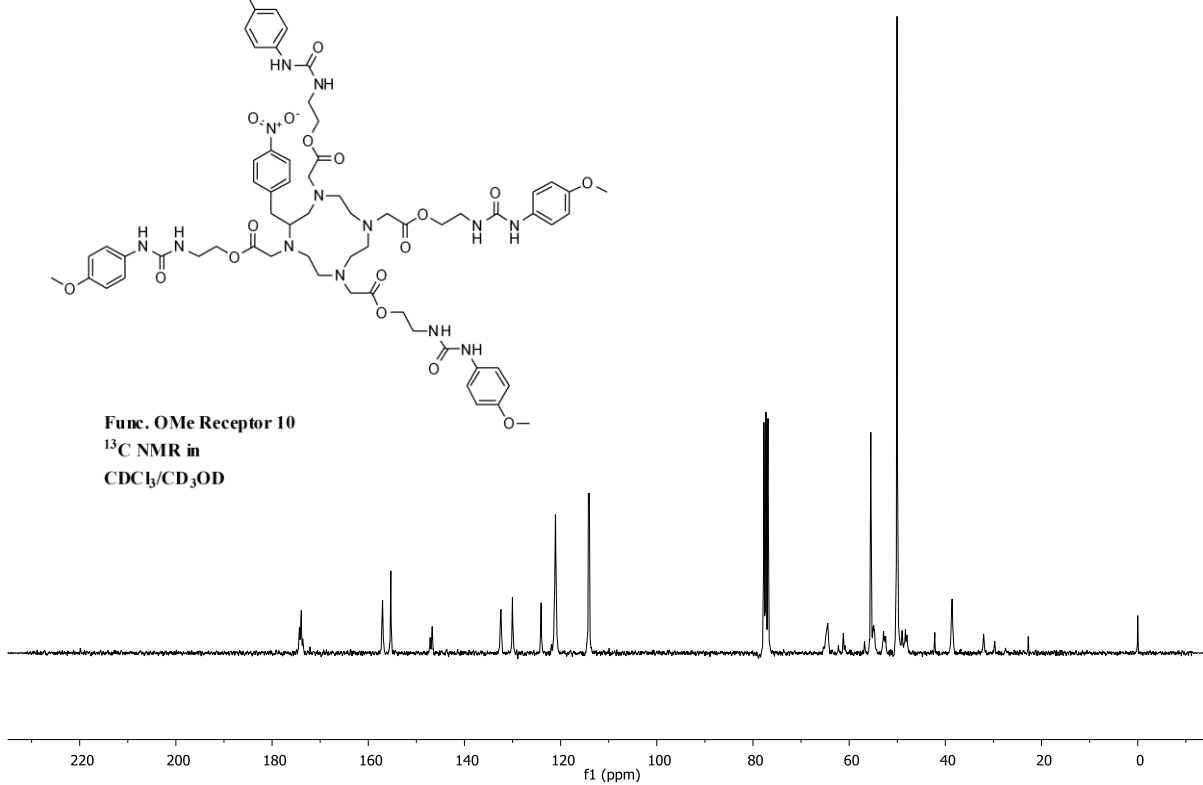


vk-5-19-11-OMe\_receptor-C13  
13C OBSERVE

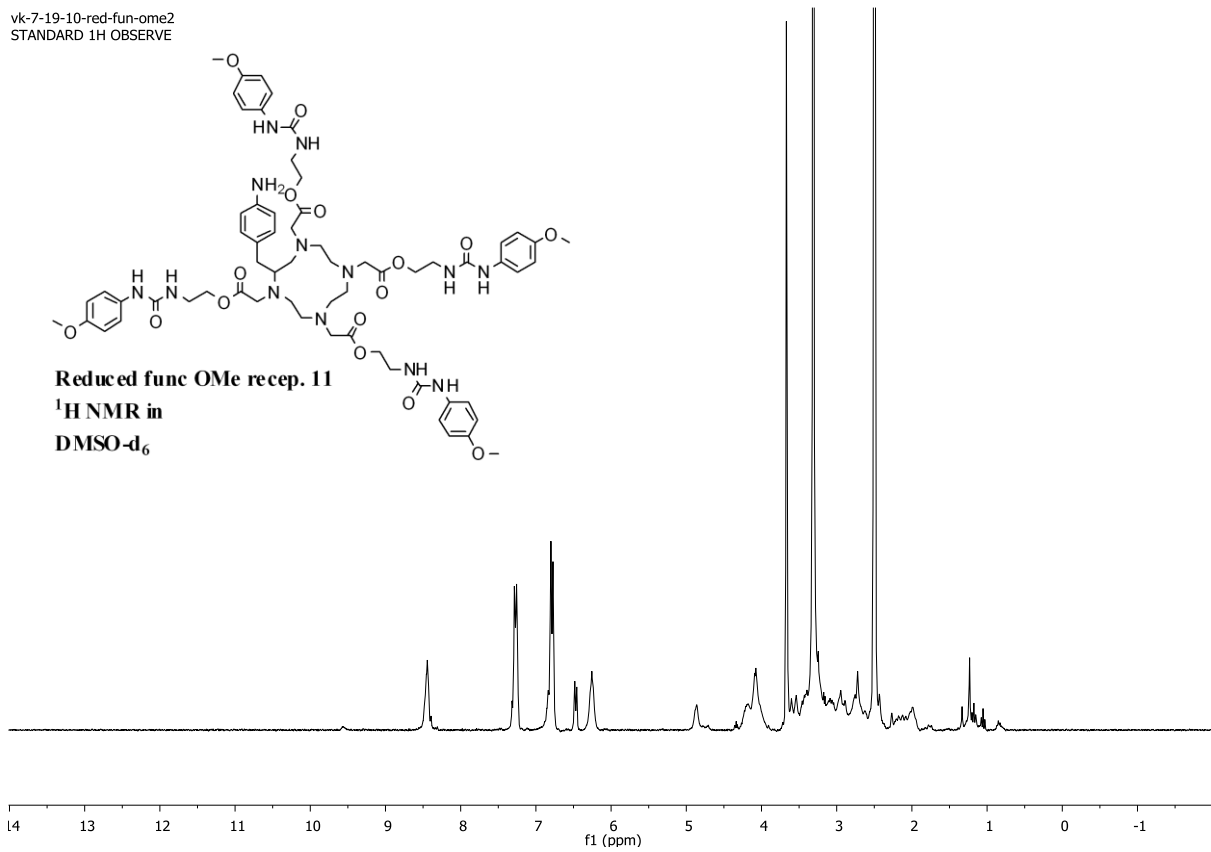
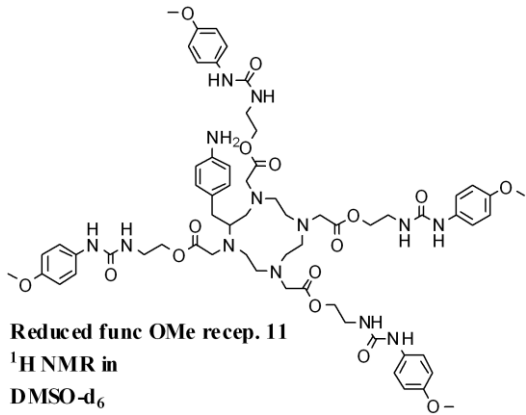


Func. OMe Receptor 10

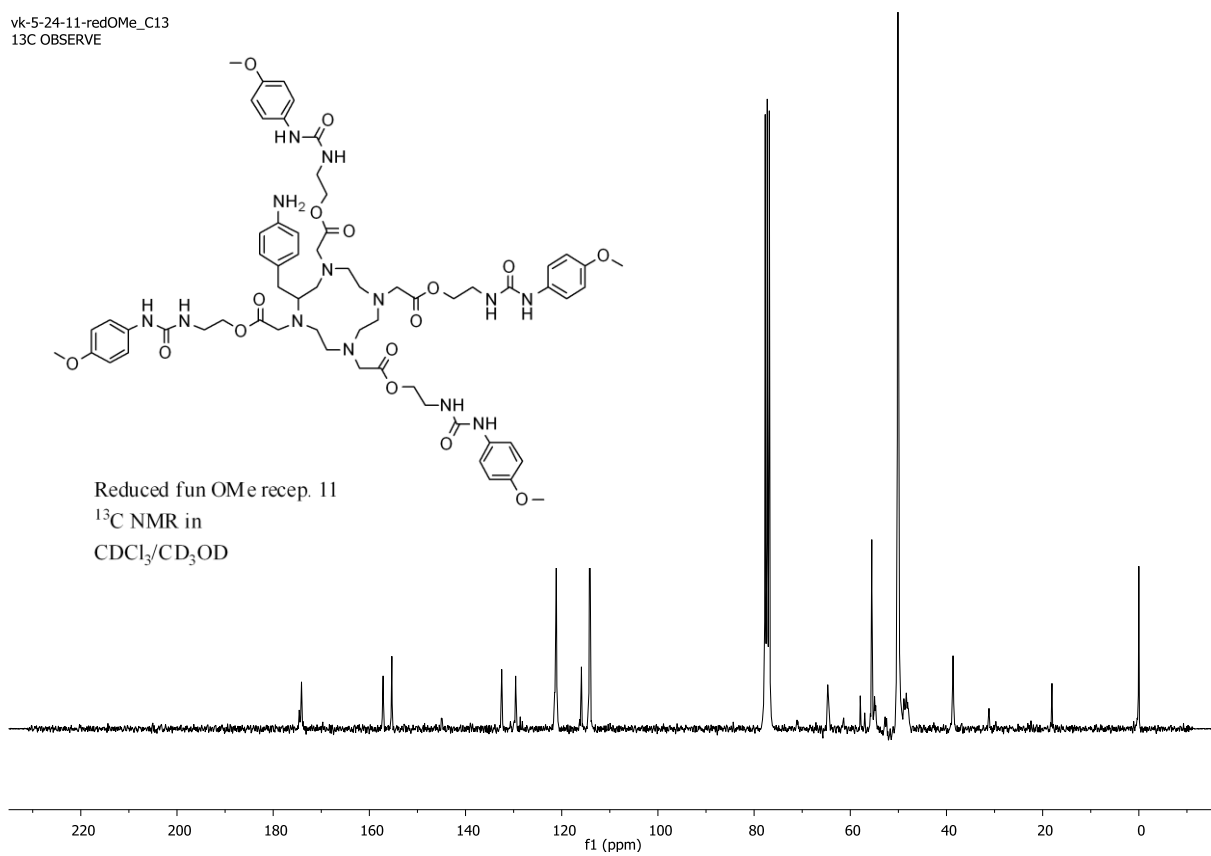
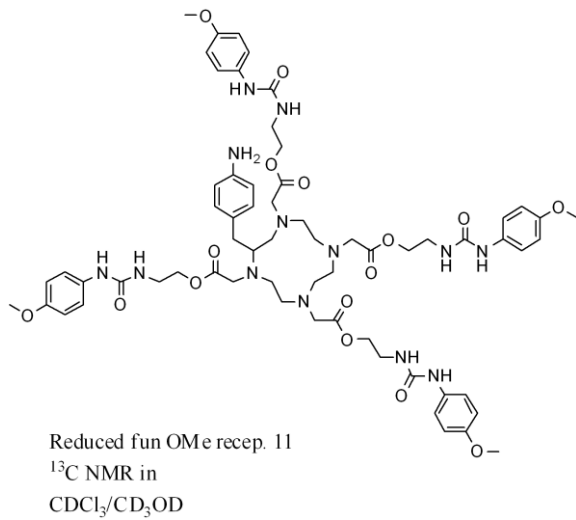
$^{13}\text{C}$  NMR in  
 $\text{CDCl}_3/\text{CD}_3\text{OD}$



vk-7-19-10-red-fun-ome2  
STANDARD 1H OBSERVE

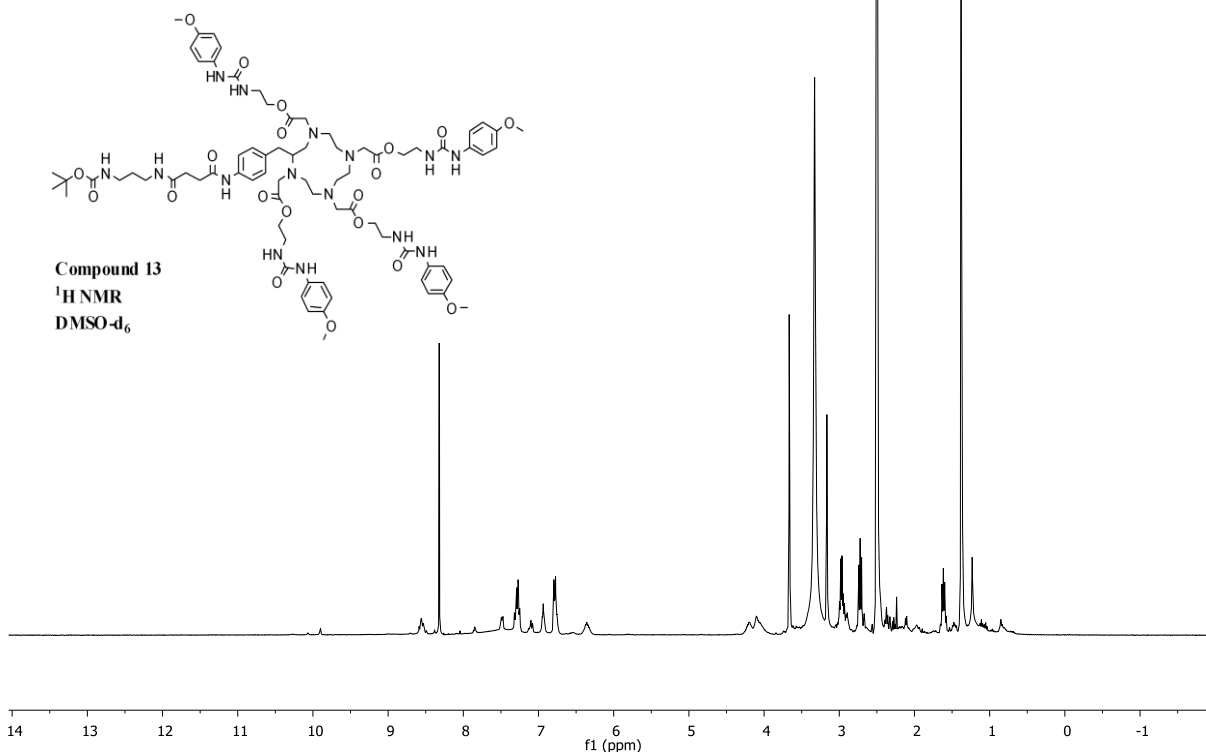


vk-5-24-11-redOMe\_C13  
13C OBSERVE

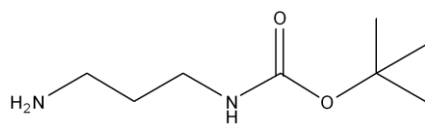




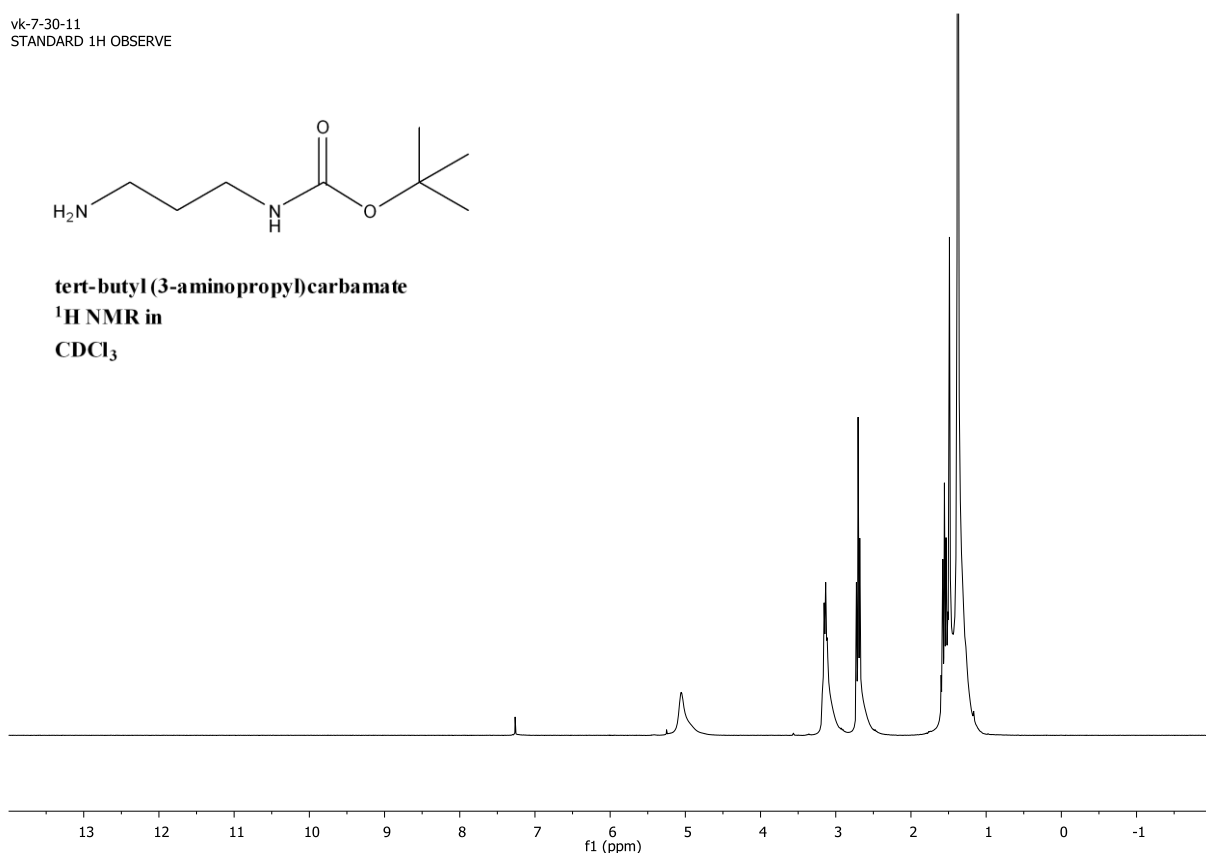
vk-4-7-11-recep-linker  
STANDARD 1H OBSERVE



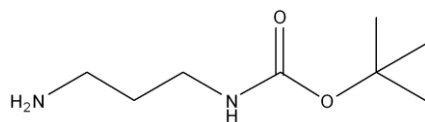
vk-7-30-11  
STANDARD 1H OBSERVE



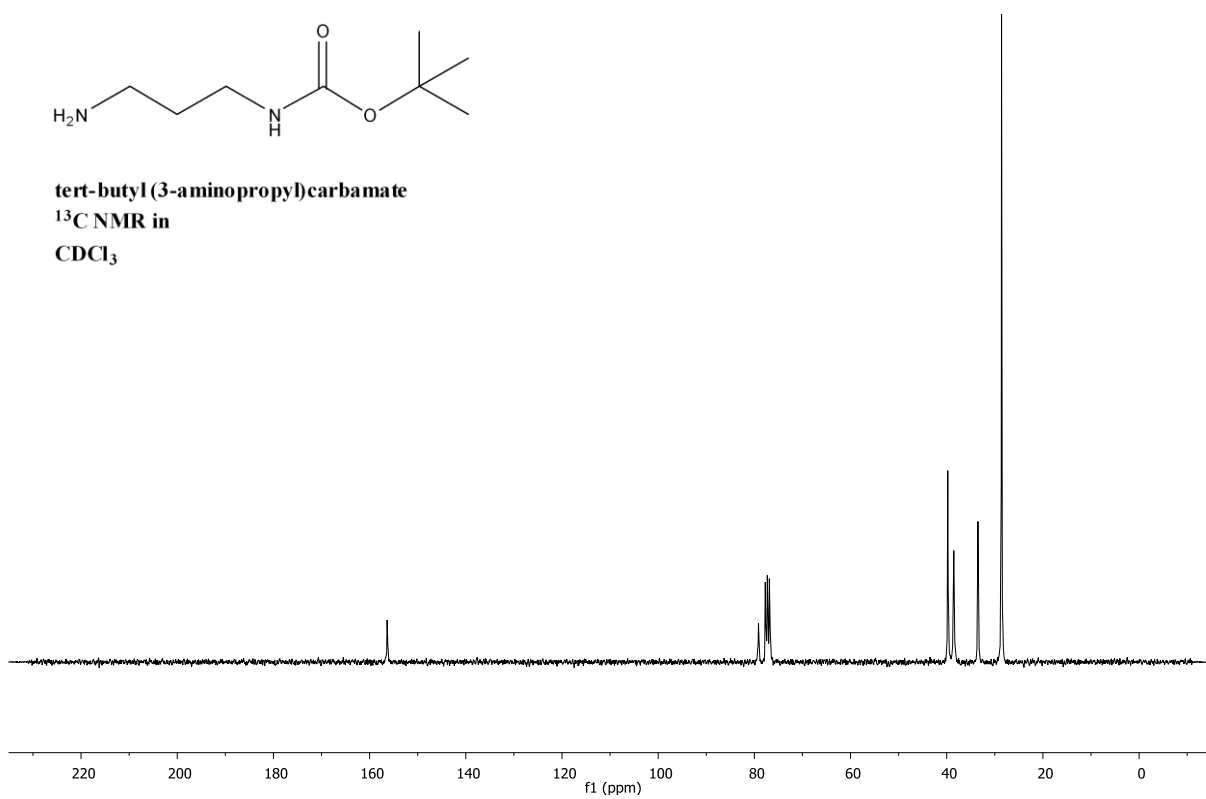
**tert-butyl (3-aminopropyl)carbamate**  
**<sup>1</sup>H NMR in**  
**CDCl<sub>3</sub>**



vk-7-30-11-C13  
13C OBSERVE



**tert-butyl (3-aminopropyl)carbamate**  
**<sup>13</sup>C NMR in**  
**CDCl<sub>3</sub>**





## VITA

Vivek Kaushik was born on July 9, 1980 Bapora, Haryana, India and is an Indian citizen. He received his Bachelor of Science Degree in Chemistry and Biology from Krukshetra University in 2001. He got his Master of Science Degree in Organic Chemistry from Dyanand University in 2004. Before coming to United States in 2005, he worked in Baba Fine Chemicals as a Chemist for one year. He joined Dr. Sidorov's research group in 2006 and he is author of two publications. He is a member of the American Chemical Society.